CHAPTER FOUR

Thin Plates

In practice we frequently encounter "thin" plates whose thickness is small compared with all other dimensions. Such a plate, undergoing small displacements, may be analyzed with the approximations that the strains vary linearly across the plate, (out-of-plane) shear deformations are negligible, and the out-of-plane normal stress σ_z and shear stresses τ_{xz}, τ_{yz} are small compared with the in-plane normal σ_x, σ_y, and shear τ_{xy} stresses.

Under certain conditions, solutions may be obtained for thin plates either by the solution of the differential equations representing equilibrium or by energy methods.[1] Here we demonstrate the use of the first method via the example of long plates and the second method via examples of rectangular plates either with symmetrical layup or with orthotropic and symmetrical layup. (For orthotropic plates the directions of orthotropy are parallel to the edges of the plate.) We chose these three types of problems because (i) they illustrate the analytical approaches and the use of the relevant equations, (ii) solutions can be obtained without extensive numerical algorithms, and last, but not least, (iii) they are of practical interest. Additionally, and importantly, these problems provide insights that are useful when analyzing plates by numerical methods.

Although the specification of orthotropy may seem to be overly restrictive, in fact it does not unduly limit the applicability of the analyses. The reason for this is that plates are often made according to the 10-percent rule, and such plates behave similarly to orthotropic plates.[2] Therefore, solutions for orthotropic plates provide good approximations of the deflections, maximum bending moments, buckling loads, and natural frequencies of nonorthotropic plates that have symmetrical layup and are constructed according to the 10-percent rule. The 10-percent rule

[1] J. M. Whitney, *Structural Analysis of Laminated Anisotropic Plates.* Technomic, Lancaster, Pennsylvania, 1987.

[2] I. Veres and L. P. Kollár, Approximate Analysis of Mid-plane Symmetric Rectangular Composite Plates. *Journal of Composite Materials*, Vol. 36, 673–684, 2002.

requires that the plate satisfy the following conditions:

- The plate is made of unidirectional plies.
- There are at least three ply orientations.
- The angles between the fibers are at least 15°.
- The number of plies in each fiber direction is at least 10 percent of the total number of plies.

Plates conforming to the 10-percent rule have better load bearing capabilities than unidirectional or angle-ply laminates for the following reasons.

Unidirectional plies are stiffer and stronger in the 0-degree fiber direction than in the 90-degree direction perpendicular to the fibers. Thus, laminates made of unidirectional plies are ill-suited to carry load in the 90-degree direction. Angle-ply laminates with only two fiber directions do not resist well tensile loads applied along the symmetry axis. Plates made by the 10-percent rule minimize these shortcomings.

The specification of symmetrical layup is less restrictive than it may appear because the analyses of symmetrical plates (for which ($[B] = 0$) can readily be extended to unsymmetrical plates ($[B] \neq 0$) with the use of the reduced bending stiffness $[D]^*$, defined as [3,4,5]

$$[D]^* = [D] - [B][A]^{-1}[B]. \tag{4.1}$$

The deflections, maximum bending moments, buckling loads, and natural frequencies of unsymmetrical plates can be approximated by replacing $[D]$ by $[D]^*$ in the expressions derived for symmetrical plates.

4.1 Governing Equations

In this section we summarize the equations used in analyzing thin plates. We employ the x, y, z coordinate system. The origin is at the midplane for plates with symmetrical layup and at a suitably chosen reference plane for plates with unsymmetrical layup.

The strains and curvatures of the reference plane (Fig. 3.10) are (Eqs. 3.1, 3.8)

$$\begin{aligned} \epsilon_x^o &= \frac{\partial u^o}{\partial x} & \epsilon_y^o &= \frac{\partial v^o}{\partial y} & \gamma_{xy}^o &= \frac{\partial u^o}{\partial y} + \frac{\partial v^o}{\partial x} \\ \kappa_x &= -\frac{\partial^2 w^o}{\partial x^2} & \kappa_y &= -\frac{\partial^2 w^o}{\partial y^2} & \kappa_{xy} &= -\frac{2\partial^2 w^o}{\partial x \partial y}, \end{aligned} \tag{4.2}$$

[3] J. M. Whitney, *Structural Analysis of Laminated Anisotropic Plates.* Technomic, Lancaster, Pennsylvania, 1987, p. 203.

[4] E. Reissner and Y. Stavsky, Bending and Stretching of Certain Types of Heterogeneous Aelotropic Elastic Plates. *Journal of Applied Mechanics*, Vol. 28, 402–408, 1961.

[5] J. E. Ashton, Approximate Solutions for Unsymmetrically Laminated Plates. *Journal of Composite Materials*, Vol. 3, 189–191, 1969.

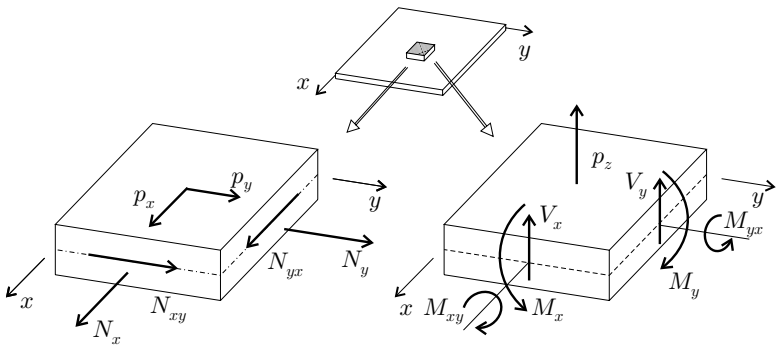

Figure 4.1: Forces and loads acting on an element of the plate.

where u^{o} and v^{o} are the displacements of the reference plane in the x and y directions, and w^{o} is the out-of-plane displacement (deflection) of this plane. The force–strain relationships are (Eq. 3.21)

$$\begin{Bmatrix} N_x \\ N_y \\ N_{xy} \\ M_x \\ M_y \\ M_{xy} \end{Bmatrix} = \begin{bmatrix} A_{11} & A_{12} & A_{16} & B_{11} & B_{12} & B_{16} \\ A_{12} & A_{22} & A_{26} & B_{12} & B_{22} & B_{26} \\ A_{16} & A_{26} & A_{66} & B_{16} & B_{26} & B_{66} \\ B_{11} & B_{12} & B_{16} & D_{11} & D_{12} & D_{16} \\ B_{12} & B_{22} & B_{26} & D_{12} & D_{22} & D_{26} \\ B_{16} & B_{26} & B_{66} & D_{16} & D_{26} & D_{66} \end{bmatrix} \begin{Bmatrix} \epsilon_x^{\mathrm{o}} \\ \epsilon_y^{\mathrm{o}} \\ \gamma_{xy}^{\mathrm{o}} \\ \kappa_x \\ \kappa_y \\ \kappa_{xy} \end{Bmatrix}. \tag{4.3}$$

In the analyses we may employ either the equilibrium equations or the strain energy.

The equilibrium equations are[6]

$$\begin{aligned} \frac{\partial N_x}{\partial x} + \frac{\partial N_{xy}}{\partial y} &= -p_x \\ \frac{\partial N_y}{\partial y} + \frac{\partial N_{xy}}{\partial x} &= -p_y \\ \frac{\partial V_x}{\partial x} + \frac{\partial V_y}{\partial y} &= -p_z \end{aligned} \tag{4.4}$$

$$V_x = \frac{\partial M_x}{\partial x} + \frac{\partial M_{xy}}{\partial y} \qquad V_y = \frac{\partial M_y}{\partial y} + \frac{\partial M_{xy}}{\partial x}, \tag{4.5}$$

where p_x, p_y, and p_z are the components of the distributed surface load (per unit area); N_x, N_y, and N_{xy} are the in-plane forces (per unit length); V_x and V_y are the transverse shear forces (per unit length); M_x, M_y and M_{xy} are, respectively, the bending moments and the twist moment (per unit length) (Fig. 4.1).

[6] S. P. Timoshenko and S. Woinowsky-Krieger, *Theory of Plates and Shells.* 2nd edition. McGraw-Hill, New York, 1959, p. 80.

4.1.1 Boundary Conditions

The conditions along each edge of the plate must be specified. Boundary conditions for an edge parallel with the y-axis are given below.

Along a built-in edge, the deflection w^{o}, the rotation of the edge $\partial w^{\mathrm{o}}/\partial x$, and the in-plane u^{o}, v^{o} displacements are zero:

$$w^{\mathrm{o}} = 0 \qquad \frac{\partial w^{\mathrm{o}}}{\partial x} = 0 \qquad u^{\mathrm{o}} = v^{\mathrm{o}} = 0. \tag{4.6}$$

Along a free edge, where no external loads are applied, the bending moment M_x, the replacement shear force[7] $V_x + \partial M_{xy}/\partial x$, and the in-plane forces N_x, N_{xy} are zero:

$$M_x = 0 \qquad V_x + \frac{\partial M_{xy}}{\partial y} = 0 \qquad N_x = N_{xy} = 0. \tag{4.7}$$

Along a simply supported edge, the deflection w^{o}, the bending moment M_x, and the in-plane forces N_x, N_{xy} are zero:

$$w^{\mathrm{o}} = 0 \qquad M_x = 0 \qquad N_x = N_{xy} = 0. \tag{4.8}$$

When in-plane motions are prevented by the support, the in-plane forces are not zero ($N_x \neq 0$, $N_{xy} \neq 0$) whereas the in-plane displacements are zero:

$$u^{\mathrm{o}} = 0 \qquad v^{\mathrm{o}} = 0. \tag{4.9}$$

For an edge parallel with the x-axis, the preceding boundary conditions hold with x and y interchanged.

4.1.2 Strain Energy

As we noted previously, solutions to plate problems may be obtained by energy methods that require knowledge of the strain energy. For a linearly elastic material the strain energy is given by Eq. (2.200). Under plane-stress condition the stress components σ_z, τ_{xz}, and τ_{yz} are zero (Eq. 2.121), and the expression for the strain energy simplifies to

$$U = \frac{1}{2}\int_0^{L_x}\int_0^{L_y}\int_{-h_{\mathrm{b}}}^{h_{\mathrm{t}}} (\sigma_x\epsilon_x + \sigma_y\epsilon_y + \tau_{xy}\gamma_{xy})\, dz dy dx, \tag{4.10}$$

where h_{t} and h_{b} are the distances from the reference plane to the plate's surfaces (Fig. 3.12). The strain components are (Eq. 3.7)

$$\begin{Bmatrix} \epsilon_x \\ \epsilon_y \\ \gamma_{xy} \end{Bmatrix} = \begin{Bmatrix} \epsilon_x^{\mathrm{o}} \\ \epsilon_y^{\mathrm{o}} \\ \gamma_{xy}^{\mathrm{o}} \end{Bmatrix} + z \begin{Bmatrix} \kappa_x \\ \kappa_y \\ \kappa_{xy} \end{Bmatrix}. \tag{4.11}$$

[7] Ibid., p. 84.

The stresses and the strains at a point are related by (Eq. 3.13)

$$\begin{Bmatrix} \sigma_x \\ \sigma_y \\ \tau_{xy} \end{Bmatrix} = [\overline{Q}] \begin{Bmatrix} \epsilon_x \\ \epsilon_y \\ \gamma_{xy} \end{Bmatrix}. \tag{4.12}$$

By substituting Eqs. (4.11) and (4.12) into Eq. (4.10) and by utilizing the definitions of the $[A]$, $[B]$, $[D]$ matrices (Eq. 3.18), we obtain the following expression for the strain energy:

$$U = \frac{1}{2} \int_0^{L_x} \int_0^{L_y} \begin{Bmatrix} \epsilon_x^o \\ \epsilon_y^o \\ \gamma_{xy}^o \\ \kappa_x \\ \kappa_y \\ \kappa_{xy} \end{Bmatrix}^T \begin{bmatrix} A_{11} & A_{12} & A_{16} & B_{11} & B_{12} & B_{16} \\ A_{12} & A_{22} & A_{26} & B_{12} & B_{22} & B_{26} \\ A_{16} & A_{26} & A_{66} & B_{16} & B_{26} & B_{66} \\ B_{11} & B_{12} & B_{16} & D_{11} & D_{12} & D_{16} \\ B_{12} & B_{22} & B_{26} & D_{12} & D_{22} & D_{26} \\ B_{16} & B_{26} & B_{66} & D_{16} & D_{26} & D_{66} \end{bmatrix} \begin{Bmatrix} \epsilon_x^o \\ \epsilon_y^o \\ \gamma_{xy}^o \\ \kappa_x \\ \kappa_y \\ \kappa_{xy} \end{Bmatrix} dydx. \tag{4.13}$$

The superscript T denotes the transpose of the vector.

4.2 Deflection of Rectangular Plates

4.2.1 Pure Bending and In-Plane Loads

We consider an unsupported rectangular plate subjected to pure bending and to in-plane loads (Fig. 4.2). The in-plane forces and moments are related to the reference plane's strains and curvatures by Eq. (4.3). Six of the twelve quantities appearing in this equation must be specified as follows:

$$\begin{array}{llll} N_x & \text{or} & \epsilon_x^o & M_x \quad \text{or} \quad \kappa_x \\ N_y & \text{or} & \epsilon_y^o & M_y \quad \text{or} \quad \kappa_y \\ N_{xy} & \text{or} & \epsilon_{xy}^o & M_{xy} \quad \text{or} \quad \kappa_{xy}. \end{array} \tag{4.14}$$

With six of the quantities chosen (Eq. 4.14), the remaining six may be obtained by solving the six simultaneous equations given by Eq. (4.3). Once the curvatures

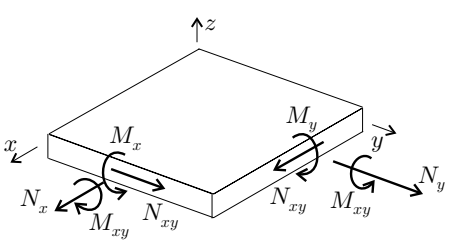

Figure 4.2: Rectangular plate subjected to bending and in-plane loads.

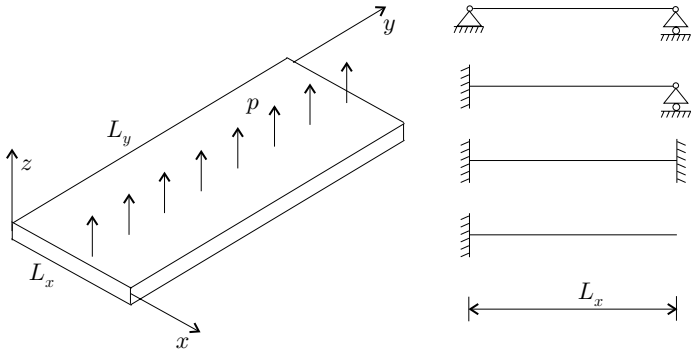

Figure 4.3: The different types of supports along the long edges of a transversely loaded long plate.

are known, the deflection of the reference surface w^o is calculated by using the relationships between the curvatures and the deflection (Eq. 4.2) as follows:

$$\kappa_x = -\frac{\partial^2 w^o}{\partial x^2} \qquad \kappa_y = -\frac{\partial^2 w^o}{\partial y^2} \qquad \kappa_{xy} = -\frac{2\partial^2 w^o}{\partial x \partial y}. \tag{4.15}$$

The following deflection satisfies these relationships:

$$w^o = -\frac{\kappa_x}{2}x^2 - \frac{\kappa_y}{2}y^2 - \frac{\kappa_{xy}}{2}xy. \tag{4.16}$$

This expression for w^o does not include the deflection of the reference plane due to rigid-body motion.

4.2.2 Long Plates

We consider a long rectangular plate whose length L_y is large compared with its width L_x. The long edges may be built-in, simply supported, or free, as shown in Figure 4.3. The plate is subjected to a distributed transverse load p. Neither this load nor the edge supports vary along the longitudinal y direction.

When the length of the plate is large compared with its width, away from the short edges the deflected surface may be assumed to be cylindrical (cylindrical deformation, Fig. 4.4), and the forces and moments do not vary appreciably along the length. With these approximations the analysis simplifies considerably. Before we undertake the analysis, we establish the length-to-width ratios for which a plate may be considered long.

For an isotropic plate the long-plate approximation for the deflection is reasonable when[8]

$$\frac{L'_y}{L'_x} > 3 \qquad \text{isotropic plate,} \tag{4.17}$$

where L'_y and L'_x are the length and the width of the isotropic plate, respectively. We now establish for orthotropic plates the length-to-width ratios at which the

[8] Ibid., p. 118.

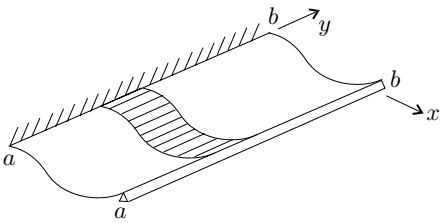

Figure 4.4: Cylindrical deformation of a long rectangular plate.

long-plate approximation may be applied. To this end we observe that the deflections of an orthotropic plate (with length L_y and width L_x) and an isotropic plate (with length L'_y and width L'_x) are similar when (page 109)

$$L'_x = \frac{L_x}{\sqrt[4]{\frac{D_{11}}{D_{22}}}} \qquad L'_y = L_y. \tag{4.18}$$

Thus, from Eqs. (4.17) and (4.18) we have that the long-plate approximation is reasonable when the following inequality is satisfied:

$$\frac{L_y}{L_x} > 3\sqrt[4]{\frac{D_{11}}{D_{22}}} \qquad \text{orthotropic plate.} \tag{4.19}$$

This formula, which is established for orthotropic plates, may also be used as a guide for plates whose layup is not orthotropic.

We now proceed with the analysis of long plates in cylindrical bending. The generator of this cylindrical surface is parallel to the longitudinal y-axis of the plate. The curvatures κ_y and κ_{xy} of the plate are zero

$$\kappa_y = 0 \qquad \kappa_{xy} = 0, \tag{4.20}$$

and κ_x is (Eq. 4.2)

$$\kappa_x = -\frac{\partial^2 w^o}{\partial x^2}. \tag{4.21}$$

Away from the short edges the forces and moments do not vary along the length of the plate. Thus, from the last of Eq. (4.4) and the first of Eq. (4.5) we have

$$\frac{dV_x}{dx} + p_z = 0 \tag{4.22}$$

$$\frac{dM_x}{dx} - V_x = 0. \tag{4.23}$$

The load is perpendicular to the surface, and for simplicity we replace p_z by p. Thus, by substituting V_x from Eq. (4.23) into Eq. (4.22) we obtain the equilibrium equation

$$\frac{d^2 M_x}{dx^2} + p = 0. \tag{4.24}$$

We note that this equation, representing equilibrium, is independent of the material.

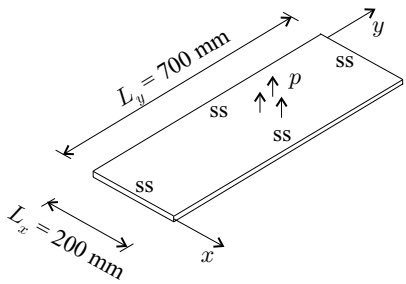

Figure 4.5: The plate in Example 4.1.

Symmetrical layup. The layup of the plate is symmetrical ($[B] = 0$). We now concern ourselves only with the bending moment M_x, which, from Eqs. (4.3) and (4.20), is

$$M_x = D_{11}\kappa_x. \tag{4.25}$$

The element D_{11} of the matrix $[D]$ is given by Eq. (3.20).

By substituting Eq. (4.25) into Eq. (4.24) and by using Eq. (4.21), we obtain the following equilibrium equation for the anisotropic long plate:

$$\frac{d^4 w^{\mathrm{o}}}{dx^4} - \frac{p}{D_{11}} = 0 \qquad \begin{array}{l}\text{long plate}\\ \text{symmetrical layup.}\end{array} \tag{4.26}$$

The equation governing the deflection of a transversely loaded isotropic beam is[9]

$$\frac{d^4 w}{dx^4} - \frac{p'}{EI} = 0 \qquad \text{isotropic beam,} \tag{4.27}$$

where E is Young's modulus, I is the moment of inertia about the y-axis, and p' is the transverse load per unit length.

By comparing Eq. (4.26) and (4.27), we see that the equations describing the deflections of a long plate (symmetrical layup) and an isotropic beam are similar. Consequently, the deflection of a long plate (symmetrical layup) with bending stiffness D_{11} is the same as the deflection of an isotropic beam with bending stiffness EI when the numerical values of the loads are equal ($p = p'$). (Note however that p is per unit area and p' is per unit length.) Thus, the deflection of a long plate with symmetrical layup can be obtained by replacing EI/p' by D_{11}/p in the expression[10] given for the deflection of the corresponding isotropic beam.

4.1 Example. *A* 0.7*-m-long and* 0.2*-m-wide rectangular plate is made of graphite epoxy. The material properties are given in Table 3.6 (page 81). The layup is* $[\pm 45_2^{\mathrm{f}}/0_{12}/\pm 45_2^{\mathrm{f}}]$. *The* 0*-degree plies are parallel to the short edge of the plate. The plate is simply supported along all four edges and is subjected to a uniformly distributed transverse load* $p = 50\,000$ *N/m*^{2} *(Fig. 4.5). Calculate the maximum*

[9] E. P. Popov, *Engineering Mechanics of Solids*. Prentice-Hall, Englewood Cliffs, New Jersey, 1990, p. 505.

[10] W. D. Pilkey, *Formulas for Stresses, Strains, and Structural Matrices.* John Wiley & Sons, New York, 1994.

deflection, the maximum bending moments, and the stresses and strains in each layer.

Solution. The bending stiffnesses of the plate are (Table 3.7, page 84) $D_{11} = 45.30\ \mathrm{N \cdot m}$ and $D_{22} = 25.26\ \mathrm{N \cdot m}$. We may treat this plate as long when the following condition is met (Eq. 4.19):

$$\frac{L_y}{L_x} > 3\sqrt[4]{\frac{D_{11}}{D_{22}}}. \tag{4.28}$$

In the present problem the terms in this inequality are $L_y/L_x = 3.5$ and $3\sqrt[4]{D_{11}/D_{22}} = 3.47$. Thus, the preceding condition is satisfied and the long-plate expressions may be used.

The maximum deflection of a simply supported beam is (Table 7.3, page 332)

$$\widetilde{w} = \frac{5}{384}\frac{p' L^4}{EI}. \tag{4.29}$$

The maximum deflection of the plate is obtained by replacing EI/p' by D_{11}/p (see page 96). For the plate under consideration $D_{11} = 45.30\,\mathrm{N \cdot m}$ and $L_x = 0.2\,\mathrm{m}$, and we have

$$\widetilde{w} = \frac{5}{384}\frac{p L_x^4}{D_{11}} = 0.0230\ \mathrm{m} = 23.0\ \mathrm{mm}. \tag{4.30}$$

The bending moments are (Eq. 3.27)

$$M_x = D_{11}\kappa_x + D_{12}\kappa_y + D_{16}\kappa_{xy} \tag{4.31}$$

$$M_y = D_{12}\kappa_x + D_{22}\kappa_y + D_{26}\kappa_{xy}. \tag{4.32}$$

For a long plate κ_y and κ_{xy} are zero (Eq. 4.20), and M_x and M_y are

$$M_x = D_{11}\kappa_x \qquad M_y = D_{12}\kappa_x. \tag{4.33}$$

The maximum bending moment M_x, which arises at $L_x/2$, is (see Table 7.3, page 332)

$$M_x = \frac{p L_x^2}{8} = 250.00\ \frac{\mathrm{N \cdot m}}{\mathrm{m}}. \tag{4.34}$$

From Eqs. (4.33) and (4.34) we have

$$\kappa_x = \frac{M_x}{D_{11}} = 5.52\ \frac{1}{\mathrm{m}}. \tag{4.35}$$

From Eqs. (4.33) and (4.34) the maximum bending moment M_y (at $L_x/2$) is

$$M_y = D_{12}\kappa_x = \underbrace{\frac{D_{12}}{D_{11}}}_{0.431} M_x = 107.75\ \frac{\mathrm{N \cdot m}}{\mathrm{m}}. \tag{4.36}$$

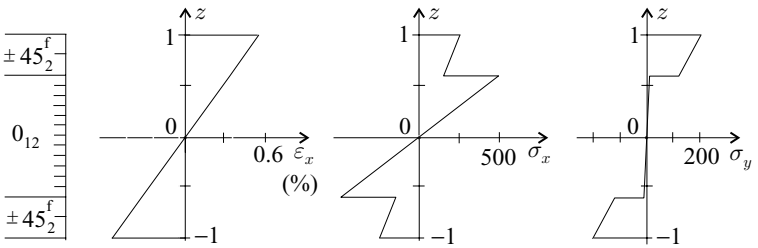

Figure 4.6: The nonzero strains and stresses across the thickness of the plate at $L_x/2$ in Example 4.1. The unit of σ is 10^6 N/m^2.

For the long plate ($\kappa_y = \kappa_{xy} = 0$) the strains at $L_x/2$ are (Eq. 3.7)

$$\begin{aligned} \epsilon_x &= \kappa_x z = 5.52z \\ \epsilon_y &= 0 \\ \gamma_{xy} &= 0. \end{aligned} \tag{4.37}$$

The strain distribution at $L_x/2$ is shown in Figure 4.6. The stresses are calculated by (Eq. 3.11)

$$\begin{Bmatrix} \sigma_x \\ \sigma_y \\ \tau_{xy} \end{Bmatrix} = \begin{bmatrix} \overline{Q}_{11} & \overline{Q}_{12} & \overline{Q}_{16} \\ \overline{Q}_{12} & \overline{Q}_{22} & \overline{Q}_{26} \\ \overline{Q}_{16} & \overline{Q}_{26} & \overline{Q}_{66} \end{bmatrix} \begin{Bmatrix} \epsilon_x \\ \epsilon_y \\ \gamma_{xy} \end{Bmatrix}. \tag{4.38}$$

The stiffness matrices for the fabric and for the unidirectional layer are given by Eqs. (3.65) and (3.66). The stresses in the top layer (where $z = h/2 = 0.001$ m) at $L_x/2$ are

$$\begin{Bmatrix} \sigma_x \\ \sigma_y \\ \tau_{xy} \end{Bmatrix} = \begin{bmatrix} \overline{Q}_{11} \\ \overline{Q}_{12} \\ \overline{Q}_{16} \end{bmatrix} \epsilon_x = \begin{bmatrix} 45.65 \\ 36.55 \\ 0 \end{bmatrix} 10^9 \times 5.52 \times 0.001 = \begin{bmatrix} 251.95 \\ 201.73 \\ 0 \end{bmatrix} 10^6 \frac{\text{N}}{\text{m}^2}. \tag{4.39}$$

The stresses in the other layers are calculated similarly. The results are shown in Figure 4.6.

Unsymmetrical layup. The layup of the plate is unsymmetrical. One of the long edges must be restrained along the lengthwise direction. With the plate thus restrained, the strain in the longitudinal y direction is zero throughout the plate:

$$\epsilon_y^{\text{o}} = 0. \tag{4.40}$$

Furthermore, we take the shear force N_{xy} to be zero:

$$N_{xy} = 0. \tag{4.41}$$

Equation (4.41) is valid when one of the long edges of the plate is free to move in the lengthwise y direction. It is only an approximation when the lengthwise motion

of both long edges of the plate is restricted, as in the top three configurations of Figure 4.3.

By substituting Eqs. (4.20), (4.40), and (4.41) into the third and fourth expressions of Eq. (4.3), we obtain

$$\begin{Bmatrix} 0 \\ M_x \end{Bmatrix} = \begin{bmatrix} A_{16} & A_{66} & B_{16} \\ B_{11} & B_{16} & D_{11} \end{bmatrix} \begin{Bmatrix} \epsilon_x^{\mathrm{o}} \\ \gamma_{xy}^{\mathrm{o}} \\ \kappa_x \end{Bmatrix}. \tag{4.42}$$

We now select a reference plane at a distance ϱ from the midplane (Fig. 3.14). The strain components and the stiffnesses referred to this reference plane are identified by the superscript ϱ. (The curvature and the M_x component of the moment are independent of the position of the reference plane and thus do not need to be identified by the superscript ϱ.) For the new reference plane Eq. (4.42) is written as

$$\begin{Bmatrix} 0 \\ M_x \end{Bmatrix} = \begin{bmatrix} A_{16}^{\varrho} & A_{66}^{\varrho} & B_{16}^{\varrho} \\ B_{11}^{\varrho} & B_{16}^{\varrho} & D_{11}^{\varrho} \end{bmatrix} \begin{Bmatrix} \epsilon_x^{\mathrm{o},\varrho} \\ \gamma_{xy}^{\mathrm{o},\varrho} \\ \kappa_x \end{Bmatrix}. \tag{4.43}$$

The first row of this equation gives

$$\gamma_{xy}^{\mathrm{o},\varrho} = -\epsilon_x^{\mathrm{o},\varrho} \frac{A_{16}^{\varrho}}{A_{66}^{\varrho}} - \kappa_x \frac{B_{16}^{\varrho}}{A_{66}^{\varrho}}. \tag{4.44}$$

Substitution of Eq. (4.44) into the second row of Eq. (4.43) yields

$$M_x = \left(B_{11}^{\varrho} - \frac{A_{16}^{\varrho} B_{16}^{\varrho}}{A_{66}^{\varrho}} \right) \epsilon_x^{\mathrm{o},\varrho} + \left(D_{11}^{\varrho} - \frac{B_{16}^{\varrho 2}}{A_{66}^{\varrho}} \right) \kappa_x. \tag{4.45}$$

In general, the bending moment M_x depends both on $\epsilon_x^{\mathrm{o},\varrho}$ and κ_x. However, there is a reference plane for which the term in the parentheses in front of $\epsilon_x^{\mathrm{o},\varrho}$ is zero:

$$B_{11}^{\varrho} - \frac{A_{16}^{\varrho} B_{16}^{\varrho}}{A_{66}^{\varrho}} = 0. \tag{4.46}$$

We recall that the stiffnesses in the midplane (Reference Plane 1) and the new reference plane (Reference Plane 2) are related by (Eq. 3.47)

$$\begin{aligned} A_{ij}^{\varrho} &= A_{ij} \\ B_{ij}^{\varrho} &= B_{ij} - \varrho A_{ij} \\ D_{ij}^{\varrho} &= D_{ij} - 2\varrho B_{ij} + \varrho^2 A_{ij}. \end{aligned} \tag{4.47}$$

Equations (4.46) and (4.47) give

$$B_{11} - \frac{A_{16} B_{16}}{A_{66}} - \varrho \left(A_{11} - \frac{A_{16}^2}{A_{66}} \right) = 0. \tag{4.48}$$

By rearranging this equation, we obtain the position of the reference plane where Eq. (4.46) is satisfied:

$$\varrho = \frac{B_{11} - \frac{A_{16}B_{16}}{A_{66}}}{A_{11} - \frac{A_{16}^2}{A_{66}}}. \tag{4.49}$$

For a reference plane at ϱ distance from the midplane, the moment M_x depends only on κ_x as follows:

$$M_x = \left[D_{11}^{\varrho} - \frac{\left(B_{16}^{\varrho}\right)^2}{A_{66}^{\varrho}} \right] \kappa_x. \tag{4.50}$$

Equations (4.50) and (4.24), together with Eq. (4.2), yield the following equilibrium equation for an anisotropic long plate:

$$\frac{d^4 w^{\mathrm{o}}}{dx^4} - \frac{p}{\Psi} = 0 \qquad \begin{array}{l} \text{long plate} \\ \text{unsymmetrical layup,} \end{array} \tag{4.51}$$

where the symbol Ψ is the bending stiffness parameter

$$\Psi = D_{11}^{\varrho} - \frac{\left(B_{16}^{\varrho}\right)^2}{A_{66}^{\varrho}}. \tag{4.52}$$

By using Eq. (4.47), Ψ may be written as

$$\Psi = D_{11} - 2\varrho B_{11} + \varrho^2 A_{11} - \frac{\left(B_{16} - \varrho A_{16}\right)^2}{A_{66}}, \tag{4.53}$$

where ϱ is given by Eq. (4.49).

By comparing Eqs. (4.51) and (4.27), we again observe that the equations governing the deflections of long plates and isotropic beams are similar. Therefore, the deflection of a long plate with unsymmetrical layup can be obtained by replacing EI/p' by Ψ/p in the expression given for the deflection of the corresponding isotropic beam.

4.2.3 Simply Supported Plates – Symmetrical Layup

We consider a rectangular plate with dimensions L_x and L_y simply supported along its four edges (Fig. 4.7). The layup of the plate is symmetrical and $[B] = [0]$. The plate is subjected to a uniformly distributed load p.

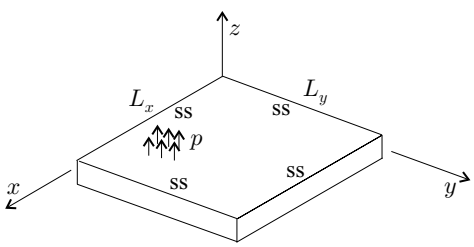

Figure 4.7: Rectangular simply supported (ss) plate subjected to a uniformly distributed transverse load.

Following Whitney,[11] we analyze the deflection of this plate by the energy method. For a simply supported plate (symmetrical layup) subjected to out-of-plane loads only, the in-plane strains in the midplane are zero, and Eq. (4.13) simplifies to

$$U = \frac{1}{2}\int_0^{L_x}\int_0^{L_y} \{\kappa_x \quad \kappa_y \quad \kappa_{xy}\} \begin{bmatrix} D_{11} & D_{12} & D_{16} \\ D_{12} & D_{22} & D_{26} \\ D_{16} & D_{26} & D_{66} \end{bmatrix} \begin{Bmatrix} \kappa_x \\ \kappa_y \\ \kappa_{xy} \end{Bmatrix} dydx. \tag{4.54}$$

By using the relationships between the curvatures and the deflections given by Eq. (4.2), we obtain

$$U = \frac{1}{2}\int_0^{L_x}\int_0^{L_y} \left[D_{11}\left(\frac{\partial^2 w^{\mathrm{o}}}{\partial x^2}\right)^2 + D_{22}\left(\frac{\partial^2 w^{\mathrm{o}}}{\partial y^2}\right)^2 + D_{66}\left(\frac{2\partial^2 w^{\mathrm{o}}}{\partial x \partial y}\right)^2 + 2\left(D_{12}\frac{\partial^2 w^{\mathrm{o}}}{\partial x^2}\frac{\partial^2 w^{\mathrm{o}}}{\partial y^2} + D_{16}\frac{\partial^2 w^{\mathrm{o}}}{\partial x^2}\frac{2\partial^2 w^{\mathrm{o}}}{\partial x \partial y} + D_{26}\frac{\partial^2 w^{\mathrm{o}}}{\partial y^2}\frac{2\partial^2 w^{\mathrm{o}}}{\partial x \partial y} \right) \right] dydx. \tag{4.55}$$

For the applied transverse load p (per unit area) the potential of the external forces is (Eq. 2.203)

$$\Omega = -\int_0^{L_x}\int_0^{L_y} (pw^{\mathrm{o}}) dydx. \tag{4.56}$$

We use the Ritz method and select an expression for the deflection that satisfies the geometrical boundary conditions. For the simply supported plate under consideration the geometrical boundary conditions require that the deflection be zero along the edges (see Eq. 4.8) as follows:

$$w^{\mathrm{o}} = 0 \quad \text{at} \quad \begin{cases} x = 0 & \text{and} \quad 0 \le y \le L_y \\ x = L_x & \text{and} \quad 0 \le y \le L_y \\ 0 \le x \le L_x & \text{and} \quad y = 0 \\ 0 \le x \le L_x & \text{and} \quad y = L_y\,. \end{cases} \tag{4.57}$$

The following deflection satisfies these conditions:

$$w^{\mathrm{o}} = \sum_{i=1}^{I}\sum_{j=1}^{J} w_{ij} \sin\frac{i\pi x}{L_x} \sin\frac{j\pi y}{L_y}, \tag{4.58}$$

where I and J are the number of terms, chosen arbitrarily, for the summations and w_{ij} are constants and are calculated from the principle of stationary potential energy (Eq. 2.206) expressed as

$$\frac{\partial \pi_{\mathrm{p}}}{\partial w_{ij}} = \frac{\partial\,(U + \Omega)}{\partial w_{ij}} = 0. \tag{4.59}$$

[11] J. M. Whitney, *Structural Analysis of Laminated Anisotropic Plates*. Technomic, Lancaster, Pennsylvania, 1987, p. 133.

We now substitute w^{o} (from Eq. 4.58) into the expressions of U and Ω (Eqs. 4.55 and 4.56) and perform the differentiations indicated above. Lengthy but straightforward algebraic manipulations result in the following system of simultaneous algebraic equations:

$$\sum_{i=1}^{I}\sum_{j=1}^{J} G_{mnij}\, w_{ij} = p_{mn} \quad \begin{cases} i, m = 1, 2, 3, \ldots, I \\ j, n = 1, 2, 3, \ldots, J\,. \end{cases} \tag{4.60}$$

For convenience, we introduce the contracted notation

$$k = (i-1)J + j \quad \begin{cases} i = 1, 2, 3, \ldots, I \\ j = 1, 2, 3, \ldots, J \end{cases} \tag{4.61}$$

$$l = (m-1)J + n \quad \begin{cases} m = 1, 2, 3, \ldots, I \\ n = 1, 2, 3, \ldots, J\,. \end{cases} \tag{4.62}$$

Equation (4.60) may now be written as

$$\sum_{k=1}^{I\times J} G_{kl}\, w_k = p_l \quad l = 1, 2, 3, \ldots, I \times J, \tag{4.63}$$

where G_{kl} $(= G_{lk})$ is given in Table 4.1 and, for a uniformly distributed load, p_l is

$$p_l = \begin{cases} \frac{4pL_xL_y}{\pi^2 mn} & \text{if } m \text{ and } n \text{ are odd} \\ 0 & \text{if } m \text{ or } n \text{ is even} \end{cases}. \tag{4.64}$$

Table 4.1. The elements of the matrix [G]

$$G_{lk} = \tfrac{1}{4}L_xL_y\pi^4\left[D_{11}\left(\tfrac{i}{L_x}\right)^4 + 2\left(D_{12}+2D_{66}\right)\left(\tfrac{i}{L_x}\right)^2\left(\tfrac{j}{L_y}\right)^2 + D_{22}\left(\tfrac{j}{L_y}\right)^4\right]\delta_{lk}$$

$$-2L_xL_y\pi^4 D_{16}\left[\left(\tfrac{i}{L_x}\right)^2\left(\tfrac{m}{L_x}\right)\left(\tfrac{n}{L_y}\right)r_{im}r_{jn} + \left(\tfrac{m}{L_x}\right)^2\left(\tfrac{i}{L_x}\right)\left(\tfrac{j}{L_y}\right)r_{mi}r_{nj}\right]$$

$$-2L_xL_y\pi^4 D_{26}\left[\left(\tfrac{j}{L_y}\right)^2\left(\tfrac{m}{L_x}\right)\left(\tfrac{n}{L_y}\right)r_{im}r_{jn} + \left(\tfrac{n}{L_y}\right)^2\left(\tfrac{i}{L_x}\right)\left(\tfrac{j}{L_y}\right)r_{mi}r_{nj}\right]$$

$$\delta_{lk} = \begin{cases} 1 & \text{if } k = l \\ 0 & \text{if } k \neq l \end{cases}$$

$$r_{ij} = \begin{cases} \frac{2i}{i^2-j^2}\frac{1}{\pi} & \text{if } (i-j) \text{ is odd} \\ 0 & \text{if } (i-j) \text{ is even} \end{cases}$$

$$k = (i-1)J + j \begin{cases} i = 1, 2, 3, \ldots, I \\ j = 1, 2, 3, \ldots, J \end{cases}$$

$$l = (m-1)J + n \begin{cases} m = 1, 2, 3, \ldots, I \\ n = 1, 2, 3, \ldots, J \end{cases}$$

In expanded form, Eq. (4.63) is

$$\begin{bmatrix} G_{11} & G_{12} & \dots & G_{1(I\times J)} \\ G_{21} & G_{22} & & \\ \vdots & & \ddots & \\ G_{(I\times J)1} & & & G_{(I\times J)(I\times J)} \end{bmatrix} \begin{Bmatrix} w_1 \\ w_2 \\ \vdots \\ w_{(I\times J)} \end{Bmatrix} = \begin{Bmatrix} p_1 \\ p_2 \\ \vdots \\ p_{(I\times J)} \end{Bmatrix}. \tag{4.65}$$

By inverting this equation, we obtain the coefficients w_k

$$\begin{Bmatrix} w_1 \\ w_2 \\ \vdots \\ w_{(I\times J)} \end{Bmatrix} = \begin{bmatrix} G_{11} & G_{12} & \dots & G_{1(I\times J)} \\ G_{21} & G_{22} & & \\ \vdots & & \ddots & \\ G_{(I\times J)1} & & & G_{(I\times J)(I\times J)} \end{bmatrix}^{-1} \begin{Bmatrix} p_1 \\ p_2 \\ \vdots \\ p_{(I\times J)} \end{Bmatrix}. \tag{4.66}$$

From Eqs. (4.2), (3.27), and (4.58) the moments are

$$\begin{Bmatrix} M_x \\ M_y \\ M_{xy} \end{Bmatrix} = [D] \begin{Bmatrix} \kappa_x \\ \kappa_y \\ \kappa_{xy} \end{Bmatrix} = [D] \begin{Bmatrix} \sum_{i=1}^{I}\sum_{j=1}^{J} w_{ij}\left(\frac{i\pi}{L_x}\right)^2 \sin\frac{i\pi x}{L_x}\sin\frac{j\pi y}{L_y} \\ \sum_{i=1}^{I}\sum_{j=1}^{J} w_{ij}\left(\frac{j\pi}{L_y}\right)^2 \sin\frac{i\pi x}{L_x}\sin\frac{j\pi y}{L_y} \\ -\sum_{i=1}^{I}\sum_{j=1}^{J} w_{ij} 2\frac{i\pi}{L_x}\frac{j\pi}{L_y}\cos\frac{i\pi x}{L_x}\cos\frac{j\pi y}{L_y} \end{Bmatrix}. \tag{4.67}$$

For an orthotropic plate $D_{16} = D_{26} = 0$, and Eq. (4.66) becomes

$$w_k = w_{ij} = \frac{16p}{\pi^6 ij\left[D_{11}\left(\frac{i}{L_x}\right)^4 + 2\left(D_{12} + 2D_{66}\right)\left(\frac{i}{L_x}\right)^2\left(\frac{j}{L_y}\right)^2 + D_{22}\left(\frac{j}{L_y}\right)^4\right]}, \tag{4.68}$$

where $i, j = 1, 3, 5, \dots$ ($w_k = w_{ij} = 0$ when i or $j = 2, 4, 6, \dots$).

Once the deflections are known, the moments can be calculated by Eq. (4.67).

4.2 Example. *A* 0.7*-m-long and* 0.2*-m-wide rectangular plate is made of graphite epoxy. The material properties are given in Table 3.6 (page 81). The layup is* $[\pm 45_2^{\mathrm{f}}/0_{12}/\pm 45_2^{\mathrm{f}}]$. *The 0-degree plies are parallel to the short edge of the plate. The plate is simply supported along all four edges and is subjected to a uniformly distributed transverse load* $p = 50\,000$ *N/m*^{2} *(Fig. 4.8). Calculate the maximum deflection and the maximum bending moments.*

Solution. The deflection of the plate is (Eq. 4.58)

$$w^{\mathrm{o}} = \sum_{i=1}^{I}\sum_{j=1}^{J} w_{ij} \sin\frac{i\pi x}{L_x}\sin\frac{j\pi y}{L_y}. \tag{4.69}$$

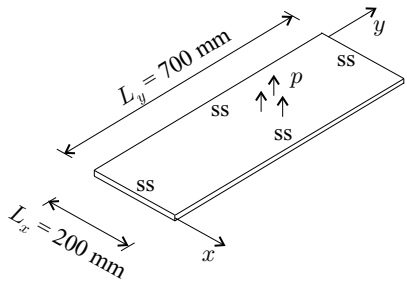

Figure 4.8: The plate in Example 4.2.

The plate is orthotropic, and the bending stiffnesses are (Table 3.7, page 84) $D_{11} = 45.30$ N · m, $D_{22} = 25.26$ N · m, $D_{12} = 19.52$ N · m, $D_{66} = 20.62$ N · m). The maximum deflection occurs at the center of the plate, where $x = L_x/2 = 0.1$ m and $y = L_y/2 = 0.35$ m. From Eq. (4.68), $w_{ij} \times 10^3$ are

$i \backslash j$	1	2	3	4	5	6	7
1	24.0389	0	2.9945	0	0.6683	0	0.2033
2	0	0	0	0	0	0	0
3	0.1181	0	0.0330	0	0.0148	0	0.0075
4	0	0	0	0	0	0	0
5	0.0093	0	0.0029	0	0.0015	0	0.0009
6	0	0	0	0	0	0	0
7	0.0017	0	0.0006	0	0.0003	0	0.0002 .

At the center of the plate the deflection is

$$w^{\mathrm{o}} = \sum_{i=1}^{7} \sum_{j=1}^{7} w_{ij} \sin \frac{i\pi}{2} \sin \frac{j\pi}{2}. \tag{4.70}$$

We chose to perform the summation up to $i = j = 7$. For $i,\ j = 2, 4, 6$, the sine is zero; for $i,\ j = 1, 5$ the sine is unity, and for $i,\ j = 3, 7$ the sine is minus one. The resulting deflection at the midpoint is

$$w^{\mathrm{o}} = 0.0214 \text{ m} = 21.4 \text{ mm}. \tag{4.71}$$

We now assess the length-to-width ratios under which the long-plate approximation is reasonable. To this end, we calculated the maximum deflections of the plate, keeping the width L_x the same while changing the length L_y. In Figure 4.9 we plot the maximum deflections thus calculated versus L_y. In this figure we also included the deflection given by the long-plate approximation (Eq. 4.30). The results in this figure show that, in accordance with Eq. (4.19), the long-plate formula approximates the deflection well (within 8 percent) when L_y is greater than $3L_x\sqrt[4]{D_{11}/D_{22}} = 0.694$ m.

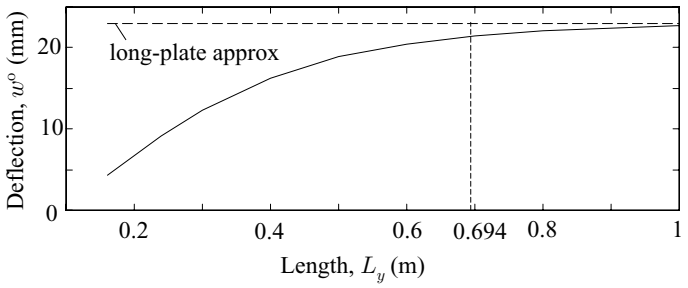

Figure 4.9: Maximum deflection of the plate in Example 4.2 as a function of the plate length.

The bending moments at the center of the plate are (Eq. 4.67)

$$\begin{Bmatrix} M_x \\ M_y \end{Bmatrix} = \begin{bmatrix} D_{11} & D_{12} \\ D_{12} & D_{22} \end{bmatrix} \begin{Bmatrix} \sum_{i=1}^{7}\sum_{j=1}^{7} w_{ij} \left(\frac{i\pi}{L_x}\right)^2 \sin\frac{i\pi}{2}\sin\frac{j\pi}{2} \\ \sum_{i=1}^{7}\sum_{j=1}^{7} w_{ij} \left(\frac{j\pi}{L_y}\right)^2 \sin\frac{i\pi}{2}\sin\frac{j\pi}{2} \end{Bmatrix}$$
$$= \begin{Bmatrix} 233.94 \\ 102.18 \end{Bmatrix} \frac{\text{N}\cdot\text{m}}{\text{m}}. \tag{4.72}$$

The twist moment at the corner of the plate ($x = y = 0$) is (Eq. 4.67)

$$M_{xy} = -D_{66} \sum_{i=1}^{7}\sum_{j=1}^{7} w_{ij} 2 \frac{i\pi}{L_x}\frac{j\pi}{L_y} \cos\frac{i\pi x}{L_x}\cos\frac{j\pi y}{L_y}$$
$$= -D_{66} \sum_{i=1}^{7}\sum_{j=1}^{7} w_{ij} 2 \frac{i\pi}{L_x}\frac{j\pi}{L_y} = -113.43 \frac{\text{N}\cdot\text{m}}{\text{m}}. \tag{4.73}$$

4.3 Example. *A 0.2-m-long and 0.2-m-wide rectangular plate is made of graphite epoxy unidirectional plies. The material properties are given in Table 3.6 (page 81). The layup is* $[0_2/45_2/90_2/-45_2]_s$. *The plate, simply supported along the four edges (Fig. 4.10), is subjected to a uniformly distributed transverse load* $p = 50\,000$ *N/m*^{2}. *Calculate the maximum deflection and the maximum moments.*

Solution. The layup of the plate is symmetrical but is not orthotropic. The bending stiffnesses are $D_{11} = 34.61$ N·m, $D_{22} = 12.34$ N·m, $D_{12} = 4.58$ N·m,

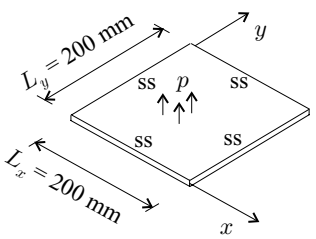

Figure 4.10: The plate in Example 4.3.

Table 4.2. The maximum deflection and the maximum bending and twist moments calculated by the numerical solution and by the orthotropic approximation for the plate in Example 4.3

	w^o	M_x	M_y	M_{xy} $x = y = 0$	M_{xy} $x = L_x,\ y = 0$
	mm			N · m/m	
numerical	17.60	160.65	64.53	−69.28	36.47
orthotropic approximation	16.93	154.07	63.21	−49.56	49.56

$D_{66} = 5.14$ N · m, $D_{16} = 3.34$ N · m, $D_{26} = 3.34$ N · m (Table 3.7, page 84). The maximum deflection and the maximum bending and twist moments must be calculated from Eqs. (4.58), (4.64), (4.66), and (4.67). With the preceding stiffnesses the calculations yield the results given in Table 4.2 (first row).

The layup follows the 10-percent rule (page 89), and we treat the plate as orthotropic. The deflection of the plate is (Eq. 4.58)

$$w^{\mathrm{o}} = \sum_{i=1}^{I} \sum_{j=1}^{J} w_{ij} \sin \frac{i\pi x}{L_x} \sin \frac{j\pi y}{L_y}. \tag{4.74}$$

Since the plate is treated as orthotropic $D_{16} = D_{26} = 0$, and the relevant bending stiffnesses are $D_{11} = 34.61$ N · m, $D_{22} = 12.34$ N · m, $D_{12} = 4.58$ N · m, $D_{66} = 5.14$ N · m (Table 3.7, page 84). The maximum deflection occurs at the center of the plate, where $x = L_x/2 = 0.1$ m and $y = L_y/2 = 0.1$ m. From Eq. (4.68) $w_{ij} \times 10^3$ are

$i \backslash j$	1	2	3	4	5	6	7
1	17.3628	0	0.3409	0	0.0314	0	0.0061
2	0	0	0	0	0	0	0
3	0.1439	0	0.0238	0	0.0052	0	0.0014
4	0	0	0	0	0	0	0
5	0.0119	0	0.0030	0	0.0011	0	0.0004
6	0	0	0	0	0	0	0
7	0.0022	0	0.0007	0	0.0003	0	0.0001

At the center of the plate the deflection is

$$w^{\mathrm{o}} = \sum_{i=1}^{7} \sum_{j=1}^{7} w_{ij} \sin \frac{i\pi}{2} \sin \frac{j\pi}{2}. \tag{4.75}$$

We perform the summation up to $i = j = 7$. For $i, j = 2, 4, 6$ the sine is zero, for $i, j = 1, 5$ the sine is unity, and for $i, j = 3, 7$ the sine is minus one. Thus, the resulting deflection at the center of the plate is

$$w^{\mathrm{o}} = 0.01693 \text{ m} = 16.93 \text{ mm}. \tag{4.76}$$

The bending moments at the center of the plate are (Eq. 4.67)

$$\begin{Bmatrix} M_x \\ M_y \end{Bmatrix} = \begin{bmatrix} D_{11} & D_{12} \\ D_{12} & D_{22} \end{bmatrix} \begin{Bmatrix} \sum_{i=1}^{7}\sum_{j=1}^{7} w_{ij}\left(\frac{i\pi}{L_x}\right)^2 \sin\frac{i\pi}{2}\sin\frac{j\pi}{2} \\ \sum_{i=1}^{7}\sum_{j=1}^{7} w_{ij}\left(\frac{j\pi}{L_y}\right)^2 \sin\frac{i\pi}{2}\sin\frac{j\pi}{2} \end{Bmatrix}$$

$$= \begin{Bmatrix} 154.07 \\ 63.21 \end{Bmatrix} \frac{\mathrm{N}\cdot\mathrm{m}}{\mathrm{m}}. \tag{4.77}$$

The twist moment at the corner of the plate ($x = y = 0$) is (Eq. 4.67)

$$M_{xy} = -D_{66}\sum_{i=1}^{7}\sum_{j=1}^{7} 2w_{ij}\frac{i\pi}{L_x}\frac{j\pi}{L_y}\cos\frac{i\pi x}{L_x}\cos\frac{j\pi y}{L_y}$$

$$= -D_{66}\sum_{i=1}^{7}\sum_{j=1}^{7} 2w_{ij}\frac{i\pi}{L_x}\frac{j\pi}{L_y} = -49.56\frac{\mathrm{N}\cdot\mathrm{m}}{\mathrm{m}}. \tag{4.78}$$

The maximum deflection and the maximum moments thus calculated are included in Table 4.2 (second row). The maximum bending moments and the maximum deflections calculated by the numerical method and the orthotropic approximation are in close agreement, but the maximum twist moments differ significantly.

4.2.4 Plates with Built-In Edges – Orthotropic and Symmetrical Layup

We consider a rectangular plate with length L_x and width L_y built-in along its four edges (Fig. 4.11). The layup is orthotropic and symmetrical. The plate is subjected to a uniformly distributed load p.

The potential energy of the plate is obtained from Eqs. (4.55) and (4.56) by setting D_{16} and D_{26} equal to zero:

$$\pi_\mathrm{p} = U + \Omega = \frac{1}{2}\int_0^{L_x}\int_0^{L_y}\left[D_{11}\left(\frac{\partial^2 w^\mathrm{o}}{\partial x^2}\right)^2 + D_{22}\left(\frac{\partial^2 w^\mathrm{o}}{\partial y^2}\right)^2 + D_{66}\left(\frac{2\partial^2 w^\mathrm{o}}{\partial x\partial y}\right)^2 + 2D_{12}\frac{\partial^2 w^\mathrm{o}}{\partial x^2}\frac{\partial^2 w^\mathrm{o}}{\partial y^2} - pw^\mathrm{o}\right]dydx. \tag{4.79}$$

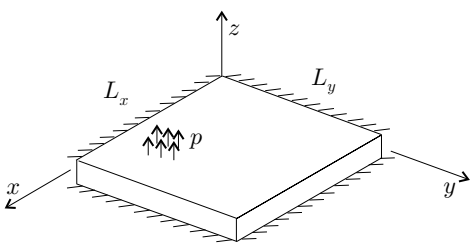

Figure 4.11: Rectangular plate with built-in edges.

The moments at a point x, y are (Eqs. 4.2 and 3.27)

$$\begin{aligned} M_x &= -D_{11}\frac{\partial^2 w^{\mathrm{o}}}{\partial x^2} - D_{12}\frac{\partial^2 w^{\mathrm{o}}}{\partial y^2} \\ M_y &= -D_{12}\frac{\partial^2 w^{\mathrm{o}}}{\partial x^2} - D_{22}\frac{\partial^2 w^{\mathrm{o}}}{\partial y^2} \\ M_{xy} &= -D_{66}\frac{2\partial^2 w^{\mathrm{o}}}{\partial x \partial y}, \end{aligned} \tag{4.80}$$

where w^{o} is the deflection and D_{11}, D_{12}, D_{22}, D_{66} are the elements of the stiffness matrix in the x–y coordinate system.

The displacements and moments can be calculated when the plate's bending stiffnesses satisfy the following Huber orthotropy relationship[12] (see Eq. 4.153 with $K = 1$):

$$D_{66} = \frac{1}{2}\left(\sqrt{D_{11}D_{22}} - D_{12}\right). \tag{4.81}$$

Although this relationship may not hold exactly, we adopt it for calculating the displacements and the moments. Possible errors introduced by this relationship are discussed on page 111.

We introduce the variable

$$x' = \frac{x}{\alpha}, \tag{4.82}$$

where α is a constant defined as

$$\alpha = \sqrt[4]{\frac{D_{11}}{D_{22}}}. \tag{4.83}$$

Equations (4.79)–(4.83) yield the potential energy and the moments (per unit length) as follows:

$$\begin{aligned} \pi_{\mathrm{p}} = \frac{1}{2}\int_0^{L_x/\alpha}\int_0^{L_y} D_{22}\Bigg[&\left(\frac{\partial^2 w^{\mathrm{o}}}{\partial x'^2}\right)^2 + \left(\frac{\partial^2 w^{\mathrm{o}}}{\partial y^2}\right)^2 + \frac{1}{2}\left(1 - \sqrt{\frac{D_{12}^2}{D_{11}D_{22}}}\right)\left(\frac{2\partial^2 w^{\mathrm{o}}}{\partial x' \partial y}\right)^2 \\ &+ 2\sqrt{\frac{D_{12}^2}{D_{11}D_{22}}}\quad \frac{\partial^2 w^{\mathrm{o}}}{\partial x'^2}\frac{\partial^2 w^{\mathrm{o}}}{\partial y^2} - pw^{\mathrm{o}}\Bigg] dy dx' \end{aligned} \tag{4.84}$$

$$\begin{aligned} M_x &= \alpha^2\left[-D_{22}\frac{\partial^2 w^{\mathrm{o}}}{\partial x'^2} - \sqrt{\frac{D_{12}^2}{D_{11}D_{22}}}\quad \left(D_{22}\frac{\partial^2 w^{\mathrm{o}}}{\partial y^2}\right)\right] \\ M_y &= \left[-\sqrt{\frac{D_{12}^2}{D_{11}D_{22}}}\quad \left(D_{22}\frac{\partial^2 w^{\mathrm{o}}}{\partial x'^2}\right) - D_{22}\frac{\partial^2 w^{\mathrm{o}}}{\partial y^2}\right] \\ M_{xy} &= \alpha\left[-D_{22}\frac{1}{2}\left(1 - \sqrt{\frac{D_{12}^2}{D_{11}D_{22}}}\right)\frac{2\partial^2 w^{\mathrm{o}}}{\partial x' \partial y}\right]. \end{aligned} \tag{4.85}$$

[12] S. P. Timoshenko and S. Woinowsky-Krieger, *Theory of Plates and Shells*. 2nd edition. McGraw-Hill, New York, 1959, p. 366.

We now consider a rectangular isotropic plate with dimensions L'_x and L_y. The potential energy and the moments (per unit length) of an isotropic plate are obtained by substituting into Eqs. (4.79) and (4.80) $D_{11} = D_{22} = D^{\text{iso}}$, $D_{12} = \nu^{\text{iso}} D^{\text{iso}}$, and $D_{66} = D^{\text{iso}}(1 - \nu^{\text{iso}})/2$ (see Eq. 3.41). In the x', y coordinate system the results are

$$\pi_{\text{p}}^{\text{iso}} = \frac{1}{2}\int_0^{L'_x}\int_0^{L_y} D^{\text{iso}}\left[\left(\frac{\partial^2 w^{\text{iso}}}{\partial x'^2}\right)^2 + \left(\frac{\partial^2 w^{\text{iso}}}{\partial y^2}\right)^2 + \frac{1}{2}\left(1-\nu^{\text{iso}}\right)\left(\frac{2\partial^2 w^{\text{iso}}}{\partial x'\partial y}\right)^2 + 2\nu^{\text{iso}}\frac{\partial^2 w^{\text{iso}}}{\partial x'^2}\frac{\partial^2 w^{\text{iso}}}{\partial y^2} - p w^{\text{iso}}\right] dy dx' \tag{4.86}$$

$$M_{x'}^{\text{iso}} = -D^{\text{iso}}\frac{\partial^2 w^{\text{iso}}}{\partial x'^2} - \nu^{\text{iso}} D^{\text{iso}}\frac{\partial^2 w^{\text{iso}}}{\partial y^2}$$

$$M_y^{\text{iso}} = -\nu^{\text{iso}} D^{\text{iso}}\frac{\partial^2 w^{\text{iso}}}{\partial x'^2} - D^{\text{iso}}\frac{\partial^2 w^{\text{iso}}}{\partial y^2} \tag{4.87}$$

$$M_{x'y}^{\text{iso}} = -D^{\text{iso}}\frac{1-\nu^{\text{iso}}}{2}\frac{2\partial^2 w^{\text{iso}}}{\partial x'\partial y}.$$

The superscript "iso" refers to the isotropic plate.

From Eqs. (4.84) and (4.86) we see that the expressions for the potential energy for the Huber orthotropic plate (with dimensions L_x, L_y and stiffnesses D_{11}, D_{12}, D_{22}) and for an isotropic plate (with dimensions L'_x and L_y) are identical when

$$L'_x = L_x/\alpha \tag{4.88}$$

$$D^{\text{iso}} = D_{22} \qquad \nu^{\text{iso}} = \sqrt{\frac{D_{12}^2}{D_{11}D_{22}}}. \tag{4.89}$$

The deflections of the plate are obtained from the potential energy. Hence, when Eqs. (4.88) and (4.89) are satisfied, the deflection of the orthotropic plate at point x, y is the same as the deflection of the corresponding isotropic plate at point x', y, that is,

$$w^{\text{o}}(x, y) = w^{\text{iso}}(x', y). \tag{4.90}$$

Equations (4.85) and (4.87) show that the moments (per unit length) of a Huber orthotropic plate are related to the moments (per unit length) of the corresponding isotropic plate by

$$M_x(x, y) = \alpha^2 M_{x'}^{\text{iso}}(x', y)$$

$$M_y(x, y) = M_y^{\text{iso}}(x', y) \tag{4.91}$$

$$M_{xy}(x, y) = \alpha M_{x'y}^{\text{iso}}(x', y).$$

By the preceding method, the deflections and moments (per unit length) of an orthotropic plate can be obtained from the deflections and moments

Table 4.3. Maximum deflections and maximum moments of rectangular plates with built-in edges subjected to a uniformly distributed load p ($\nu^{\text{iso}} = 0.3$). The locations P_1, P_2, and P_3 are shown in Figure 4.12.

	$w^{\text{iso}} = \frac{1}{384}\frac{pL_x'^4}{D^{\text{iso}}}c_1$	$M_{x'}^{\text{iso}} = -\frac{pL_x'^2}{12}c_2$	$M_y^{\text{iso}} = -\frac{pL_x'^2}{12}c_3$	$M_{x'}^{\text{iso}} = \frac{pL_x'^2}{24}c_4$	$M_y^{\text{iso}} = \frac{pL_x'^2}{24}c_5$
	at P_1	at P_2	at P_3	at P_1	at P_1
$\frac{L_y}{L_x'}$	c_1	c_2	c_3	c_4	c_5
1.0	0.484	0.616	0.616	0.554	0.554
1.1	0.576	0.697	0.646	0.634	0.554
1.2	0.661	0.767	0.665	0.718	0.547
1.4	0.795	0.871	0.682	0.838	0.509
1.6	0.883	0.936	0.685	0.914	0.463
1.8	0.941	0.974	0.685	0.962	0.418
2.0	0.975	0.995	0.685	0.989	0.379
∞	1.000	1.000	0.685	1.000	0.300

(per unit length) of the corresponding isotropic plate. The calculation steps are as follows.

Step 1. We calculate the equivalent length L_x', stiffness D^{iso}, and Poisson's ratio ν^{iso} of the isotropic plate (width L_y):

$$L_x' = \frac{L_x}{\alpha} \qquad D^{\text{iso}} = D_{22} \qquad \nu^{\text{iso}} = \sqrt{\frac{D_{12}^2}{D_{11}D_{22}}}, \tag{4.92}$$

where

$$\alpha = \sqrt[4]{\frac{D_{11}}{D_{22}}}. \tag{4.93}$$

Step 2. We determine the deflections w^{iso} and moments (per unit length) $M_{x'}^{\text{iso}}$, M_y^{iso}, and $M_{x'y}^{\text{iso}}$ of the "equivalent" isotropic plate. Maximum deflections and maximum bending moments (per unit length) of isotropic plates (width a, length b, bending stiffness D) subjected to a uniformly distributed load are given by Timoshenko and Woinowsky-Krieger.[13] We modified these results and adopted them for Huber orthotropic plates. The resulting maximum deflections and maximum bending moments are given in Table 4.3.

Step 3. The deflection w^{o} and moments (per unit length) M_x, M_y, and M_{xy} of the orthotropic plate are calculated by (Eqs. 4.90 and 4.91)

$$w^{\text{o}} = w^{\text{iso}} \qquad M_x = \alpha^2 M_{x'}^{\text{iso}} \qquad M_y = M_y^{\text{iso}} \qquad M_{xy} = \alpha M_{x'y}^{\text{iso}}. \tag{4.94}$$

[13] Ibid., p. 202.

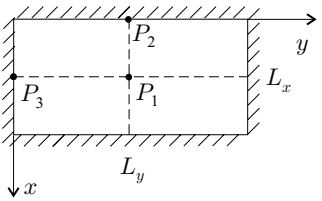

Figure 4.12: Locations where the moments and the deflection are calculated.

The preceding approximate procedure yields the deflections and bending moments of orthotropic plates with built-in edges within about 10 percent.[14]

4.4 Example. *A 0.2-m-long and 0.2-m-wide rectangular plate is made of graphite epoxy unidirectional plies. The material properties are given in Table 3.6 (page 81). The layup is* $[0_2/45_2/90_2/-45_2]_s$ *. The plate, built-in along the four edges (Fig. 4.13), is subjected to a uniformly distributed transverse load* $p = 50\,000$ *N/m*^{2}*. Calculate the maximum deflection and the maximum bending moments.*

Solution. We treat this plate as Huber orthotropic. The bending stiffnesses are $D_{11} = 34.61\ \mathrm{N\cdot m}$, $D_{22} = 12.34\ \mathrm{N\cdot m}$, $D_{12} = 4.58\ \mathrm{N\cdot m}$, $D_{66} = 5.14\ \mathrm{N\cdot m}$ (Table 3.7, page 84). From Eqs. (4.83) and (4.89) we have

$$\alpha = \sqrt[4]{\frac{D_{11}}{D_{22}}} = 1.29\ \mathrm{N\cdot m} \qquad L_x' = \frac{L_x}{\alpha} = 0.155\ \mathrm{m} \tag{4.95}$$

$$D^{\mathrm{iso}} = D_{22} = 12.34\ \mathrm{N\cdot m} \qquad \nu^{\mathrm{iso}} = \sqrt{\frac{D_{12}^2}{D_{11}D_{22}}} = 0.222. \tag{4.96}$$

From Table 4.3 (at $L_y/L_x' = 1.29$) we obtain the constants $c_1 = 0.724$, $c_2 = 0.816$, $c_3 = 0.673$, $c_4 = 0.774$, and $c_5 = 0.529$. With the values of these constants the maximum deflection and the maximum bending moments of the corresponding isotropic plate are (Table 4.3)

$$w^{\mathrm{iso}}\big|_{\text{at } P_1} = \frac{1}{384}\frac{pL_x'^4}{D^{\mathrm{iso}}}c_1 = 0.0044\ \mathrm{m} \tag{4.97}$$

$$M_{x'}^{\mathrm{iso}}\big|_{\text{at } P_2} = -\frac{pL_x'^2}{12}c_2 = -81.21\ \frac{\mathrm{N\cdot m}}{\mathrm{m}} \tag{4.98}$$

$$M_{y}^{\mathrm{iso}}\big|_{\text{at } P_3} = -\frac{pL_x'^2}{12}c_3 = -66.96\ \frac{\mathrm{N\cdot m}}{\mathrm{m}} \tag{4.99}$$

$$M_{x'}^{\mathrm{iso}}\big|_{\text{at } P_1} = \frac{pL_x'^2}{24}c_4 = 38.52\ \frac{\mathrm{N\cdot m}}{\mathrm{m}} \tag{4.100}$$

$$M_{y}^{\mathrm{iso}}\big|_{\text{at } P_1} = \frac{pL_x'^2}{24}c_5 = 26.33\ \frac{\mathrm{N\cdot m}}{\mathrm{m}}. \tag{4.101}$$

[14] I. Veres and L. P. Kollár, Approximate Analysis of Mid-plane Symmetric Rectangular Composite Plates. *Journal of Composite Materials*, Vol 36, 673–684, 2002.

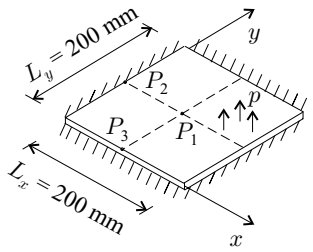

Figure 4.13: The plate in Example 4.4.

The points P_1–P_3 are shown in Figure 4.13. The maximum deflection and the maximum bending moments of the composite plate are (Eq. 4.94)

$$w^{\mathrm{o}}\big|_{\text{at } P_1} = w^{\mathrm{iso}}\big|_{\text{at } P_1} = 0.0044 \text{ m} \tag{4.102}$$

$$M_x|_{\text{at } P_2} = \alpha^2 \, M^{\mathrm{iso}}_{x'}\big|_{\text{at } P_2} = -135.98 \, \frac{\mathrm{N}\cdot\mathrm{m}}{\mathrm{m}} \tag{4.103}$$

$$M_y\big|_{\text{at } P_3} = M^{\mathrm{iso}}_{y}\big|_{\text{at } P_3} = -66.96 \, \frac{\mathrm{N}\cdot\mathrm{m}}{\mathrm{m}} \tag{4.104}$$

$$M^{\mathrm{iso}}_{x'}\big|_{\text{at } P_1} = \alpha^2 \, M^{\mathrm{iso}}_{x'}\big|_{\text{at } P_1} = 64.50 \, \frac{\mathrm{N}\cdot\mathrm{m}}{\mathrm{m}} \tag{4.105}$$

$$M^{\mathrm{iso}}_{y}\big|_{\text{at } P_1} = M^{\mathrm{iso}}_{y}\big|_{\text{at } P_1} = 26.33 \, \frac{\mathrm{N}\cdot\mathrm{m}}{\mathrm{m}}. \tag{4.106}$$

4.3 Buckling of Rectangular Plates

4.3.1 Simply Supported Plates – Symmetrical Layup

We consider a rectangular plate with dimensions L_x and L_y simply supported along its four edges (Fig. 4.14). The layup of the plate is symmetrical, $[B] = [0]$.

The plate is subjected to uniformly distributed in-plane loads N_{x0}, N_{y0}, and N_{xy0} around the edges. These loads are increased proportionally, that is, the loads are λN_{x0}, λN_{y0}, λN_{xy0}, where λ is the load parameter. For a buckled plate the load parameter is denoted by λ_{cr}. Following Whitney,[15] we obtain λ_{cr} by the energy method.

The strain energy is (Eq. 4.55)

$$U = \frac{1}{2}\int_0^{L_x}\int_0^{L_y}\left[D_{11}\left(\frac{\partial^2 w^{\mathrm{o}}}{\partial x^2}\right)^2 + D_{22}\left(\frac{\partial^2 w^{\mathrm{o}}}{\partial y^2}\right)^2 + D_{66}\left(\frac{2\partial^2 w^{\mathrm{o}}}{\partial x \partial y}\right)^2 + 2\left(D_{12}\frac{\partial^2 w^{\mathrm{o}}}{\partial x^2}\frac{\partial^2 w^{\mathrm{o}}}{\partial y^2} + D_{16}\frac{\partial^2 w^{\mathrm{o}}}{\partial x^2}\frac{2\partial^2 w^{\mathrm{o}}}{\partial x \partial y} + D_{26}\frac{\partial^2 w^{\mathrm{o}}}{\partial y^2}\frac{2\partial^2 w^{\mathrm{o}}}{\partial x \partial y}\right)\right] dy dx. \tag{4.107}$$

[15] J. M. Whitney, *Structural Analysis of Laminated Anisotropic Plates.* Technomic, Lancaster, Pennsylvania, 1987, p. 151.

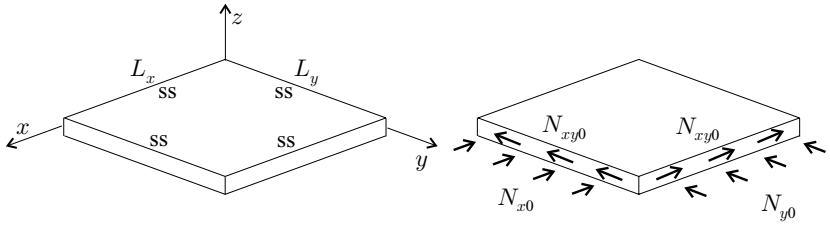

Figure 4.14: Rectangular simply supported (ss) plate subjected to compressive and shear edge loads.

For a plate subjected only to in-plane loads, which do not vary with x and y, the potential of the external forces is[16]

$$\Omega = \frac{1}{2}\int_0^{L_x}\int_0^{L_y}\left[N_x\left(\frac{\partial w^{\mathrm{o}}}{\partial x}\right)^2 + N_y\left(\frac{\partial w^{\mathrm{o}}}{\partial y}\right)^2 + 2N_{xy}\frac{\partial w^{\mathrm{o}}}{\partial x}\frac{\partial w^{\mathrm{o}}}{\partial y}\right]dydx, \quad (4.108)$$

where N_x, N_y, N_{xy} are the in-plane forces (per unit length) inside the plate. These internal in-plane forces are related to the edge loads λN_{x0}, λN_{y0}, λN_{xy0} by

$$N_x = -\lambda N_{x0} \qquad N_y = -\lambda N_{y0} \qquad N_{xy} = -\lambda N_{xy0}. \quad (4.109)$$

We use the Ritz method to obtain the deflection. For the simply supported plate under consideration the geometrical boundary conditions require that the deflection be zero along the edges (Eq. 4.57):

$$w^{\mathrm{o}} = 0 \quad \text{at} \quad \begin{cases} x = 0 & \text{and} \quad 0 \le y \le L_y \\ x = L_x & \text{and} \quad 0 \le y \le L_y \\ 0 \le x \le L_x & \text{and} \quad y = 0 \\ 0 \le x \le L_x & \text{and} \quad y = L_y\,. \end{cases} \quad (4.110)$$

The following deflection satisfies these geometrical boundary conditions:

$$w^{\mathrm{o}} = \sum_{i=1}^{I}\sum_{j=1}^{J} w_{ij}\sin\frac{i\pi x}{L_x}\sin\frac{j\pi y}{L_y}, \quad (4.111)$$

where I and J are the number of terms, chosen arbitrarily, in the summations; w_{ij} are constants and are calculated from the principle of stationary potential energy (Eq. 2.206) expressed as

$$\frac{\partial \pi_{\mathrm{p}}}{\partial w_{ij}} = \frac{\partial\,(U+\Omega)}{\partial w_{ij}} = 0. \quad (4.112)$$

We now substitute w^{o} (from Eq. 4.111) into the expressions of U and Ω (Eqs. 4.107 and 4.108) and perform the differentiation indicated by Eq. (4.112).

[16] S. P. Timoshenko and J. Gere, *Theory of Elastic Stability.* 2nd edition. McGraw-Hill, New York, 1961, p. 349.

Algebraic manipulations result in the following system of simultaneous algebraic equations:

$$\sum_{i=1}^{I}\sum_{j=1}^{J}\left(G_{mnij}-\lambda b_{mnij}\right)w_{ij}=0 \quad \begin{cases} i,m=1,2,3,\ldots,I \\ j,n=1,2,3,\ldots,J. \end{cases} \tag{4.113}$$

For convenience, we introduce the contracted notation

$$k=(i-1)J+j \quad \begin{cases} i=1,2,3,\ldots,I \\ j=1,2,3,\ldots,J \end{cases} \tag{4.114}$$

$$l=(m-1)J+n \quad \begin{cases} m=1,2,3,\ldots,I \\ n=1,2,3,\ldots,J. \end{cases} \tag{4.115}$$

Equation (4.113) may now be written as

$$\sum_{k=1}^{I\times J}G_{kl}w_k=\lambda\sum_{k=1}^{I\times J}b_{kl}w_k, \quad l=1,2,3,\ldots,I\times J, \tag{4.116}$$

where G_{kl} $(=G_{lk})$ is given in Table 4.1 (page 102) and b_{kl} $(=b_{lk})$ is

$$\begin{aligned} b_{lk}=&\frac{1}{4}L_xL_y\pi^2\left[N_{x0}\left(\frac{i}{L_x}\right)^2+N_{y0}\left(\frac{j}{L_y}\right)^2\right]\delta_{lk} \\ &+L_xL_y\pi^2N_{xy0}\left(\frac{i}{L_x}\frac{n}{L_y}r_{mi}r_{jn}+\frac{j}{L_y}\frac{m}{L_x}r_{im}r_{nj}\right). \end{aligned} \tag{4.117}$$

The Kronecker delta δ_{lk} and the parameter r_{ij} are also given in Table 4.1. In expanded form Eq. (4.116) is

$$\left(\begin{bmatrix} G_{11} & \cdots & G_{1(I\times J)} \\ \vdots & \ddots & \\ G_{(I\times J)1} & & G_{(I\times J)(I\times J)} \end{bmatrix}-\lambda\begin{bmatrix} b_{11} & \cdots & b_{1(I\times J)} \\ \vdots & \ddots & \\ b_{(I\times J)1} & & b_{(I\times J)(I\times J)} \end{bmatrix}\right)\begin{Bmatrix} w_1 \\ \vdots \\ w_{(I\times J)} \end{Bmatrix}=\begin{Bmatrix} 0 \\ \vdots \\ 0 \end{Bmatrix}. \tag{4.118}$$

When the plate is not buckled, the deflection is zero, whereas for a buckled plate it is nonzero. The values of λ for the buckled plate (denoted by λ_{cr}) are the eigenvalues of Eq. (4.118), and these can be calculated by commercial software. There are $J\times I$ eigenvalues, of which the lowest gives the lowest buckling load.

We now consider an orthotropic plate subjected to N_{x0} and N_{y0} edge loads. The forces inside the plate are

$$N_x=-\lambda N_{x0} \qquad N_y=-\lambda N_{y0} \qquad N_{xy}=0. \tag{4.119}$$

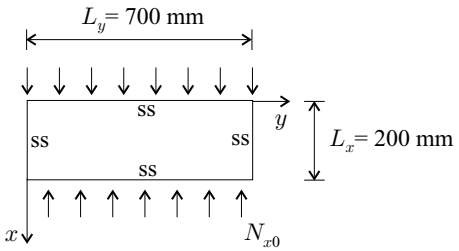

Figure 4.15: The plate in Example 4.5.

For orthotropic laminates we have (Table 3.4, page 76)

$$D_{16} = D_{26} = 0. \tag{4.120}$$

The eigenvalues of Eq. (4.118) can now be calculated directly. The result is

$$(\lambda_{\text{cr}})_{ij} = \frac{\pi^2\Big[D_{11}\big(\frac{i}{L_x}\big)^4 + 2(D_{12}+2D_{66})\big(\frac{i}{L_x}\big)^2\big(\frac{j}{L_y}\big)^2 + D_{22}\big(\frac{j}{L_y}\big)^4\Big]}{N_{x0}\big(\frac{i}{L_x}\big)^2 + N_{y0}\big(\frac{j}{L_y}\big)^2}. \tag{4.121}$$

$(\lambda_{\text{cr}})_{ij}$ must be calculated for different sets of i and j, ($i, j = 1, 2, \dots$). The lowest resulting value of $(\lambda_{\text{cr}})_{ij}$ is the value of interest.

Libove[17] showed that, for simply supported orthotropic plates, the lowest buckling load corresponds to a mode that has a half wave in at least one direction. (In this direction either i or j is equal to unity.) When the plate is subjected to uniaxial compression, or to compression in one direction and tension in the other direction, buckling occurs with a half wave perpendicular to the compressive load.[18]

4.5 Example. *A 0.7-m-long and 0.2-m-wide rectangular plate is made of graphite epoxy. The material properties are given in Table 3.6 (page 81). The layup is* $[\pm 45_2^{\text{f}}/0_{12}/\pm 45_2^{\text{f}}]$. *The 0-degree plies are parallel to the short edge of the plate. The plate is simply supported along all four edges. (Fig. 4.15). The plate is subjected to uniform compressive loads along the long edges. Calculate the buckling load.*

Solution. From Eq. (4.121), with $N_{y0} = 0$ and with the stiffnesses $D_{11} = 45.30\,\text{N}\cdot\text{m}$, $D_{22} = 25.26\ \text{N}\cdot\text{m}$, $D_{12} = 19.52\ \text{N}\cdot\text{m}$, $D_{66} = 20.62\ \text{N}\cdot\text{m}$ (Table 3.7, page 84) we have

$$\begin{aligned} N_{x0}\,(\lambda_{\text{cr}})_{ij} &= \pi^2\left[D_{11}\left(\frac{i}{L_x}\right)^2 + 2\,(D_{12}+2D_{66})\left(\frac{j}{L_y}\right)^2 + D_{22}\left(\frac{j}{L_y}\right)^4\left(\frac{L_x}{i}\right)^2\right] \\ &= \left(11.18i^2 + 2.45\,j^2 + 0.0415\frac{j^4}{i^2}\right)10^3. \end{aligned} \tag{4.122}$$

[17] C. Libove, Buckle Pattern for Biaxially Compressed Simply Supported Orthotropic Rectangular Plates. *Journal of Composite Materials*, Vol. 17, 45–48, 1983.

[18] T. K. Tung and J. Surdenas, Buckling of Rectangular Orthotropic Plates under Biaxial Loading. *Journal of Composite Materials,* Vol. 21, 124–128, 1987.

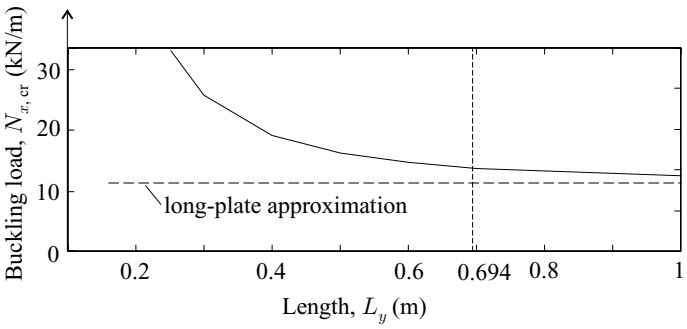

Figure 4.16: The lowest buckling load of the plate in Example 4.5 as a function of the plate length.

The values of $N_{x0}\,(\lambda_{\mathrm{cr}})_{ij} \times 10^{-3}$ are

$i \setminus j$	1	2	3
1	13.67	21.63	36.57
2	47.17	54.66	67.58
3	103.04	110.46	122.99.

(4.123)

The lowest value is $N_{x0}\,(\lambda_{\mathrm{cr}})_{ij} = 13.67$ kN/m, which corresponds to $i = j = 1$. Thus, the lowest buckling load is

$$N_{x,\mathrm{cr}} = (\lambda_{\mathrm{cr}})_{11}\, N_{x0} = 13.67 \text{ kN/m}. \tag{4.124}$$

We now assess the length-to-width ratios under which the long-plate approximation is reasonable. To this end, we calculate the lowest buckling loads of the plate, keeping the width L_x the same while changing the length L_y. In Figure 4.16 we plot the buckling loads thus calculated versus L_y. In this figure we also include the lowest buckling load given by the long-plate approximation (Eq. 4.170). The results in this figure show that, in accordance with Eq. (4.19), the long-plate formula is reasonable when L_y is greater than $3L_x\sqrt[4]{D_{11}/D_{22}} = 0.694$ m. At $L_y = 0.694$ m the long-plate formula underestimates the buckling load by about 18 percent.

4.6 Example. *A 0.2-m-long and 0.2-m-wide rectangular plate is made of graphite epoxy unidirectional plies. The material properties are given in Table 3.6 (page 81). The layup is* $[45_2/-45_2/0_{12}/-45_2/45_2]$. *The plate, simply supported along four edges, is subjected to uniform compressive loads along all four edges (Fig. 4.17). Determine the buckling load.*

Solution. The layup of the plate is symmetrical but is not orthotropic. The bending stiffnesses are $D_{11} = 45.30$ N · m, $D_{22} = 25.26$ N · m, $D_{12} = 19.52$ N · m, $D_{66} = 20.62$ N · m, $D_{16} = 4.45$ N · m, $D_{26} = 4.45$ N · m (Table 3.7, page 84). The buckling load is calculated from Eqs. (4.117) and (4.118). With the preceding stiffnesses and

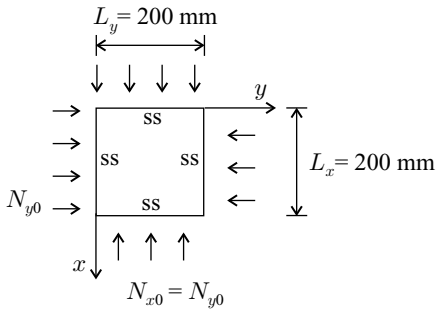

Figure 4.17: The plate in Example 4.6.

with $I = J = 7$, these calculations yield the following results for $(N_{\text{cr}})_{ij} \times 10^{-3}$:

$i \setminus j$	1	2	3
1	23.47	45.05	76.62
2	61.25	94.61	132.38
3	119.45	164.43	214.29.

(4.125)

The lowest buckling load is

$$N_{\text{cr}} = (N_{\text{cr}})_{ij} = 23.47 \text{ kN/m}. \tag{4.126}$$

The layup follows the 10-percent rule (page 89), and we may treat the plate as orthotropic. With $N_{x0} = N_{y0} = N_0$, from Eq. (4.121) we have

$$\begin{aligned} N_0(\lambda_{\text{cr}})_{ij} &= \frac{\pi^2\Big[D_{11}\big(\frac{i}{L_x}\big)^4 + 2\big(D_{12} + 2D_{66}\big)\big(\frac{i}{L_x}\big)^2\big(\frac{j}{L_y}\big)^2 + D_{22}\big(\frac{j}{L_y}\big)^4\Big]}{\big(\frac{i}{L_x}\big)^2 + \big(\frac{j}{L_y}\big)^2} \\ &= \frac{(279.4i^4 + 749.5i^2j^2 + 155.8i^4)10^3}{25i^2 + 25j^2}. \end{aligned} \tag{4.127}$$

The values of $N_0\,(\lambda_{\text{cr}})_{ij} \times 10^{-3}$ are

$i \setminus j$	1	2	3
1	23.70	46.16	78.58
2	61.00	94.78	135.61
3	118.14	160.34	213.26.

(4.128)

The lowest value is $N_0\,(\lambda_{\text{cr}})_{ij} = 23.70$ kN/m, which corresponds to $i = j = 1$. Thus, the lowest buckling load is

$$N_{\text{cr}} = (\lambda_{\text{cr}})_{11}\, N_0 = 23.70 \text{ kN/m}. \tag{4.129}$$

This buckling load, based on the orthotropy approximation, is within 1 percent of the buckling load given by Eq. (4.126).

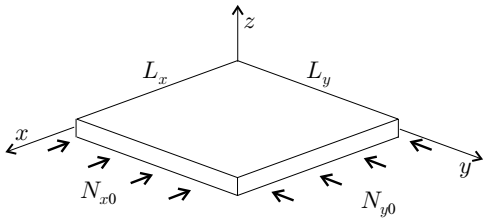

Figure 4.18: Rectangular plate subjected to uniform biaxial compressive edge loads.

4.3.2 Plates with Built-In and Simply Supported Edges – Orthotropic and Symmetrical Layup

We consider rectangular plates with length L_x and width L_y (Fig. 4.18). The layup of the plate is orthotropic and symmetrical. Each edge of the plate is either simply supported or built-in. Uniformly distributed in-plane loads N_{x0} and N_{y0} act along the edges.

The edge loads are increased proportionally to $\lambda N_{x0}, \lambda N_{y0}$, where λ is the load parameter. For the buckled plate the load parameter is denoted by λ_{cr}. We apply the Ritz method to find λ_{cr}.[19]

The expression of the potential energy is obtained by setting N_{xy} and D_{16} and D_{26} equal to zero (orthotropy) in Eqs. (4.107) and (4.108)

$$\pi_{\text{p}} = U + \Omega = \frac{1}{2}\int_0^{L_x}\int_0^{L_y}\left[D_{11}\left(\frac{\partial^2 w^{\text{o}}}{\partial x^2}\right)^2 + D_{22}\left(\frac{\partial^2 w^{\text{o}}}{\partial y^2}\right)^2 + D_{66}\left(\frac{2\partial^2 w^{\text{o}}}{\partial x \partial y}\right)^2 + 2D_{12}\frac{\partial^2 w^{\text{o}}}{\partial x^2}\frac{\partial^2 w^{\text{o}}}{\partial y^2} + N_x\left(\frac{\partial w^{\text{o}}}{\partial x}\right)^2 + N_y\left(\frac{\partial w^{\text{o}}}{\partial y}\right)^2\right] dydx, \tag{4.130}$$

where N_x and N_y are the in-plane loads (per unit length) inside the plate, which are related to the edge forces by

$$N_x = -\lambda N_{x0}, \qquad N_y = -\lambda N_{y0}, \tag{4.131}$$

and w^{o} is the deflection of the midplane, which is assumed to be of the form

$$w^{\text{o}} = AX_i(x)Y_j(y), \tag{4.132}$$

where A is an unknown amplitude. For the $X_i(x)$ and $Y_j(y)$ displacement functions we adopt the shape of a freely vibrating beam. (The $X_i(x)$ function is illustrated in Fig. 4.19.) For different end supports $X_i(x)$ and $Y_j(y)$ are given in Table 4.4 (page 119).

By virtue of the principle of stationary potential energy (Eq. 2.206), we have

$$\frac{\partial \pi_{\text{p}}}{\partial A} = 0. \tag{4.133}$$

[19] I. Veres and L. P. Kollár, Buckling of Orthotropic Plates with Different Edge Supports. *Journal of Composite Materials*, Vol. 35, 625–635, 2001.

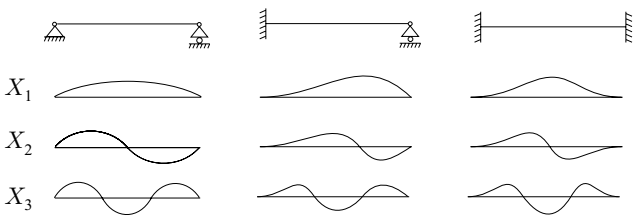

Figure 4.19: Freely vibrating beam. The displacements correspond to $X_i(x)$, $i = 1, 2, 3$.

Equations (4.130) and (4.133), together with Eq. (4.132) and the expressions in Table 4.4, yield

$$\left[\frac{D_{11}}{L_x^4}\alpha_1^4 + \frac{D_{22}}{L_y^4}\alpha_3^4 + 2\left(D_{12}+2D_{66}\right)\frac{1}{L_x^2 L_y^2}\alpha_2 - \lambda_{\mathrm{cr}}\left(\frac{N_{x0}}{L_x^2}\alpha_4 + \frac{N_{y0}}{L_y^2}\alpha_5\right)\right] = 0. \tag{4.134}$$

The parameters α_1, α_2, α_3, α_4, α_5 are defined in Table 4.5 (page 120). The integrations indicated in Table 4.5 simplify when $X_i(x)$ and $Y_j(y)$ are calculated by the approximate expressions of μ_i given in Table 4.4. The resulting approximate expressions for α_1 through α_5 are given in Tables 4.6 and 4.7, and α_2 is

$$\alpha_2 = \alpha_4\alpha_5. \tag{4.135}$$

By rearranging Eq. (4.134), we obtain the following expression for λ_{cr}:

$$(\lambda_{\mathrm{cr}})_{ij} = \frac{D_{11}\frac{\alpha_1^4}{L_x^4} + D_{22}\frac{\alpha_3^4}{L_y^4} + 2\left(D_{12}+2D_{66}\right)\frac{\alpha_4\alpha_5}{L_x^2 L_y^2}}{\left(N_{x0}\frac{\alpha_4}{L_x^2} + N_{y0}\frac{\alpha_5}{L_y^2}\right)}. \tag{4.136}$$

This equation applies when each edge is either simply supported or built-in. When all four edges are simply supported, Eq. (4.136) simplifies to Eq. (4.121).

Table 4.4. The displacement function X_i of a freely vibrating beam. The parameter μ_i is to be determined either from the exact or from the approximate expression. (Also: $\xi = \frac{x}{L_x}$.) For Y_j the same formulas apply with ξ, x, L_x, i replaced by η, y, L_y, j, respectively.

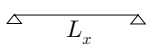	$X_i = \sin(i\pi\xi)$
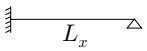	$X_i = \gamma_i\cos(\mu_i\xi) - \gamma_i\cosh(\mu_i\xi) + \sin(\mu_i\xi) - \sinh(\mu_i\xi)$ $\tan\mu_i - \tanh\mu_i = 0$ (Exact) $\mu_i \approx (i+0.25)\pi$ (Approximate) $\gamma_i = \frac{\sin\mu_i - \sinh\mu_i}{\cosh\mu_i - \cos\mu_i}$
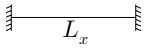	$X_i = \gamma_i\cos(\mu_i\xi) - \gamma_i\cosh(\mu_i\xi) + \sin(\mu_i\xi) - \sinh(\mu_i\xi)$ $\cos\mu_i\cosh\mu_i = 1$ (Exact) $\mu_i \approx (i+0.5)\pi$ (Approximate) $\gamma_i = \frac{\cos\mu_i - \cosh\mu_i}{\sin\mu_i + \sinh\mu_i}$

Table 4.5. The coefficients α_1 through α_5

$$\alpha_1 \equiv \sqrt[4]{\frac{1}{c_x^2}\int_0^1 \left(\frac{\partial^2 X_i}{\partial \xi^2}\right)^2 d\xi} \qquad \alpha_3 \equiv \sqrt[4]{\frac{1}{c_y^2}\int_0^1 \left(\frac{\partial^2 Y_j}{\partial \eta^2}\right)^2 d\eta}$$

$$\alpha_4 \equiv \frac{1}{c_x^2}\int_0^1 \left(\frac{\partial X_i}{\partial \xi}\right)^2 d\xi \qquad \alpha_5 \equiv \frac{1}{c_y^2}\int_0^1 \left(\frac{\partial Y_j}{\partial \eta}\right)^2 d\eta$$

$$\alpha_2 \equiv \frac{1}{c_x^2}\frac{1}{c_y^2}\int_0^1 \left(\frac{\partial X_i}{\partial \xi}\right)^2 d\xi \int_0^1 \left(\frac{\partial Y_j}{\partial \eta}\right)^2 d\eta$$

$$c_x \equiv \sqrt{\int_0^1 X_i^2 d\xi} \qquad c_y \equiv \sqrt{\int_0^1 Y_j^2 d\eta}$$

Table 4.6. Approximate expressions for the coefficients α_1 and α_4 (*i* represents the number of half waves in the *x* direction)

	α_1	α_4	*i*
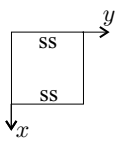	$i\pi$	$i^2\pi^2$	1, 2, 3, ...
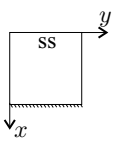	$(i+0.25)\,\pi$	$\alpha_1\,(\alpha_1-1)$	1, 2, 3, ...
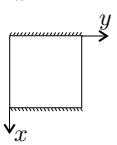	4.730 $(i+0.5)\,\pi$	$\alpha_1\,(\alpha_1-2)$ $\alpha_1\,(\alpha_1-2)$	1 2, 3, 4, ...

Table 4.7. Approximate expressions for the coefficients α_3 and α_5 (*j* represents the number of half waves in the *y* direction)

	α_3	α_5	*j*
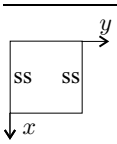	$j\pi$	$j^2\pi^2$	1, 2, 3, ...
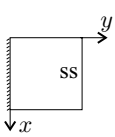	$(j+0.25)\,\pi$	$\alpha_3\,(\alpha_3-1)$	1, 2, 3, ...
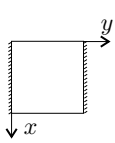	4.730 $(j+0.5)\,\pi$	$\alpha_3\,(\alpha_3-2)$ $\alpha_3\,(\alpha_3-2)$	1 2, 3, 4, ...

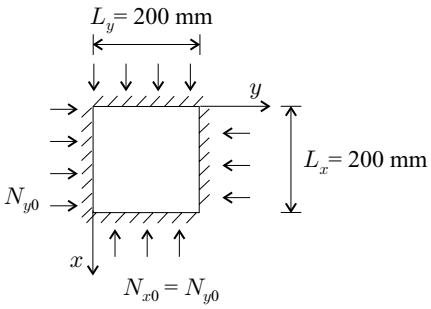

Figure 4.20: The plate in Example 4.7.

The critical load parameter must be calculated for different sets of i and j, (i, $j = 1, 2, \dots$). The lowest resulting value of λ_{cr} is the value of interest. The lowest buckling load (as in the case of simply supported plates) corresponds to a mode that has a half wave in at least one direction. (In this direction either i or j is equal to unity.) When the plate is subjected to uniaxial compression, or to compression in one direction and tension in the other direction, buckling occurs with a half wave perpendicular to the compressive load.

4.7 Example. *A 0.2-m-long and 0.2-m-wide rectangular plate is made of graphite epoxy unidirectional plies. The material properties are given in Table 3.6 (page 81). The layup is* $[45_2/-45_2/0_{12}/-45_2/45_2]$. *The plate, built-in along the four edges, is subjected to uniform compressive loads along all four edges (Fig. 4.20). Determine the buckling load.*

Solution. The layup follows the 10-percent rule (page 89), and we treat the plate as orthotropic. With the stiffnesses $D_{11} = 45.30\ \text{N}\cdot\text{m}$, $D_{22} = 25.26\ \text{N}\cdot\text{m}$, $D_{12} = 19.52\ \text{N}\cdot\text{m}$, $D_{66} = 20.62\ \text{N}\cdot\text{m}$ (Table 3.7, page 84) and with $N_{x0} = N_{y0} = N_0$, from Eq. (4.136) we have

$$N_0\left(\lambda_{\text{cr}}\right)_{ij} = \frac{D_{11}\frac{\alpha_1^4}{L_x^4} + D_{22}\frac{\alpha_3^4}{L_y^4} + 2\left(D_{12} + 2D_{66}\right)\frac{\alpha_4\alpha_5}{L_x^2 L_y^2}}{\frac{\alpha_4}{L_x^2} + \frac{\alpha_5}{L_y^2}}, \tag{4.137}$$

where α_1 and α_4 depend on i ($i = 1, 2, \dots$) and α_3 and α_5 depend on j ($j = 1, 2, \dots$) as given in Tables 4.6 and 4.7, third row. From these tables the values are

	$i=1$	$i=2$	$i=3$
α_1	4.73	7.85	11.00
α_4	12.91	45.98	98.91

	$j=1$	$j=2$	$j=3$
α_3	4.73	7.85	11.00
α_5	12.91	45.98	98.91 .

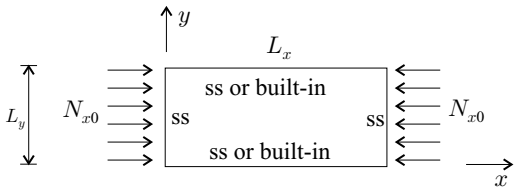

Figure 4.21: Uniaxially loaded rectangular plate.

The values of $N_0\,(\lambda_{\rm cr})_{ij} \times 10^{-3}$ are (Eq. 4.137)

$i \setminus j$	1	2	3
1	53.80	81.05	122.31
2	109.16	142.82	188.79
3	185.55	226.18	280.57.

The lowest value is $N_0\,(\lambda_{\rm cr})_{ij} = 53.80$ kN/m, which corresponds to $i = j = 1$, Thus, the lowest buckling load is

$$N_{\rm cr} = (\lambda_{\rm cr})_{11}\, N_0 = 53.80 \text{ kN/m}. \tag{4.138}$$

Uniform compressive load in the x direction. We consider a plate with the edges parallel to the y-axis simply supported and the edges parallel to the x-axis either simply supported or built-in (Fig. 4.21). The plate is subjected to a uniaxial compressive load N_{x0} in the x direction. By introducing the notation $N_{x,\rm cr} = \lambda_{\rm cr} N_{x0}$ and by setting $N_{y0} = 0$, Eq. (4.136) may be rearranged to yield

$$N_{x,\rm cr} = D_{11}\frac{\alpha_1^4}{\alpha_4}\frac{1}{L_x^2} + D_{22}\frac{\alpha_3^4}{\alpha_4}\frac{L_x^2}{L_y^4} + 2\,(D_{12} + 2D_{66})\,\frac{\alpha_5}{L_y^2}, \tag{4.139}$$

where α_1 and α_4 depend on i ($i = 1, 2, \dots$) and α_3 and α_5 depend on j ($j = 1, 2, \dots$) (Tables 4.6 and 4.7). The values of i and j (and the corresponding values of $\alpha_1, \alpha_4, \alpha_3$, and α_5) that yield the lowest value of $N_{x,\rm cr}$ are determined as follows.

To determine j, we observe that both α_3 and α_5 increase monotonically with j (Table 4.7). Hence, the right-hand side of Eq. (4.139) also increases with j. Thus, the lowest buckling load corresponds to $j = 1$. At this load the buckled shape is a half wave in the direction perpendicular to the load. This is illustrated in Figure 4.22 for a simply supported plate.

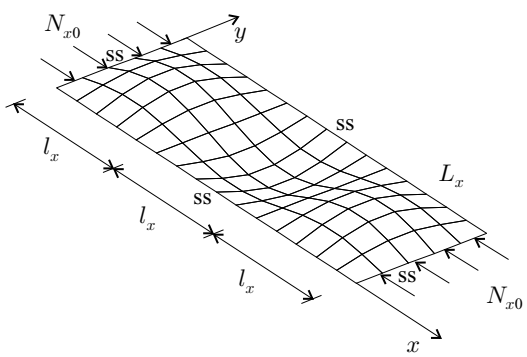

Figure 4.22: Buckled shape of a uniaxially loaded rectangular plate with simply supported edges.

Table 4.8. Buckling loads of unidirectionally loaded plates (orthotropic and symmetrical layup) with simply supported, built-in, and rotationally restrained edges ($l_x = L_x/i$, $i = 1, 2, \ldots$, $\xi = \frac{1}{1+10\zeta}$, $\zeta = \frac{D_{22}}{\widetilde{k}L_y}$); L_x, L_y are the length and the width, respectively, and $\widetilde{k}$ is the spring constant

Supports	Buckling load $N_{x,\mathrm{cr}}$
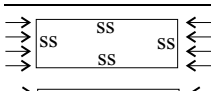	$\frac{\pi^2}{L_y^2}\left(D_{11}\frac{L_y^2}{l_x^2} + D_{22}\frac{l_x^2}{L_y^2} + 2\left(D_{12}+2D_{66}\right)\right)$
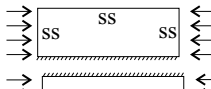	$\frac{\pi^2}{L_y^2}\left(D_{11}\frac{L_y^2}{l_x^2} + 2.441\,D_{22}\frac{l_x^2}{L_y^2} + 2.33\left(D_{12}+2D_{66}\right)\right)$
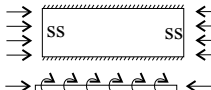	$\frac{\pi^2}{L_y^2}\left(D_{11}\frac{L_y^2}{l_x^2} + 5.139\,D_{22}\frac{l_x^2}{L_y^2} + 2.62\left(D_{12}+2D_{66}\right)\right)$
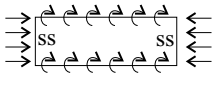	$\frac{\pi^2}{L_y^2}\left(D_{11}\frac{L_y^2}{l_x^2} + (1+4.139\xi)D_{22}\frac{l_x^2}{L_y^2} + (2+0.62\xi^2)(D_{12}+2D_{66})\right)$

To determine α_1 and α_4 we recall that the edges parallel to the y-axis are simply supported. The corresponding values of α_1 and α_4 are given in the first row of Table 4.6 and are

$$\alpha_1 = i\pi \qquad \alpha_4 = i^2\pi^2. \tag{4.140}$$

With these values of α_1 and α_4 Eq. (4.139) becomes

$$N_{x,\mathrm{cr}} = D_{11}\pi^2\frac{1}{l_x^2} + D_{22}\frac{\alpha_3^4}{\pi^2}\frac{l_x^2}{L_y^4} + 2\left(D_{12}+2D_{66}\right)\frac{\alpha_5}{L_y^2}, \tag{4.141}$$

where l_x is the length of the half buckling wave

$$l_x = \frac{L_x}{i}. \tag{4.142}$$

The values of α_3 and α_5 to be used are those given in Table 4.7 for $j = 1$. The resulting buckling loads are listed in the first three rows of Table 4.8.

The value of $N_{x,\mathrm{cr}}$ must be calculated for different values of i ($i = 1, 2, \ldots$), and, generally the lowest resulting value is of interest.

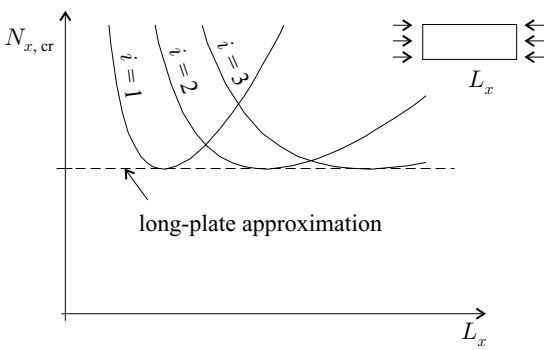

Figure 4.23: Buckling loads of unidirectionally loaded rectangular plates with simply supported or built-in edges. The plate's length is L_x.

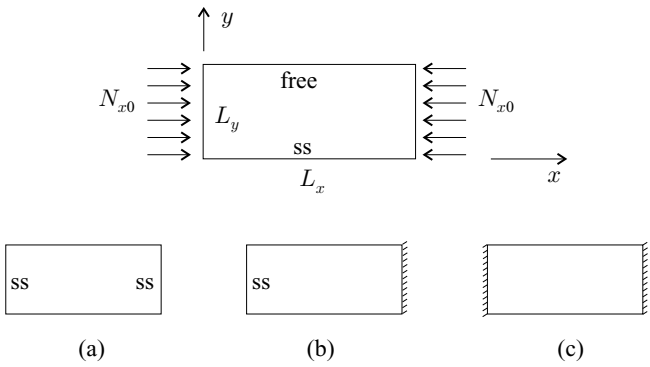

Figure 4.24: Supports along edges parallel (top) and perpendicular (bottom) to the load direction.

The buckling loads of plates with simply supported or built-in edges (Fig. 4.21) are illustrated in Figure 4.23. For each value of i the lowest buckling load is the same as the lowest buckling load of the corresponding long plate that will be given, subsequently, in the first three rows of Table 4.11 (page 136).

4.3.3 Plates with One Free Edge – Orthotropic and Symmetrical Layup

We consider a rectangular plate with length L_x and width L_y. The layup of the plate is orthotropic and symmetrical.

One Edge Parallel to the x Axis is Simply Supported; the Other is Free

The plate is simply supported along the $y = 0$ edge and is free along the $y = L_y$ edge (Fig. 4.24, top). The edges parallel to the y-axis may be either simply supported or built-in (Fig. 4.24, bottom). The plate is subjected to uniform uniaxial compression N_{x0} in the x direction (Fig. 4.24, top). We wish to determine the lowest value of the load at which the plate buckles.

Edges parallel to the y-axis are simply supported. We consider plates whose edges parallel to the y-axis are simply supported (Fig. 4.24, a). The buckling loads are denoted by $N_{x,\mathrm{cr}}$. An exact analysis resulting in a transcendental equation for $N_{x,\mathrm{cr}}$ is given by Whitney.[20] Here, we present an approximate analysis, which yields a closed-form expression for $N_{x,\mathrm{cr}}$. In our analysis we apply the Ritz method and approximate the buckled shape (shown in Fig. 4.25) by

$$w^{\mathrm{o}} = Ay \sin\left(\frac{\pi x}{L_x}\right), \tag{4.143}$$

where A is a constant and w^{o} is the deflection, which satisfies the geometrical boundary condition ($w^{\mathrm{o}} = 0$) along the simply supported edges.

[20] J. M. Whitney, *Structural Analysis of Laminated Anisotropic Plates.* Technomic, Lancaster, Pennsylvania, 1987, p. 108.

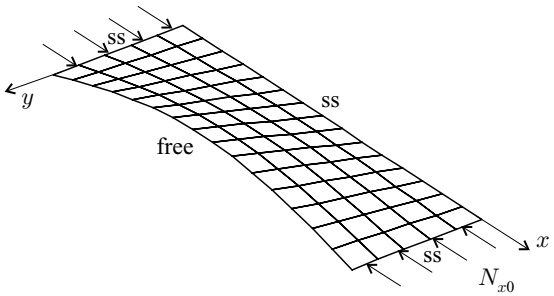

Figure 4.25: Buckled shape of a rectangular plate with one free and three simply supported edges.

We express the potential energy of the plate by setting $N_y = 0$ and $N_x = -N_{x0}$ in Eq. (4.130):

$$\pi_{\mathrm{p}} = \frac{1}{2}\int_0^{L_x}\int_0^{L_y}\left[D_{11}\left(\frac{\partial^2 w^{\mathrm{o}}}{\partial x^2}\right)^2 + D_{22}\left(\frac{\partial^2 w^{\mathrm{o}}}{\partial y^2}\right)^2 + D_{66}\left(\frac{2\partial^2 w^{\mathrm{o}}}{\partial x \partial y}\right)^2 + 2\left(D_{12}\frac{\partial^2 w^{\mathrm{o}}}{\partial x^2}\frac{\partial^2 w^{\mathrm{o}}}{\partial y^2}\right)\right] dydx - \frac{1}{2}\int_0^{L_x}\int_0^{L_y}\left[N_{x0}\left(\frac{\partial w^{\mathrm{o}}}{\partial x}\right)^2\right] dydx. \quad (4.144)$$

By introducing Eq. (4.143) into Eq. (4.144), we arrive at the following expression for the potential energy:

$$\pi_{\mathrm{p}} = \frac{A^2 L_x}{4}\left\{D_{11}\frac{L_y^3}{3}\frac{\pi^4}{L_x^4} + 4D_{66}L_y\frac{\pi^2}{L_x^2} - N_{x0}\frac{L_y^3}{3}\frac{\pi^2}{L_x^2}\right\}. \quad (4.145)$$

Table 4.9. Buckling loads of unidirectionally loaded plates (orthotropic and symmetrical layup) with one free edge ($l_x = L_x/i$, $i = 1, 2, \ldots$, $\zeta = \frac{D_{22}}{\widetilde{k}L_y}$); L_x, L_y are the length and the width, respectively, and $\widetilde{k}$ is the spring constant

Supports	Buckling load $N_{x,\mathrm{cr}}$
free; ss, ss, ss; N_{x0}	$\frac{\pi^2 D_{11}}{L_x^2} + \frac{12D_{66}}{L_y^2}$
free; ss, ss; N_{x0}	$\frac{\pi^2 D_{11}}{(0.7L_x)^2} + \frac{12D_{66}}{L_y^2}$
free; ss; N_{x0}	$\frac{\pi^2 D_{11}}{(0.5L_x)^2} + \frac{12D_{66}}{L_y^2}$
free; ss, ss; N_{x0}	$\frac{1.25l_x^2 D_{22}}{L_y^4} + \frac{\pi^2 D_{11}}{l_x^2} + \frac{12D_{66}}{L_y^2}$
free; ss, ss; N_{x0}	$\frac{1.25}{1+4.12\zeta}\frac{l_x^2 D_{22}}{L_y^4} + \frac{\pi^2 D_{11}}{l_x^2} + \frac{12D_{66}}{L_y^2}$

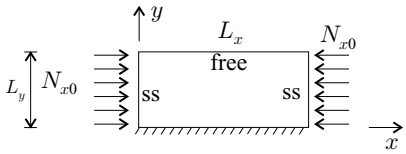

Figure 4.26: Support along the edges of a uniaxially loaded rectangular plate.

By virtue of the principle of stationary potential energy $\partial \pi_p / \partial A = 0$ (Eq. 2.206), and we have

$$N_{x,\mathrm{cr}} = \frac{\pi^2 D_{11}}{L_x^2} + \frac{12 D_{66}}{L_y^2}. \tag{4.146}$$

One or Both Edges Parallel to the *y*-Axis are Built-in

The buckling loads of plates that have one or both edges parallel to the y-axis built-in (Fig. 4.24, b and c) can be derived in a way similar to that of Eq. (4.146). The details are not given here; the resulting buckling loads are given in Table 4.9.

One edge parallel to the x-axis is built-in; the other is free. The plate is built-in along the $y = 0$ edge, is free along the $y = L_y$ edge, and is simply supported along the $x = 0$ and $x = L_x$ edges (Fig. 4.26). The plate is subjected to uniform uniaxial compression N_{x0} in the x direction. We wish to determine the lowest value of the load at which the plate buckles (Fig. 4.27). An exact analysis, resulting in transcendental equations for the buckling loads $N_{x,\mathrm{cr}}$, is given by Bank and Yin.[21] An approximate expression for $N_{x,\mathrm{cr}}$ is[22]

$$N_{x,\mathrm{cr}} = \frac{\pi^2 D_{11}}{l_x^2} + 1.25 \frac{l_x^2 D_{22}}{L_y^4} + \frac{12 D_{66}}{L_y^2}, \tag{4.147}$$

where $l_x = L_x / i$ is the length of the half buckling wave in the x direction and $i = 1, 2, \ldots$ is the number of half waves in the x direction.

Equation (4.147) underestimates the buckling loads by less than 14 percent.

The value of $N_{x,\mathrm{cr}}$ must be calculated for different values of i ($i = 1, 2, \ldots$) and, in general, the lowest resulting value is of interest.

The buckling load is a function of the length of the plate L_x (Fig. 4.23). For each value of i the lowest buckling load is the same as the lowest buckling load of the corresponding long plate given subsequently in the fifth row of Table 4.11 (page 136).

4.8 Example. *A rectangular plate with length $L_x = 0.5$ m and width $L_y = 0.05$ m is made of graphite epoxy unidirectional plies with the fibers oriented along the x-axis of the plate (Fig. 4.28). The material properties are given in Table 3.6 (page 81). The layup is* $[0_{20}]$. *One of the long edges is built-in; the other long edge is free. The short edges are simply supported. The plate is subjected to uniform compressive loads in the x direction. Calculate the buckling load.*

[21] L. C. Bank and J. Yin, Buckling of Orthotropic Plates with Free and Rotationally Restrained Unloaded Edges. *Thin-Walled Structures*, Vol. 24, 83–96, 1996.

[22] L. P. Kollár, Buckling of Unidirectionally Loaded Composite Plates with One Free and One Rotationally Restrained Unloaded Edge. *Journal of Structural Engineering*, Vol. 128, 1202–1211, 2002.

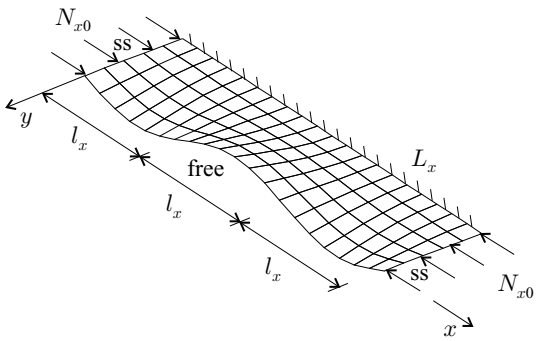

Figure 4.27: Buckled shape of a uniaxially loaded rectangular plate with a built-in and a free longitudinal edge.

Solution. The expression in Table 4.9, fourth row (page 125), together with the stiffnesses $D_{11} = 99.25\,\mathrm{N\cdot m}$, $D_{22} = 6.47\,\mathrm{N\cdot m}$, $D_{12} = 1.94\,\mathrm{N\cdot m}$, $D_{66} = 3.03\,\mathrm{N\cdot m}$ (Table 3.7, page 84) gives

$$\begin{aligned} N_{x,\mathrm{cr}} &= \frac{\pi^2 D_{11}}{l_x^2} + 1.25\frac{l_x^2 D_{22}}{L_y^4} + \frac{12 D_{66}}{L_y^2} \\ &= 979.5\frac{1}{l_x^2} + 1.294 \times 10^6 l_x^2 + 14\,560, \end{aligned} \tag{4.148}$$

where $l_x = L_x/i$. The buckling loads for $i = 1, 2, 3, 4, 5, 6$ are

i	1	2	3	4	5	6
$N_{x,\mathrm{cr}}$ (kN/m)	342.04	111.12	85.78	97.47	125.46	164.60

The lowest buckling load corresponds to $i = 3$ and is 85.78 kN/m.

The buckling loads of plates of the same width but with different lengths are given by solid lines in Figure 4.29. The buckling loads calculated by the equations of Bank and Yin[23] are also included in this figure. The approximate formula (Eq. 4.148) underestimates $N_{x,\mathrm{cr}}$, and, hence, is a conservative estimate.

The long-plate expression gives the lowest buckling load of this plate as 90.64 kN/m (Example 4.11, page 138). This value is also shown in Figure 4.29.

4.3.4 Plates with Rotationally Restrained Edges – Orthotropic and Symmetrical Layup

We consider a rectangular plate with length L_x and width L_y. The layup of the plate is orthotropic and symmetrical. The plate is simply supported along the edges parallel to the y-axis. The $y = 0$ edge is rotationally restrained, the $y = L_y$ edge is either rotationally restrained (Fig. 4.30, left) or free (Fig 4.30, right). Along a rotationally restrained edge the bending moment is proportional to the rotation

[23] L. C. Bank and J. Yin, Buckling of Orthotropic Plates with Free and Rotationally Restrained Unloaded Edges. *Thin-Walled Structures*, Vol. 24, 83–96, 1996.

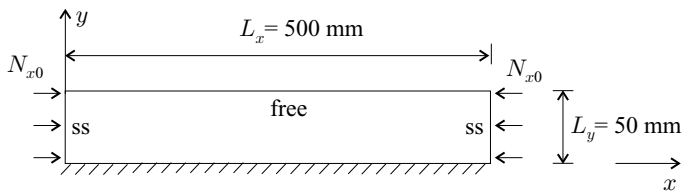

Figure 4.28: The plate in Example 4.8.

of the edge

$$M_y = \widetilde{k}\frac{\partial w}{\partial y}, \tag{4.149}$$

where $\widetilde{k}$ is the rotational spring constant. The rotational spring constant is further discussed in Section 6.9.3.

The plate is subjected to uniform uniaxial compression N_{x0} in the x direction. We wish to determine the lowest value of the load at which the plate buckles.

Both Unloaded Edges are Rotationally Restrained

We consider a plate that is rotationally restrained along the $y = 0$ and the $y = L_y$ edges (Fig. 4.30, left). An exact analysis resulting in a transcendental equation for the buckling loads $N_{x,\mathrm{cr}}$ is given by Qiao et al.[24] Here, we present an approximate analysis, which yields a closed-form expression for $N_{x,\mathrm{cr}}$.

The buckling load of a plate with rotationally restrained edges must be between the buckling load of a simply supported plate (Table 4.8, first row, page 123) and the buckling load of a plate with built-in edges (Table 4.8, third row). We combine the expressions for plates with simply supported and built-in edges and write

$$N_{x,\mathrm{cr}} = \frac{\pi^2}{L_y^2}\left(D_{11}\frac{L_y^2}{l_x^2} + (1+4.139\xi)\,D_{22}\frac{l_x^2}{L_y^2} + (2+0.62\xi')\,(D_{12}+2D_{66})\right), \tag{4.150}$$

where ξ and ξ' are parameters that depend on the support conditions along the unloaded edges. These parameters are zero for a plate with simply supported unloaded edges and are unity for a plate with built-in unloaded edges. The values of ξ and ξ' may be approximated by[25]

$$\xi = \frac{1}{1+10\zeta} \qquad \xi' = \xi^2, \tag{4.151}$$

where ζ is the parameter of restraint

$$\zeta = \frac{D_{22}}{\widetilde{k}L_y}. \tag{4.152}$$

[24] P. Qiao, J. F. Davalos, and J. Wang, Local Buckling of Composite FRP Shapes by Discrete Plate Analysis. *Journal of Structural Engineering*, Vol. 127, 245–255, 2001.

[25] L. P. Kollár, Discussion on the paper of Qiao, P. Davalos, J. F. and Wang, J.: Local Buckling of Composite FRP Shapes by Discrete Plate Analysis. *Journal of Structural Engineering,* Vol 128, 1091–1093, 2002.

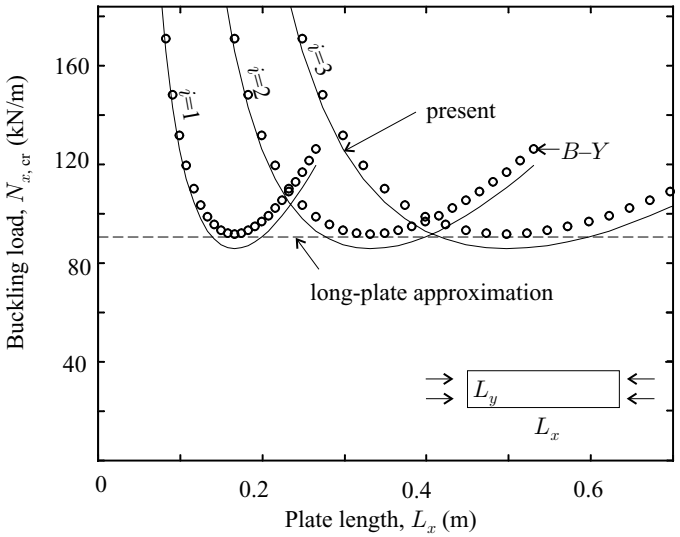

Figure 4.29: Buckling loads of the plate in Example 4.8. The results shown are by Eq. (4.148) (labeled as "present"), by Bank and Yin's equations, and by the long-plate approximation.

With these approximations of ξ and ξ', Eq. (4.150) overestimates the buckling load by less than 3.5 percent when $0 < K \leq 1$ and by less than 6.5 percent when $1 < K \leq 3$, where K is a stiffness parameter defined as

$$K = \frac{2D_{66} + D_{12}}{\sqrt{D_{11}D_{22}}}. \tag{4.153}$$

For most practical layups K is less than 3.

Equation (4.150) is included in Table 4.8 (page 123).

The value of $N_{x,\mathrm{cr}}$ must be calculated for different values of i ($i = 1, 2, \ldots$), and, generally, the lowest resulting value is of interest.

The buckling load is a function of the length of the plate L_x (Fig. 4.23). For each value of i the lowest buckling load is the same as the lowest buckling load of the corresponding long plate given subsequently in the fourth row of Table 4.11 (page 136).

One Unloaded Edge is Rotationally Restrained; the Other is Free

The plate is rotationally restrained along the $y = 0$ edge and is free along the $y = L_y$ edge (Fig. 4.30, right). An exact analysis resulting in transcendental equations

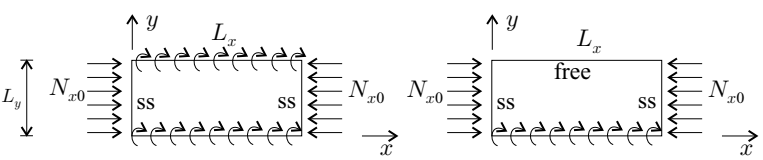

Figure 4.30: Uniaxially loaded rectangular plate with two rotationally restrained edges or with one rotationally restrained and one free edge.

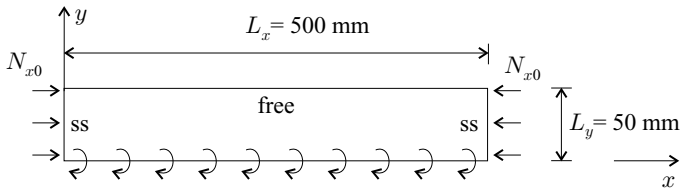

Figure 4.31: The plate in Example 4.9.

for the buckling loads $N_{x,\mathrm{cr}}$ is given by Bank and Yin.[26] Here, we present an approximate analysis, which yields a closed-form expression for $N_{x,\mathrm{cr}}$.

The buckling load of a plate with a rotationally restrained edge must be between the buckling load of a plate with a simply supported edge (Table 4.9, first row, page 125) and the buckling load of a plate with a built-in edge (Table 4.9, fourth row). We combine the expressions for plates with a simply supported and with a built-in edge and write

$$N_{x,\mathrm{cr}} = \frac{\pi^2 D_{11}}{l_x^2} + \xi'' \frac{1.25 l_x^2 D_{22}}{L_y^4} + \frac{12 D_{66}}{L_y^2}, \tag{4.154}$$

where $l_x = L_x/i$ is the length of the half buckling wave in the x direction, $i = 1, 2, \ldots$ is the number of half waves in the x direction, and ξ'' is a parameter that depends on the supports along the unloaded edge. This parameter is zero for a plate with a simply supported unloaded edge and is equal to unity for a plate with a built-in unloaded edge. The value of ξ'' may be approximated by[27]

$$\xi'' = \frac{1}{1 + 4.12\zeta}, \tag{4.155}$$

where ζ is the parameter of restraint given by Eq. (4.152).

Equation (4.154) may underestimate the buckling load by up to 14 percent.

The value of $N_{x,\mathrm{cr}}$ must be calculated for different values of i ($i = 1, 2, \ldots$), and, generally, the lowest resulting $N_{x,\mathrm{cr}}$ is the value of interest.

The buckling load is a function of the length of the plate L_x (Fig. 4.23). For each value of i the lowest buckling load is the same as the lowest buckling load of the corresponding long plate given subsequently in the sixth row of Table 4.11 (page 136).

4.9 Example. *A rectangular plate with length $L_x = 0.5$ m and width $L_y = 0.05$ m is made of graphite epoxy unidirectional plies with the fibers oriented along the x-axis of the plate (Fig. 4.31). The material properties are given in Table 3.6 (page 81). The layup is* $[0_{20}]$. *One of the long edges is rotationally restrained while the other long edge is free. The short edges are simply supported. The rotational spring constant of the edge is $\widetilde{k} = 129.4$ N. The plate is subjected to uniform compressive loads in the x direction. Calculate the buckling load.*

[26] L. C. Bank and J. Yin, Buckling of Orthotropic Plates with Free and Rotationally Restrained Unloaded Edges. *Thin-Walled Structures*, Vol. 24, 83–96, 1996.

[27] L. P. Kollár, Buckling of Unidirectionally Loaded Composite Plates with One Free and One Rotationally Restrained Unloaded Edge. *Journal of Structural Engineering*, Vol 128, 1202–1211, 2002.

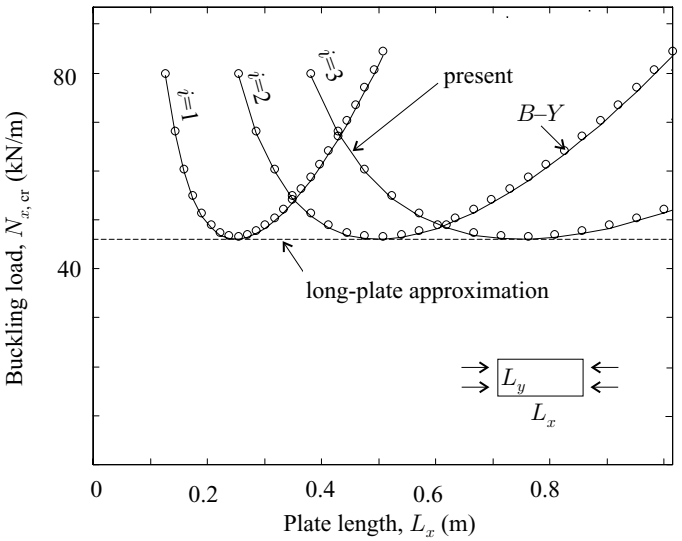

Figure 4.32: Buckling loads of the plate in Example 4.9. The results shown are by Eq. (4.156) (labeled as "present"), by Bank and Yin's equations, and by the long-plate approximation.

Solution. The expression in Table 4.9, fifth row (page 125), together with the stiffnesses $D_{11} = 99.25\,\mathrm{N\cdot m}$, $D_{22} = 6.47\,\mathrm{N\cdot m}$, $D_{12} = 1.94\,\mathrm{N\cdot m}$, $D_{66} = 3.03\,\mathrm{N\cdot m}$ (Table 3.7, page 84) gives

$$N_{x,\mathrm{cr}} = \frac{\pi^2 D_{11}}{l_x^2} + \frac{1.25}{1+4.12\zeta}\frac{l_x^2 D_{22}}{L_y^4} + \frac{12 D_{66}}{L_y^2}$$
$$= 979.5\frac{1}{l_x^2} + 0.253\times 10^6 l_x^2 + 14\,560, \tag{4.156}$$

where $l_x = L_x/i$ and ζ is the parameter of restraint (Eq. 4.152):

$$\zeta = \frac{D_{22}}{\widetilde{k} L_y} = 1. \tag{4.157}$$

The buckling loads for $i = 1, 2, 3, 4, 5, 6$ are

i	1	2	3	4	5	6
$N_{x,\mathrm{cr}}$ (kN/m)	81.67	46.03	56.85	81.20	115.04	157.37

The lowest buckling load corresponds to $i = 2$ and is 46.03 kN/m.

The buckling loads for plates with the same width but with different lengths are given by solid lines in Figure 4.32. The buckling loads calculated by the equations of Bank and Yin[28] are also included in this figure. The approximate expression (Eq. 4.156) underestimates $N_{x,\mathrm{cr}}$, and, hence, is a conservative estimate.

The long-plate expression gives the buckling load of this plate as 46.16 kN/m (Example 4.12, page 139). This value is also shown in Figure 4.32.

[28] L. C. Bank and J. Yin, Buckling of Orthotropic Plates with Free and Rotationally Restrained Unloaded Edges. *Thin-Walled Structures*, Vol. 24, 83–96, 1996.

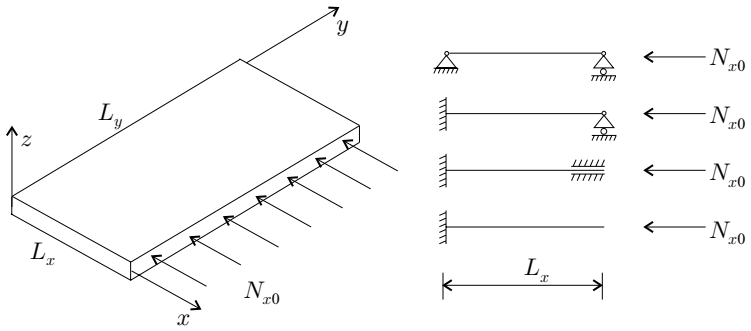

Figure 4.33: Long plate subjected to a uniform compressive edge load and the different types of supports along the long edges.

4.3.5 Long Plates

We consider a long rectangular plate of constant thickness whose length is large compared with its width.

Uniform Compressive Load Along the Long Edge

The length of the plate is L_y and the width is L_x ($L_y \gg L_x$). The supports along the long edges are as shown in Figure 4.33. A uniform compressive load N_{x0} is applied along one of the long edges of the plate. We wish to determine the lowest value of the applied under which the plate buckles.

We treat the plate as long and assume that it undergoes cylindrical deformation along its length (Fig. 4.4). This approximation is reasonable when $L_y > 3L_x\sqrt[4]{D_{11}/D_{22}}$ (Eq. 4.19).

When three in-plane loads N_{x0}, N_{y0}, and N_{xy0} act on the plate (Fig. 4.14, right), the equilibrium equations in the x, y, and z directions (Fig. 4.1) are[29]

$$\begin{aligned}
\frac{\partial N_x}{\partial x} + \frac{\partial N_{xy}}{\partial y} &= 0 \\
\frac{\partial N_y}{\partial y} + \frac{\partial N_{xy}}{\partial x} &= 0 \\
\frac{\partial V_x}{\partial x} + \frac{\partial V_y}{\partial y} &= N_{x0}\frac{d^2w^o}{dx^2} + N_{y0}\frac{d^2w^o}{dy^2} + 2N_{xy0}\frac{d^2w^o}{dxdy},
\end{aligned} \tag{4.158}$$

where N_x, N_y, and N_{xy} are the in-plane forces (per unit length), and V_x and V_y are the transverse shear forces (per unit length) (Fig. 4.1). Moment equilibria about the y- and z- axes give (Eq. 4.5)

$$V_x = \frac{\partial M_x}{\partial x} + \frac{\partial M_{xy}}{\partial y} \qquad V_y = \frac{\partial M_y}{\partial y} + \frac{\partial M_{xy}}{\partial x}, \tag{4.159}$$

where M_x and M_{xy} are, respectively, the bending moment and twist moment per unit length. Away from the short edges the forces and moments do not vary along

[29] S. P. Timoshenko and J. Gere, *Theory of Elastic Stability*. 2nd edition. McGraw-Hill, New York, 1961, pp. 333–334.

the length of the plate. Thus, from the last of Eq. (4.158) and from the first of Eq. (4.159) we have

$$\frac{dV_x}{dx} - N_{x0}\frac{d^2w^o}{dx^2} = 0 \tag{4.160}$$

$$\frac{dM_x}{dx} - V_x = 0. \tag{4.161}$$

By substituting V_x from Eq. (4.161) into Eq. (4.160) we obtain the equilibrium equation

$$\frac{d^2M_x}{dx^2} - N_{x0}\frac{d^2w^o}{dx^2} = 0. \tag{4.162}$$

As was shown in Section 4.2.2, when the plate is symmetrical, the bending moment M_x is (see Eq. 4.25)

$$M_x = D_{11}\kappa_x. \tag{4.163}$$

Equations (4.162), (4.21), and (4.163) yield

$$D_{11}\frac{d^4w^o}{dx^4} + N_{x0}\frac{d^2w^o}{dx^2} = 0 \qquad \begin{matrix}\text{long plate}\\ \text{symmetrical layup.}\end{matrix} \tag{4.164}$$

The equation describing the buckling of an isotropic beam subjected to an axial load $\widehat{N}_{x0}$ is[30]

$$EI\frac{d^4w}{dx^4} + \widehat{N}_{x0}\frac{d^2w}{dx^2} = 0 \qquad \text{isotropic beam.} \tag{4.165}$$

The structure of the two preceding equations is the same. Therefore, the buckling load of a long plate (symmetrical layup) may be obtained by substituting the value of D_{11} for EI in the expression for the buckling load of the corresponding isotropic beam.

It was shown in Section 4.2.2 that when the layup of the plate is unsymmetrical, the deflection may be obtained by replacing EI/p' by Ψ/p in the expression for the deflection of the corresponding isotropic beam. By similar arguments it can be shown that the buckling load of a long plate with unsymmetrical layup may be obtained by substituting the value of Ψ for EI in the expression for the buckling load of the corresponding isotropic beam. (Ψ is given by Eq. 4.52.)

4.10 Example. *A* 0.7*-m-long and* 0.2*-m-wide rectangular plate is made of graphite epoxy. The material properties are given in Table 3.6 (page 81). The layup is* $[\pm 45_2^f/0_{12}/\pm 45_2^f]$. *The 0-degree plies are parallel to the short edge of the plate. The plate is either simply supported or built-in along all four edges. The plate is subjected to uniform compressive loads along the long edges (Fig. 4.34). Calculate the buckling load.*

[30] Ibid., p. 2.

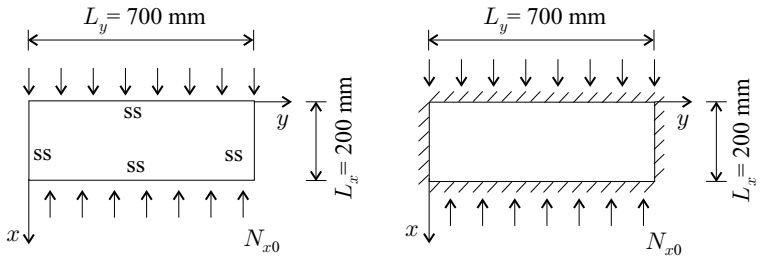

Figure 4.34: The plates in Example 4.10.

Solution. The plate may be treated as "long" (Example 4.1, page 96). The buckling loads of the corresponding beam are (Eq. 6.337)

$$\widehat{N}_{\text{cr}} = \frac{\pi^2 EI}{L^2} \qquad \text{(ss)} \tag{4.166}$$

$$\widehat{N}_{\text{cr}} = \frac{4\pi^2 EI}{L^2} \qquad \text{(built-in).} \tag{4.167}$$

The buckling loads of the plate are obtained by replacing EI by D_{11} (see page 133) as follows:

$$N_{x,\text{cr}} = \frac{\pi^2 D_{11}}{L_x^2} \qquad \text{(ss)} \tag{4.168}$$

$$N_{x,\text{cr}} = \frac{4\pi^2 D_{11}}{L_x^2} \qquad \text{(built-in).} \tag{4.169}$$

With the value of $D_{11} = 45.30\ \text{N} \cdot \text{m}$ (Table 3.7, page 84) and with $L_x = 0.2$ m, the buckling loads are

$$N_{x,\text{cr}} = 11.18\ \text{kN/m} \qquad \text{(ss)} \tag{4.170}$$

$$N_{x,\text{cr}} = 44.71\ \text{kN/m} \qquad \text{(built-in).} \tag{4.171}$$

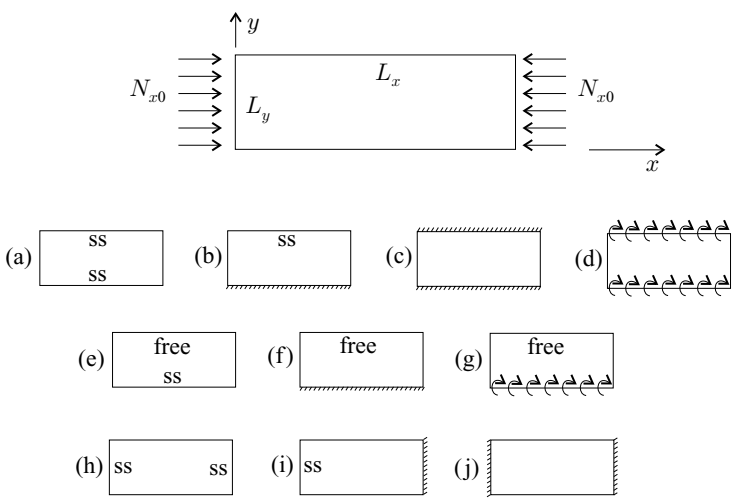

Figure 4.35: Long plate subjected to uniaxial load (top) and the supports along the long (a to g) and short edges (h to j).

Uniform Compressive Load Along the Short Edge – Orthotropic and Symmetrical Layup

We consider a plate with length L_x and width L_y ($L_x \gg L_y$) (Fig. 4.35). The layup of the plate is orthotropic and symmetrical. The possible edge supports are shown in Figure 4.35. The plate is subjected to a uniaxial compressive load N_{x0} (Fig. 4.35, top).

Simply supported and built-in edges. The buckling loads of long plates whose long edges are either simply supported or built-in (Fig. 4.35, a, b, c) are given below.

The buckled shape of a long plate away from the loaded edges is the same as the buckled shape of a plate simply supported along the loaded edges. Therefore, the buckling loads of the long plate are also given by Eq. (4.141). We are interested in the lowest buckling load. We denote the buckling length corresponding to this buckling load by l_x^o. With this notation, Eq. (4.141) becomes

$$N_{x,\mathrm{cr}} = D_{11}\pi^2 \frac{1}{l_x^{o2}} + D_{22}\frac{\alpha_3^4}{\pi^2}\frac{l_x^{o2}}{L_y^4} + 2\left(D_{12} + 2D_{66}\right)\frac{\alpha_5}{L_y^2}. \tag{4.172}$$

The necessary condition that gives the lowest $N_{x,\mathrm{cr}}$ is $d\left(N_{x,\mathrm{cr}}\right)/d(l_x^o) = 0$. This condition and Eq. (4.172) give

$$l_x^o = \frac{\pi}{\alpha_3} L_y \sqrt[4]{\frac{D_{11}}{D_{22}}}. \tag{4.173}$$

Table 4.10. The buckling lengths corresponding to the lowest buckling load with unidirectionally loaded long plates (orthotropic and symmetrical layup, $\xi = \frac{1}{1+10\zeta}$, $\zeta = \frac{D_{22}}{\widetilde{k}L_y}$); L_y is the width, and $\widetilde{k}$ is the spring constant. Plates with one simply supported and one free long edge buckle with a long wave in the x direction, as illustrated in Figure 4.25.

Supports	Buckling length l_x^o
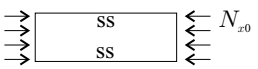	$L_y\sqrt[4]{\frac{D_{11}}{D_{22}}}$
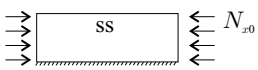	$0.8L_y\sqrt[4]{\frac{D_{11}}{D_{22}}}$
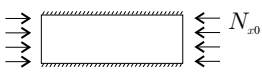	$0.664L_y\sqrt[4]{\frac{D_{11}}{D_{22}}}$
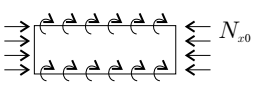	$\sqrt[4]{\frac{1}{1+4.139\xi}}L_y\sqrt[4]{\frac{D_{11}}{D_{22}}}$
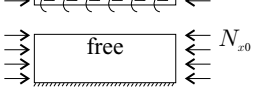	$1.675L_y\sqrt[4]{\frac{D_{11}}{D_{22}}}$
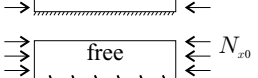	$1.675\sqrt[4]{1+4.12\zeta}\,L_y\sqrt[4]{\frac{D_{11}}{D_{22}}}$
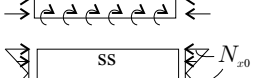	$0.707L_y\sqrt[4]{\frac{D_{11}}{D_{22}}}$

Table 4.11. The lowest buckling loads of long plates with orthotropic and symmetrical layup ($\xi = \frac{1}{1+10\zeta}$, $\zeta = \frac{D_{22}}{\widetilde{k}L_y}$, $\nu = \frac{D_{12}}{2D_{66}+D_{12}}$, $K = \frac{2D_{66}+D_{12}}{\sqrt{D_{11}D_{22}}}$, $\eta = \frac{1}{\sqrt{1+(7.22-3.55\nu)\zeta}}$). L_y is the width, and $\widetilde{k}$ is the spring constant. The buckling loads of long plates with one simply supported and one free long edge are given in the first three rows of Table 4.9 (page 125).

Supports	Buckling load $N_{x,\mathrm{cr}}$ or $N_{xy,\mathrm{cr}}$
ss, ss; N_{x0}	$\frac{\pi^2}{L_y^2}[2\sqrt{D_{11}D_{22}} + 2(D_{12}+2D_{66}])$
ss; N_{x0}	$\frac{\pi^2}{L_y^2}[3.125\sqrt{D_{11}D_{22}} + 2.33(D_{12}+2D_{66})]$
N_{x0}	$\frac{\pi^2}{L_y^2}[4.53\sqrt{D_{11}D_{22}} + 2.62(D_{12}+2D_{66})]$
N_{x0}	$\frac{\pi^2}{L_y^2}[2\sqrt{1+4.139\xi}\sqrt{D_{11}D_{22}} + (2+0.62\xi^2)(D_{12}+2D_{66})]$
free; N_{x0}	$\frac{\sqrt{D_{11}D_{22}}}{L_y^2}[15.1K\sqrt{1-\nu} + 7(1-K)]$ when $K \le 1$
	$\frac{\sqrt{D_{11}D_{22}}}{L_y^2}[15.1\sqrt{1-\nu} + (K-1)6(1-\nu)]$ when $1 < K$
free; N_{x0}	$\frac{\sqrt{D_{11}D_{22}}}{L_y^2}\left[K(\eta 15.1\sqrt{1-\nu} + (1-\eta)6(1-\nu)) + \frac{7(1-K)}{\sqrt{1+4.12\zeta}}\right]$ when $K \le 1$
	$\frac{\sqrt{D_{11}D_{22}}}{L_y^2}[\eta 15.1\sqrt{1-\nu} + (K-\eta)6(1-\nu)]$ when $1 < K$
ss, ss; N_{x0}	$\frac{\pi^2}{L_y^2}\left[13.9\sqrt{D_{11}D_{22}} + 11.1(D_{12}+2D_{66})\right]$
ss, ss; N_{xy0}	$\frac{4}{L_y^2}\sqrt[4]{D_{11}D_{22}^3}(8.125 + 5.045K)$ when $K \le 1$
	$\frac{4}{L_y^2}\sqrt{D_{22}(D_{12}+2D_{66})}\left(11.71 + \frac{1.46}{K^2}\right)$ when $1 < K$
N_{xy0}	$\frac{4}{L_y^2}\sqrt[4]{D_{11}D_{22}^3}(15.07 + 7.08K)$ when $K \le 1$
	$\frac{4}{L_y^2}\sqrt{D_{22}(D_{12}+2D_{66})}\left(18.59 + \frac{3.56}{K^2}\right)$ when $1 < K$

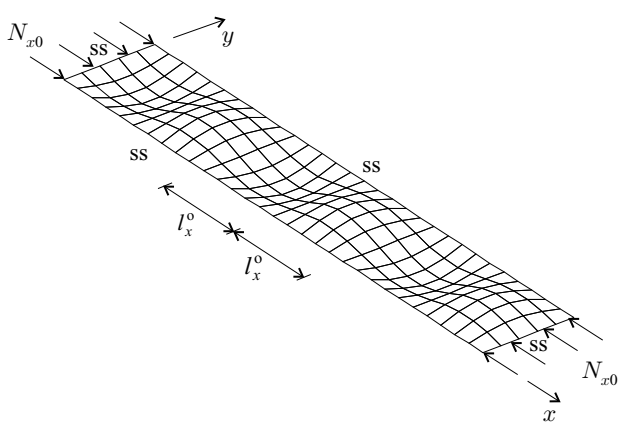

Figure 4.36: Buckled shape of a long plate with simply supported edges.

As before, the buckling length l_x^o is the half wavelength of the buckled shape. We obtain the lowest buckling load by introducing Eq. (4.173) into Eq. (4.172) as follows:

$$N_{x,\mathrm{cr}} = \frac{2}{L_y^2}\left[\alpha_3^2\sqrt{D_{11}D_{22}} + \alpha_5\left(D_{12} + 2D_{66}\right)\right]. \tag{4.174}$$

The values of α_3 and α_5 to be used are those given in Table 4.7 (page 120) for $j = 1$. The resulting buckling lengths and buckling loads are listed in the first three rows of Tables 4.10 and 4.11.

Both long edges are rotationally restrained. The plate is rotationally restrained along the unloaded long edges (Fig. 4.35, d). The buckling load for a plate with arbitrary length is given by Eq. (4.150). The value of l_x that results in the lowest buckling load is denoted by l_x^o. When the plate is long, the necessary condition that gives the lowest $N_{x,\mathrm{cr}}$ is $d\left(N_{x,\mathrm{cr}}\right)/d\left(l_x^o\right) = 0$. This condition and Eq. (4.150), with l_x replaced by l_x^o, give

$$l_x^o = \sqrt[4]{\frac{1}{1+4.139\xi}}\,L_y\sqrt[4]{\frac{D_{11}}{D_{22}}}, \tag{4.175}$$

where ξ is given by Eq. (4.151). Equations (4.150), (4.151), and (4.175) yield

$$N_{x,\mathrm{cr}} = \frac{\pi^2}{L_y^2}\left[2\sqrt{1+4.139\xi}\sqrt{D_{11}D_{22}} + \left(2+0.62\xi^2\right)\left(D_{12}+2D_{66}\right)\right]. \tag{4.176}$$

This result is included in Table 4.11.

One long edge is simply supported; the other is free. The buckling loads are given in the first three rows of Table 4.9 (page 125) for plates with one of the edges parallel to the load direction simply supported and the other edge free. These expressions are applicable regardless of the aspect ratio of the plate and hence may be used to calculate the buckling loads of long plates with one simply supported and one free long edge (Fig. 4.35, e).

One long edge is built-in; the other is free. The buckling loads of plates with one of the unloaded edges built-in and the other one free (Fig. 4.35, f) can be calculated by Eq. (4.147). The value of l_x that results in the lowest buckling load is denoted by l_x^o. When the plate is long, the necessary condition that gives the lowest $N_{x,\mathrm{cr}}$ is $d\left(N_{x,\mathrm{cr}}\right)/d\left(l_x^o\right) = 0$. This condition and Eq. (4.147), with l_x replaced by l_x^o,

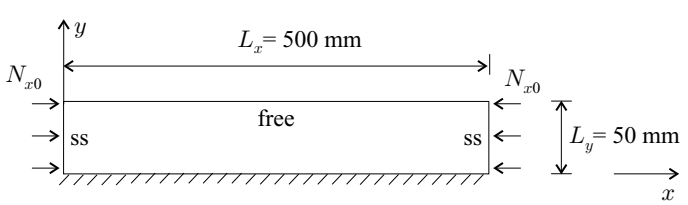

Figure 4.37: The plate in Example 4.11.

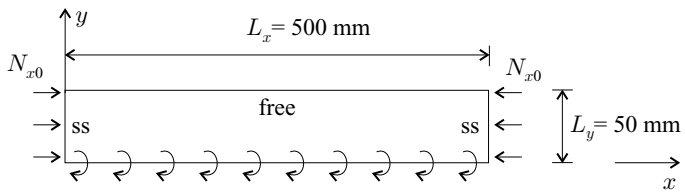

Figure 4.38: Illustration of the plate in Example 4.12.

give

$$l_x^{\mathrm{o}} = 1.675 L_y \sqrt[4]{\frac{D_{11}}{D_{22}}}. \tag{4.177}$$

Equations (4.147) and (4.177) yield

$$N_{x,\mathrm{cr}} = 7\frac{\sqrt{D_{11}D_{22}}}{L_y^2} + 12\frac{D_{66}}{L_y^2}. \tag{4.178}$$

This expression gives a conservative estimate of the buckling load and underestimates it by less than 14 percent. More accurate expressions, determined by Kollár,[31] are given in Table 4.11 (page 136). The accuracy of these equations is about 2 percent when $0 < K \leq 1$ and is about 5 percent when $1 < K \leq 3$.

4.11 Example. *A rectangular plate with length $L_x = 0.5$ m and width $L_y = 0.05$ m is made of graphite epoxy unidirectional plies with the fibers oriented along the x-axis of the plate (Fig. 4.37). The material properties are given in Table 3.6 (page 81). The layup is* $[0_{20}]$. *One of the long edges is built-in; the other long edge is free. The short edges are simply supported. The plate is subjected to uniform compressive loads in the x direction. Calculate the buckling load.*

Solution. The stiffnesses of the plate are $D_{11} = 99.25$ N · m, $D_{22} = 6.47$ N · m, $D_{12} = 1.94$ N · m, $D_{66} = 3.03$ N · m (Table 3.7, page 84). The buckling length l_x^{o} is (Eq. 4.177)

$$l_x^{\mathrm{o}} = 1.675 L_y \sqrt[4]{\frac{D_{11}}{D_{22}}} = 0.166 \text{ m}. \tag{4.179}$$

Since the plate is longer than the buckling length ($L_x > l_x^{\mathrm{o}}$), we may treat the plate as "long." From Table 4.11 (page 136), K and ν are

$$K = \frac{2D_{66} + D_{12}}{\sqrt{D_{11}D_{22}}} = 0.316 \qquad \nu = \frac{D_{12}}{2D_{66} + D_{12}} = 0.242. \tag{4.180}$$

[31] L. P. Kollár, Buckling of Unidirectionally Loaded Composite Plates with One Free and One Rotationally Restrained Unloaded Edge. *Journal of Structural Engineering*, Vol 128, 1202–1211, 2002.

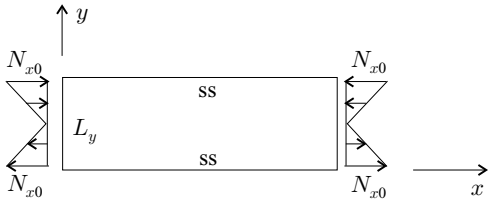

Figure 4.39: Long rectangular plate subjected to linearly varying load.

From Table 4.11 (fifth row) we obtain ($K < 1$)

$$N_{x,\mathrm{cr}} = \frac{\sqrt{D_{11}D_{22}}}{L_y^2}(15.1K\sqrt{1-\nu} + 7\,(1-K)\,) = 90.640 \text{ kN/m}. \tag{4.181}$$

One long edge is rotationally restrained the other is free. The buckling loads of plates with one of the unloaded edges rotationally restrained and the other one free (Fig. 4.35, g) can be calculated by Eq. (4.154). The value of l_x that results in the lowest buckling load is denoted by l_x^{o}. When the plate is long the necessary condition that gives the lowest $N_{x,\mathrm{cr}}$ is $d\,(N_{x,\mathrm{cr}})\,/d\,(l_x^{\mathrm{o}}) = 0$. This condition and Eq. (4.154), with l_x replaced by l_x^{o}, give

$$l_x^{\mathrm{o}} = 1.675 L_y \sqrt[4]{\frac{D_{11}}{D_{22}}\,(1 + 4.12\zeta\,)}, \tag{4.182}$$

where ζ is the parameter of restraint given by Eq. (4.152). Equations (4.154) and (4.182) yield

$$N_{x,\mathrm{cr}} = \frac{7}{\sqrt{1+4.12\zeta}}\frac{\sqrt{D_{11}D_{22}}}{L_y^2} + 12\frac{D_{66}}{L_y^2}. \tag{4.183}$$

This expression gives a conservative estimate of the buckling load and underestimates it by less than 14 percent. More accurate expressions, determined by Kollár,[32] are included in Table 4.11 (page 136). The accuracy of these equations is about 2 percent when $0 < K \leq 1$ and is about 5 percent when $1 < K \leq 3$.

4.12 Example. *A rectangular plate with length $L_x = 0.5\,m$ and width $L_y = 0.05\,m$ is made of graphite epoxy unidirectional plies with the fibers oriented along the x-axis of the plate (Fig. 4.38). The material properties are given in Table 3.6 (page 81). The layup is* $[0_{20}]$. *One of the long edges is rotationally restrained while the other long edge is free. The short edges are simply supported. The rotational spring constant of the edge is $\widetilde{k} = 129.4\,N$. The plate is subjected to uniform compressive loads in the x direction. Calculate the buckling load.*

Solution. The bending stiffnesses of the plate are $D_{11} = 99.25$ N·m, $D_{22} = 6.47$ N·m, $D_{12} = 1.94$ N·m, $D_{66} = 3.03$ N·m (Table 3.7, page 84) and $\zeta = 1$

[32] Ibid.

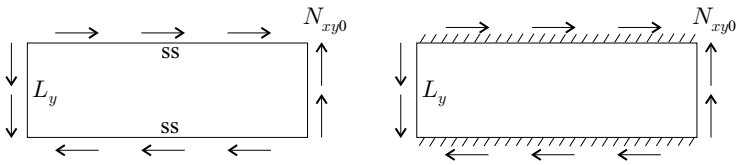

Figure 4.40: Long rectangular plate subjected to shear load.

(Eq. 4.157). The buckling length l_x^o is (Eq. 4.182)

$$l_x^o = 1.675 L_y \sqrt[4]{\frac{D_{11}}{D_{22}}(1 + 4.12\zeta)} = 0.249 \text{ m}. \tag{4.184}$$

Since the plate is longer than the buckling length ($L_x > l_x^o$), we may treat the plate as "long." With the parameters K and ν given by Eq. (4.180), from Table 4.11, sixth row (page 136) we obtain ($K < 1$)

$$\begin{aligned} N_{x,\text{cr}} &= \frac{\sqrt{D_{11} D_{22}}}{L_y^2}\left\{K\left[\eta 15.1\sqrt{1-\nu} + (1-\eta)6(1-\nu)\right] + \frac{7(1-K)}{\sqrt{1+4.12\zeta}}\right\} \\ &= 46.16 \text{ kN/m}, \end{aligned} \tag{4.185}$$

where η is (Table 4.11)

$$\eta = \frac{1}{\sqrt{1 + (7.22 - 3.55\nu)\,\zeta}} = 0.369. \tag{4.186}$$

Linearly Varying Load Along the Short Edge – Orthotropic and Symmetrical Layup

The layup of the plate is orthotropic and symmetrical. The short edges of the plate are either simply supported or built-in, as shown in the bottom row of Figure 4.35. Both long edges are simply supported. Along the short edges the plate is subjected to a linearly varying normal load with maximum intensity N_{xo} (Fig. 4.39). The lowest buckling load $N_{x,\text{cr}}$ at which the plate buckles is given by Lekhnitskii[33]

$$N_{x,\text{cr}} = \frac{\pi^2}{L_y^2}\left[13.9\sqrt{D_{11} D_{22}} + 11.1(D_{12} + 2D_{66})\right]. \tag{4.187}$$

This result is included in Table 4.11 (page 136). The buckling length is given in Table 4.10 (page 135).

Shear Load – Orthotropic and Symmetrical Layup

The layup of the plate is orthotropic and symmetrical. Both long edges are either simply supported or built-in (Fig. 4.40). Regardless of the manner in which the long edges are supported, the short edges may be either simply supported or built-in.

[33] S. G. Lekhnitskii, *Anisotropic Plates*. Gordon and Breach Science Publishers, New York, 1968, pp. 462–463.

Table 4.12. The parameter β_1 in Eq. (4.188) as a function of $K = \frac{2D_{66}+D_{12}}{\sqrt{D_{11}D_{22}}}$

	$0 \le K \le 1$	$1 < K \le \infty$
Simply supported	$8.125 + 5.045K$	$11.71 + \frac{1.46}{K^2}$
Built-in	$15.07 + 7.08K$	$18.59 + \frac{3.56}{K^2}$

The plate is subjected to a uniform shear load N_{xy0}. We wish to determine the lowest value of the load $N_{xy,\,\mathrm{cr}}$ at which the plate buckles.

Seydel derived the lowest buckling loads for infinitely long plates. The resulting expressions, as quoted by Whitney,[34] are

$$N_{xy,\,\mathrm{cr}} = \begin{cases} \dfrac{4\beta_1}{L_y^2}\sqrt[4]{D_{11}D_{22}^3} & 0 \le K \le 1 \\ \dfrac{4\beta_1}{L_y^2}\sqrt{D_{22}\,(D_{12}+2D_{66})} & 1 < K \le \infty\,. \end{cases} \tag{4.188}$$

Seydel gave numerical values for β_1. These values can be approximated within 2 percent by the expressions in Table 4.12.

4.4 Free Vibration of Rectangular Plates

When a plate undergoes free, undamped vibration, the deflection of the plate is sinusoidal with respect to time t,

$$w^{\mathrm{o}} = \overline{w}^{\mathrm{o}} \sin(\omega t) = \overline{w}^{\mathrm{o}} \sin(2\pi f t)\,, \tag{4.189}$$

where ω is the circular frequency and f is the natural frequency. The period of vibration T is

$$T = \frac{1}{f} \qquad \omega = 2\pi f = \frac{2\pi}{T}, \tag{4.190}$$

and $\overline{w}^{\mathrm{o}}$ is the deflection of the plate at time $t = T/4$.

In this section we obtain the natural frequencies and, hence, the periods of vibration, of freely vibrating plates.

4.4.1 Long Plates

We consider a long rectangular plate whose length L_y is large compared with its width L_x. The mass of the plate is uniform. The edges may be built-in, simply supported, or free (Fig. 4.41).

[34] J. M. Whitney, *Structural Analysis of Laminated Anisotropic Plates.* Technomic, Lancaster, Pennsylvania, 1987, p. 118.

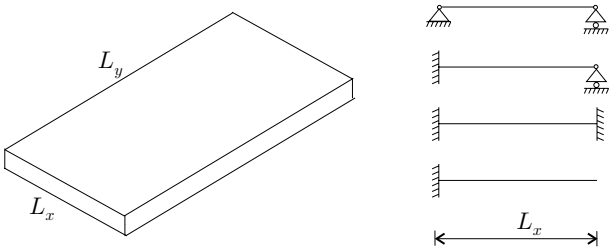

Figure 4.41: The different types of supports along the long edges of a freely vibrating long plate.

When $L_y > 3L_x\sqrt[4]{D_{11}/D_{22}}$ (Eq. 4.19), a laterally loaded plate may be approximated as a long plate undergoing cylindrical deformation (Fig. 4.4), and the equilibrium equations are (Eqs. 4.22 and 4.23)

$$\frac{dV_x}{dx} + p = 0 \tag{4.191}$$

$$\frac{dM_x}{dx} - V_x = 0, \tag{4.192}$$

where p is the lateral force (per unit area) acting on the plate. In the case of a freely vibrating plate, p is the inertia force, which, with the use of Eq. (4.189), is

$$p = -\rho\frac{\partial^2 w^o}{\partial t^2} = \rho\,(2\pi f)^2\,\overline{w}^o \sin(2\pi f t)\,, \tag{4.193}$$

where ρ is the mass of the plate per unit area. Equations (4.191)–(4.193) give

$$\frac{d^2 M_x}{dx^2} + \rho\,(2\pi f)^2\,w^o = 0. \tag{4.194}$$

When the plate is symmetrical, the bending moment is (see Eqs. 4.25 and 4.21)

$$M_x = D_{11}\kappa_x = -D_{11}\frac{\partial^2 w^o}{\partial x^2}\cdot \tag{4.195}$$

With this moment, Eq. (4.194) yields

$$\frac{d^4 w^o}{dx^4} - \frac{\rho}{D_{11}}\,(2\pi f)^2\,w^o = 0 \qquad \begin{array}{l}\text{long plate}\\ \text{symmetrical layup.}\end{array} \tag{4.196}$$

The equation of a freely vibrating isotropic beam is[35]

$$\frac{d^4 w}{dx^4} - \frac{\rho'}{EI}\,(2\pi f)^2\,w = 0 \qquad \text{isotropic beam,} \tag{4.197}$$

where ρ' is the mass of the beam per unit length.

[35] W. Weaver, S. P. Timoshenko, and D. H. Young, *Vibration Problems in Engineering.* 5th edition. John Wiley & Sons, New York, 1990, p. 417.

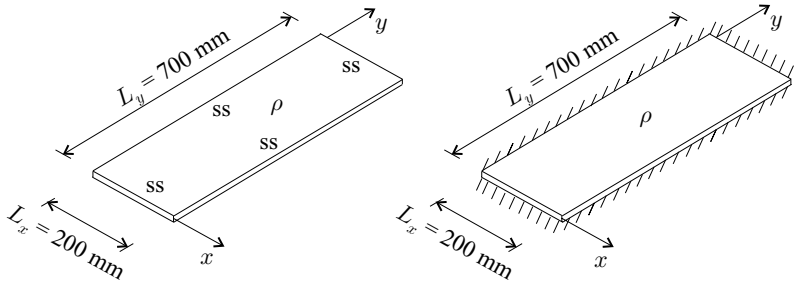

Figure 4.42: The plates in Example 4.13.

From Eqs. (4.196) and (4.197) we observe that the natural frequencies of a long plate (symmetrical layup) with bending stiffness D_{11} and mass ρ are the same as the natural frequencies of an isotropic beam with bending stiffness EI and mass ρ'. Thus, the natural frequencies of a long plate (symmetrical layup) may be obtained by replacing EI/ρ' by D_{11}/ρ in the expression for the natural frequencies of the corresponding isotropic beam.

The natural frequencies of a long plate with unsymmetrical layup may be obtained by replacing EI/ρ' by Ψ/ρ in the expression for the natural frequencies of the corresponding isotropic beam (where Ψ is given by Eq. 4.52).

4.13 Example. *A* 0.7*-m-long and* 0.2*-m-wide rectangular plate is made of graphite epoxy. The material properties are given in the Table 3.6 (page 81). The layup is* $[\pm 45_2^{\mathrm{f}}/0_{12}/\pm 45_2^{\mathrm{f}}]$. *The 0-degree plies are parallel to the short edge of the plate. The plate is either simply supported or built-in along all four edges (Fig. 4.42). The mass of the plate is uniform (*$\rho = 3.2$ *kg/m*^{2}*). Calculate the circular and natural frequencies.*

Solution. The plate may be treated as "long" (Example 4.1, page 96). The circular frequencies of the corresponding beam are (Eq. 6.398, and Table 6.13, page 308)

$$\omega_i = \sqrt{\frac{EI}{\rho'}}\frac{\mu_{Bi}^2}{L^2} \quad \mu_{Bi} = \pi, 2\pi, 3\pi, \ldots \qquad \text{(ss)} \tag{4.198}$$

$$\omega_i = \sqrt{\frac{EI}{\rho'}}\frac{\mu_{Bi}^2}{L^2} \quad \mu_{Bi} = 4.730, 7.853, 10.996, \ldots \qquad \text{(built-in).} \tag{4.199}$$

The circular frequencies of the plate are obtained by replacing EI/ρ' by D_{11}/ρ as follows:

$$\omega_i = \sqrt{\frac{D_{11}}{\rho}}\frac{\mu_{Bi}^2}{L_x^2} \quad \mu_{Bi} = \pi, 2\pi, 3\pi, \ldots \qquad \text{(ss)} \tag{4.200}$$

$$\omega_i = \sqrt{\frac{D_{11}}{\rho}}\frac{\mu_{Bi}^2}{L_x^2} \quad \mu_{Bi} = 4.730, 7.853, 10.996, \ldots \qquad \text{(built-in).} \tag{4.201}$$

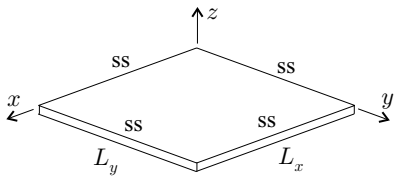

Figure 4.43: Rectangular simply supported (ss) plate.

With $D_{11} = 45.30\ \mathrm{N \cdot m}$ (Table 3.7, page 84) and $L_x = 0.2$ m, the circular frequencies are

$$\omega_1 = 928 \qquad \omega_2 = 3\,713 \qquad \omega_3 = 8\,355 \ \ 1/\mathrm{s} \qquad \text{(ss)} \tag{4.202}$$

$$\omega_1 = 2\,104 \qquad \omega_2 = 5\,801 \qquad \omega_3 = 11\,3731/\mathrm{s} \qquad \text{(built-in).} \tag{4.203}$$

The natural frequencies are $f = \omega/2\pi$ (Eq. 6.397)

$$f_1 = 148 \qquad f_2 = 591 \qquad f_3 = 1\,330\ \mathrm{Hz} \qquad \text{(ss)} \tag{4.204}$$

$$f_1 = 335 \qquad f_2 = 923 \qquad f_3 = 1\,810\ \mathrm{Hz} \qquad \text{(built-in).} \tag{4.205}$$

4.4.2 Simply Supported Plates – Symmetrical Layup

We consider a rectangular plate with dimensions L_x and L_y simply supported along its four edges (Fig. 4.43). The layup of the plate is symmetrical, $[B] = [0]$. The mass of the plate is uniform.

Following Whitney,[36] we obtain the natural frequencies of this plate by the energy method. By introducing w^{o} (see Eq. 4.189) into the expression for U (Eq. 4.55), we obtain

$$U = \overline{U} \sin^2(2\pi f t), \tag{4.206}$$

where $\overline{U}$ is defined as

$$\overline{U} = \frac{1}{2}\int_0^{L_x}\int_0^{L_y}\left[D_{11}\left(\frac{\partial^2 \overline{w}^{\mathrm{o}}}{\partial x^2}\right)^2 + D_{22}\left(\frac{\partial^2 \overline{w}^{\mathrm{o}}}{\partial y^2}\right)^2 + D_{66}\left(\frac{2\partial^2 \overline{w}^{\mathrm{o}}}{\partial x \partial y}\right)^2 + 2\left(D_{12}\frac{\partial^2 \overline{w}^{\mathrm{o}}}{\partial x^2}\frac{\partial^2 \overline{w}^{\mathrm{o}}}{\partial y^2} + D_{16}\frac{\partial^2 \overline{w}^{\mathrm{o}}}{\partial x^2}\frac{2\partial^2 \overline{w}^{\mathrm{o}}}{\partial x \partial y} + D_{26}\frac{\partial^2 \overline{w}^{\mathrm{o}}}{\partial y^2}\frac{2\partial^2 \overline{w}^{\mathrm{o}}}{\partial x \partial y}\right)\right] dy dx. \tag{4.207}$$

The kinetic energy of the plate is

$$K = \frac{1}{2}\int_0^{L_x}\int_0^{L_y}\rho\left(\frac{dw^{\mathrm{o}}}{dt}\right)^2 dy dx. \tag{4.208}$$

[36] J. M. Whitney, *Structural Analysis of Laminated Anisotropic Plates.* Technomic, Lancaster, Pennsylvania, 1987, p. 166.

Substitution of the deflection, given by Eq. (4.189), into this equation yields

$$K = \frac{1}{2}(2\pi f)^2 \cos^2(2\pi f t) \int_0^{L_x}\int_0^{L_y} \rho \overline{w}^{o2} dy dx. \tag{4.209}$$

According to the law of conservation of energy the change in strain energy from time $t = 0$ to time t equals the change in kinetic energy during this time

$$(U_t - U_{t=0}) = -(K_t - K_{t=0}). \tag{4.210}$$

Initially, at time $t = 0$ the strain energy is zero (Eq. 4.206), but at time $t = \frac{1}{4f}$ the kinetic energy is zero (Eq. 4.209). Thus, we have

$$U_{t=\frac{1}{4f}} = K_{t=0}. \tag{4.211}$$

Equation (4.211), together with Eqs. (4.206) and (4.209), yields

$$\frac{1}{2}(2\pi f)^2 \int_0^{L_x}\int_0^{L_y} \rho \overline{w}^{o2} dy dx = \overline{U}. \tag{4.212}$$

From this equation we obtain

$$(2\pi f)^2 = \frac{\overline{U}}{\frac{1}{2}\int_0^{L_x}\int_0^{L_y} \rho \overline{w}^{o2} dy dx}. \tag{4.213}$$

We use Rayleigh's energy method[37] to obtain the deflection. For the simply supported plate under consideration the geometrical boundary conditions require that the deflections be zero along the edges (Eq. 4.57) as follows:

$$w^o = 0 \quad \text{at} \quad \begin{cases} x = 0 & \text{and} \quad 0 \le y \le L_y \\ x = L_x & \text{and} \quad 0 \le y \le L_y \\ 0 \le x \le L_x & \text{and} \quad y = 0 \\ 0 \le x \le L_x & \text{and} \quad y = L_y. \end{cases} \tag{4.214}$$

The following deflection satisfies these geometrical boundary conditions:

$$w^o = \overline{w}^o \sin(2\pi f t), \tag{4.215}$$

where $\overline{w}^o$ is

$$\overline{w}^o = \sum_{i=1}^{I}\sum_{j=1}^{J} w_{ij} \sin\frac{i\pi x}{L_x} \sin\frac{j\pi y}{L_y}, \tag{4.216}$$

where I and J are the number of terms, chosen arbitrarily, for the summations and w_{ij} are constants. According to the Rayleigh principle the frequency of vibration of a conservative system has a minimum value in the neighborhood of the fundamental mode.[38] We express this principle in the form

$$\frac{\partial f}{\partial w_{ij}} = 0. \tag{4.217}$$

[37] L. Meirovitch, *Principles and Techniques of Vibrations*. Prentice-Hall, Upper Saddle River, New Jersey, 1997, pp. 518–522.

[38] Ibid., p. 520.

To determine the values of w_{ij}, we substitute Eqs. (4.207), (4.213), and (4.216) into this expression. Algebraic manipulations yield the following system of simultaneous algebraic equations:

$$\sum_{i=1}^{I}\sum_{j=1}^{J}\left(G_{mnij}-\lambda\delta_{mnij}\right)w_{ij}=0 \quad \begin{cases} i,m=1,2,3,\ldots,I \\ j,n=1,2,3,\ldots,J\,, \end{cases} \tag{4.218}$$

where λ is given by

$$\lambda=\frac{1}{4}\left(2\pi f\right)^2\rho L_x L_y. \tag{4.219}$$

For convenience, we introduce the contracted notation

$$k=(i-1)J+j \quad \begin{cases} i=1,2,3,\ldots,I \\ j=1,2,3,\ldots,J \end{cases} \tag{4.220}$$

$$l=(m-1)J+n \quad \begin{cases} m=1,2,3,\ldots,I \\ n=1,2,3,\ldots,J\,, \end{cases} \tag{4.221}$$

Equation (4.218) may now be written as

$$\sum_{k=1}^{I\times J}G_{kl}w_k=\lambda\sum_{k=1}^{I\times J}\delta_{kl}w_k \quad l=1,2,3,\ldots,I\times J, \tag{4.222}$$

where $G_{kl}\,(=G_{lk})$ and the Kronecker delta $\delta_{lk}\,(=\delta_{kl})$ are given in Table 4.1 (page 102). In expanded form Eq. (4.222) is

$$\left(\begin{bmatrix} G_{11} & \ldots & G_{1(I\times J)} \\ \vdots & \ddots & \\ G_{(I\times J)1} & & G_{(I\times J)(I\times J)} \end{bmatrix}-\lambda\begin{bmatrix} \delta_{11} & \ldots & \delta_{1(I\times J)} \\ \vdots & \ddots & \\ \delta_{(I\times J)1} & & \delta_{(I\times J)(I\times J)} \end{bmatrix}\right)\begin{Bmatrix} w_1 \\ \vdots \\ w_{(I\times J)} \end{Bmatrix}=\begin{Bmatrix} 0 \\ \vdots \\ 0 \end{Bmatrix}. \tag{4.223}$$

In the case of free vibration the deflection is nonzero. For nonzero deflections, Eq. (4.223) is satisfied when the determinant of the matrix in the parentheses is zero. At this condition λ is the eigenvalue of Eq. (4.223). There are $J\times I$ eigenvalues, denoted by λ_{ij}, which may readily be calculated by commercial software.

The natural frequencies are calculated from Eq. (4.219) as follows:

$$f_{ij}=\frac{1}{\pi}\sqrt{\frac{\lambda_{ij}}{\rho L_x L_y}}. \tag{4.224}$$

For an orthotropic plate $D_{16}=D_{26}=0$, and the eigenvalues of Eq. (4.223) can directly be calculated. The result is

$$\lambda_{ij}=\frac{1}{4}L_x L_y\pi^4\left[D_{11}\left(\frac{i}{L_x}\right)^4+2\left(D_{12}+2D_{66}\right)\left(\frac{i}{L_x}\right)^2\left(\frac{j}{L_y}\right)^2+D_{22}\left(\frac{j}{L_y}\right)^4\right]. \tag{4.225}$$

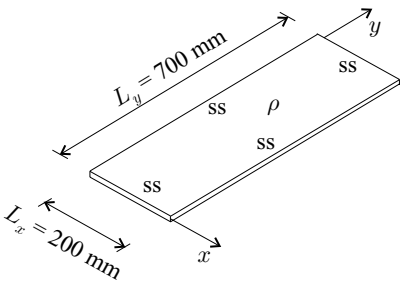

Figure 4.44: The plate in Example 4.14.

Equations (4.224) and (4.225) give the natural frequencies of an orthotropic plate as follows:

$$f_{ij} = \sqrt{\frac{\pi^2}{4\rho}\left\{D_{11}\left(\frac{i}{L_x}\right)^4 + 2\left(D_{12}+2D_{66}\right)\left(\frac{i}{L_x}\right)^2\left(\frac{j}{L_y}\right)^2 + D_{22}\left(\frac{j}{L_y}\right)^4\right\}}. \tag{4.226}$$

The values of f_{ij} must be calculated for different values of i and j.

4.14 Example. *A* 0.7*-m-long and* 0.2*-m-wide rectangular plate is made of graphite epoxy. The material properties are given in Table 3.6 (page 81). The layup is* $[\pm 45_2^{\mathrm{f}}/0_{12}/\pm 45_2^{\mathrm{f}}]$. *The 0-degree plies are parallel to the short edge of the plate. The plate is simply supported along all four edges (Fig. 4.44). The mass of the plate is uniform (*$\rho = 3.2$ *kg/m*^{2}*). Calculate the natural frequencies.*

Solution. From Eq. (4.226), with the stiffnesses $D_{11} = 45.30\ \mathrm{N\cdot m}$, $D_{22} = 25.26\ \mathrm{N\cdot m}$, $D_{12} = 19.52\ \mathrm{N\cdot m}$, $D_{66} = 20.62\ \mathrm{N\cdot m}$ (Table 3.7, page 84) we have

$$\begin{aligned} f_{ij} &= \sqrt{\frac{\pi^2}{4\rho}\left[D_{11}\left(\frac{i}{L_x}\right)^4 + 2\left(D_{12}+2D_{66}\right)\left(\frac{i}{L_x}\right)^2\left(\frac{j}{L_y}\right)^2 + D_{22}\left(\frac{j}{L_y}\right)^4\right]} \\ &= \sqrt{21\,830 i^4 + 4\,780 i^2 j^2 + 81.11 j^4}. \end{aligned} \tag{4.227}$$

This yields the following values of f_{ij} (Hz):

$i \setminus j$	1	2	3
1	163	205	267
2	607	653	727
3	1 346	1 393	1 470.

The lowest natural frequency corresponds to $i = j = 1$, and is

$$f_{11} = 163\ \mathrm{Hz}. \tag{4.228}$$

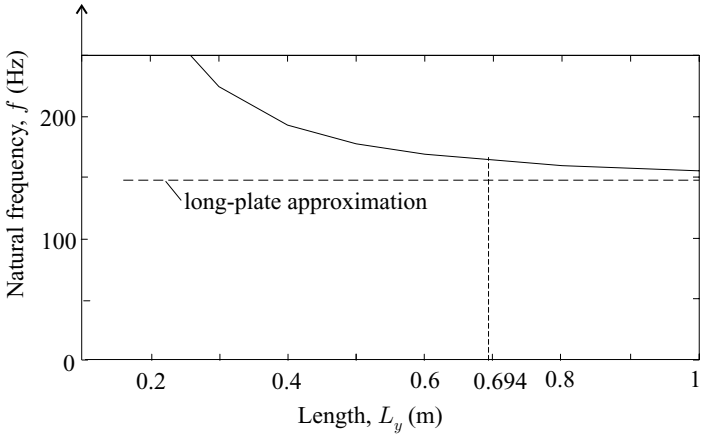

Figure 4.45: The lowest natural frequency of the plate in Example 4.14 as a function of the plate length.

We now assess the length-to-width ratios under which the long-plate approximation is reasonable. To this end, we calculated the lowest natural frequency of the plate, keeping the width L_x the same while changing the length L_y. In Figure 4.45 we plot the lowest natural frequency thus calculated versus L_y. In this figure we also included the lowest natural frequency given by the long-plate approximation (Eq. 4.204). The results in this figure show that, in accordance with Eq. (4.19), the long-plate formula approximates within 10 percent the natural frequency when L_y is greater than $3L_x\sqrt[4]{D_{11}/D_{22}} = 0.694$ m.

4.15 Example. *A 0.2-m-long and 0.2-m-wide rectangular plate is made of graphite epoxy unidirectional plies. The material properties are given in Table 3.6 (page 81). The layup is* $[0_2/45_2/90_2/-45_2]_s$. *The plate is simply supported along the four edges (Fig. 4.46). The mass of the plate is uniform* ($\rho = 2.56$ *kg/m*^{2}). *Calculate the natural frequencies.*

Solution. The layup of the plate is symmetrical but not orthotropic. The bending stiffnesses are $D_{11} = 34.61$ N$\cdot$m, $D_{22} = 12.34$ N$\cdot$m, $D_{12} = 4.58$ N$\cdot$m, $D_{66} = 5.14$ N$\cdot$m, $D_{16} = 3.34$ N$\cdot$m, $D_{26} = 3.34$ N$\cdot$m (Table 3.7, page 84). The natural frequencies are calculated from Eqs. (4.224) and (4.223). With the preceding

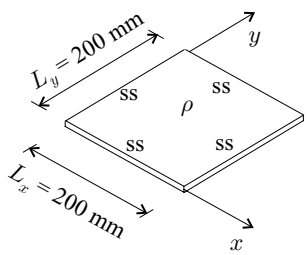

Figure 4.46: The plate in Example 4.15.

stiffnesses, and with $I = J = 7$, these calculations yield the following f_{ij} (Hz) values:

$i \setminus j$	1	2	3
1	211	446	910
2	640	797	1 179
3	1 359	1 569	1 955.

(4.229)

The layup follows the 10-percent rule (page 89), and we may treat the plate as orthotropic. From Eq. (4.226) we have

$$f_{ij} = \sqrt{\frac{\pi^2}{4\rho}\left[D_{11}\left(\frac{i}{L_x}\right)^4 + 2\left(D_{12}+2D_{66}\right)\left(\frac{i}{L_x}\right)^2\left(\frac{j}{L_y}\right)^2 + D_{22}\left(\frac{j}{L_y}\right)^4\right]}$$

$$= \sqrt{20\,850 i^4 + 17\,910 i^2 j^2 + 7\,435 j^4}. \tag{4.230}$$

The values of f_{ij} (Hz) are

$i \setminus j$	1	2	3
1	215	460	886
2	642	860	1 257
3	1 363	1 566	1 934.

(4.231)

We see that these natural frequencies (which are based on the orthotropy approximation) are within 8 percent of the natural frequencies resulting from the exact calculations (see Eq. 4.229).

4.4.3 Plates with Built-In and Simply Supported Edges – Orthotropic and Symmetrical Layup

We consider rectangular plates with length L_x and width L_y. Each edge of the plate is either simply supported or built-in. The layup of the plate is orthotropic and symmetrical. Following Hearmon[39] the natural frequencies of the plate are calculated by the Rayleigh energy method.

Under free vibration the deflection of the plate is (Eq. 4.189)

$$w^{\mathrm{o}} = \overline{w}^{\mathrm{o}} \sin\left(2\pi f t\right). \tag{4.232}$$

By introducing this w^{o} into the expression of the strain energy (Eq. 4.107), and by setting $D_{16} = D_{26} = 0$, we obtain

$$U = \overline{U} \sin^2\left(2\pi f t\right), \tag{4.233}$$

[39] R. F. S. Hearmon, The Frequency of Flexural Vibration of Rectangular Orthotropic Plates with Clamped or Simply Supported Edges. *Journal of Applied Mechanics*, Vol. 26, 537–540, 1959.

where $\overline{U}$ is defined as

$$\overline{U} = \frac{1}{2}\int_0^{L_x}\int_0^{L_y}\left[D_{11}\left(\frac{\partial^2\overline{w}^{\mathrm{o}}}{\partial x^2}\right)^2 + D_{22}\left(\frac{\partial^2\overline{w}^{\mathrm{o}}}{\partial y^2}\right)^2 + D_{66}\left(\frac{2\partial^2\overline{w}^{\mathrm{o}}}{\partial x\partial y}\right)^2 + 2\left(D_{12}\frac{\partial^2\overline{w}^{\mathrm{o}}}{\partial x^2}\frac{\partial^2\overline{w}^{\mathrm{o}}}{\partial y^2}\right)\right]dydx. \tag{4.234}$$

By following the same steps as in Section 4.4.2, we arrive at

$$(2\pi f)^2 = \frac{\overline{U}}{\frac{1}{2}\int_0^{L_x}\int_0^{L_y}\rho\overline{w}^{\mathrm{o}2}dydx}. \tag{4.235}$$

The deflection is assumed to be of the form

$$\overline{w}^{\mathrm{o}} = AX_i(x)Y_j(y), \tag{4.236}$$

where A is the, as yet unknown, amplitude. For $X_i(x)$ and $Y_j(y)$ we adopt the shape of a freely vibrating beam. For different end supports these functions are given in Table 4.4 (page 119). The variables i and j represent the number of half waves in the x and y directions, respectively (Fig. 4.19).

By introducing Eq. (4.236) into Eq. (4.235), and by performing the integration, we obtain

$$\lambda_{ij} = \frac{1}{4}L_xL_y\left(D_{11}\frac{\alpha_1^4}{L_x^4} + D_{22}\frac{\alpha_3^4}{L_y^4} + 2\left(D_{12}+2D_{66}\right)\frac{\alpha_2}{L_x^2L_y^2}\right), \tag{4.237}$$

where λ_{ij} is the eigenvalue, which is defined as

$$\lambda_{ij} = \frac{1}{4}\left(2\pi f_{ij}\right)^2\rho L_xL_y. \tag{4.238}$$

The parameters α_1, α_2, α_3, α_4, α_5 are given in Table 4.5. The values of α_1 through α_5 must be calculated numerically. The integrations simlify when $X_i(x)$ and $Y_j(y)$ are calculated by the approximate expressions of μ_i given in Table 4.4. The resulting approximate expressions for α_1 through α_5 are given in Tables 4.6 and 4.7, whereas α_2 is

$$\alpha_2 = \alpha_4\alpha_5. \tag{4.239}$$

The parameters α_1–α_5 and the corresponding eigenvalues λ_{ij} must be calculated for different sets of i and j, $(i, j = 1, 2, \dots)$. The natural frequencies are then calculated by

$$f_{ij} = \frac{1}{\pi}\sqrt{\frac{\lambda_{ij}}{\rho L_xL_y}} = \frac{1}{2\pi}\sqrt{\frac{1}{\rho}\left(D_{11}\frac{\alpha_1^4}{L_x^4} + D_{22}\frac{\alpha_3^4}{L_y^4} + 2\left(D_{12}+2D_{66}\right)\frac{\alpha_2}{L_x^2L_y^2}\right)}. \tag{4.240}$$

4.16 Example. *A* 0.2*-m-long and* 0.2*-m-wide rectangular plate is made of graphite epoxy unidirectional plies. The material properties are given in Table 3.6*

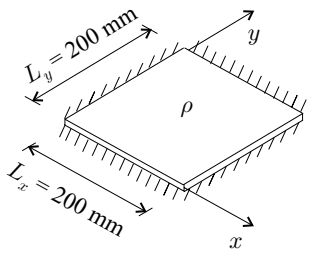

Figure 4.47: The plate in Example 4.16.

(page 81). The layup is $[0_2/45_2/90_2/-45_2]_s$. *The plate is built-in along the four edges (Fig. 4.47). The mass of the plate is uniform* ($\rho = 2.56$ *kg/m*^{2}). *Calculate the natural frequencies.*

Solution. The layup follows the 10-percent rule (page 89), and we treat the plate as orthotropic. With the stiffnesses $D_{11} = 34.61$ N · m, $D_{22} = 12.34$ N · m, $D_{12} = 4.58$ N · m, $D_{66} = 5.14$ N · m, $D_{16} = 3.34$ N · m, $D_{26} = 3.34$ N · m (Table 3.7, page 84) Eq. (4.240) yields

$$f_{ij} = \frac{1}{2\pi}\sqrt{\frac{1}{\rho}\left[D_{11}\frac{\alpha_1^4}{L_x^4} + D_{22}\frac{\alpha_3^4}{L_y^4} + 2\left(D_{12} + 2D_{66}\right)\frac{\alpha_2}{L_x^2 L_y^2}\right]}$$
$$= \sqrt{214\alpha_1^4 + 184\alpha_3^4 + 76.3\alpha_4\alpha_5}, \tag{4.241}$$

where α_1 and α_4 depend on i ($i = 1, 2, \dots$) and α_3 and α_5 depend on j ($j = 1, 2, \dots$) as given in Tables 4.6 and 4.7, third row. From these tables the values are

	$i=1$	$i=2$	$i=3$
α_1	4.73	7.85	11.00
α_4	12.91	45.98	98.91

	$j=1$	$j=2$	$j=3$
α_3	4.73	7.85	11.00
α_5	12.91	45.98	98.91 .

The values of f_{ij} (Hz) are (Eq. 4.241)

$i \setminus j$	1	2	3
1	420	712	1 207
2	981	1 222	1 663
3	1 844	2 063	2 458 .

4.5 Hygrothermal Effects

We consider a small element of a thin plate. The temperature and moisture concentration (both of which may vary across the thickness of the plate) are T and c,

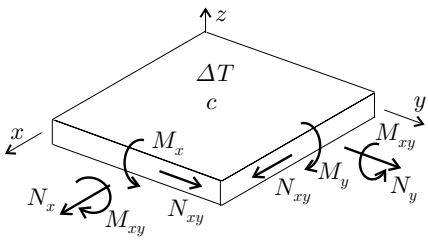

Figure 4.48: Hygrothermal and mechanical loads on a plate element.

respectively. In-plane forces and moments may also act on the element (Fig. 4.48). Owing to these hygrothermal and mechanical loads, under plane-stress condition, the strains at a point are (see Eqs. 2.155 and 2.156)

$$\begin{Bmatrix} \epsilon_x \\ \epsilon_y \\ \gamma_{xy} \end{Bmatrix} = \begin{bmatrix} \overline{S}_{11} & \overline{S}_{12} & \overline{S}_{16} \\ \overline{S}_{21} & \overline{S}_{22} & \overline{S}_{26} \\ \overline{S}_{61} & \overline{S}_{62} & \overline{S}_{66} \end{bmatrix} \begin{Bmatrix} \sigma_x \\ \sigma_y \\ \tau_{xy} \end{Bmatrix} + \Delta T \begin{Bmatrix} \widetilde{\alpha}_x \\ \widetilde{\alpha}_y \\ \widetilde{\alpha}_{xy} \end{Bmatrix} + c \begin{Bmatrix} \widetilde{\beta}_x \\ \widetilde{\beta}_y \\ \widetilde{\beta}_{xy} \end{Bmatrix}, \tag{4.242}$$

where ΔT is the temperature difference relative to a reference temperature

$$\Delta T = T - T_{\text{ref}}, \tag{4.243}$$

and $\widetilde{\alpha}$ and $\widetilde{\beta}$ are the thermal expansion and moisture expansion coefficients (Section 2.6). The stress at a point is obtained by inverting Eq. (4.242) as follows:

$$\begin{Bmatrix} \sigma_x \\ \sigma_y \\ \tau_{xy} \end{Bmatrix} = [\overline{Q}] \left(\begin{Bmatrix} \epsilon_x \\ \epsilon_y \\ \gamma_{xy} \end{Bmatrix} - \Delta T \begin{Bmatrix} \widetilde{\alpha}_x \\ \widetilde{\alpha}_y \\ \widetilde{\alpha}_{xy} \end{Bmatrix} - c \begin{Bmatrix} \widetilde{\beta}_x \\ \widetilde{\beta}_y \\ \widetilde{\beta}_{xy} \end{Bmatrix} \right). \tag{4.244}$$

By definition, the forces and moments are (Eq. 3.9)

$$\begin{Bmatrix} N_x \\ N_y \\ N_{xy} \end{Bmatrix} = \int_{-h_{\text{b}}}^{h_{\text{t}}} \begin{Bmatrix} \sigma_x \\ \sigma_y \\ \tau_{xy} \end{Bmatrix} dz \qquad \begin{Bmatrix} M_x \\ M_y \\ M_{xy} \end{Bmatrix} = \int_{-h_{\text{b}}}^{h_{\text{t}}} z \begin{Bmatrix} \sigma_x \\ \sigma_y \\ \tau_{xy} \end{Bmatrix} dz. \tag{4.245}$$

It is convenient to define the following equivalent generalized hygrothermal forces:

$$\begin{Bmatrix} N_x^{\text{ht}} \\ N_y^{\text{ht}} \\ N_{xy}^{\text{ht}} \end{Bmatrix} = \int_{-h_{\text{b}}}^{h_{\text{t}}} [\overline{Q}] \left(\Delta T \begin{Bmatrix} \widetilde{\alpha}_x \\ \widetilde{\alpha}_y \\ \widetilde{\alpha}_{xy} \end{Bmatrix} + c \begin{Bmatrix} \widetilde{\beta}_x \\ \widetilde{\beta}_y \\ \widetilde{\beta}_{xy} \end{Bmatrix} \right) dz \tag{4.246}$$

$$\begin{Bmatrix} M_x^{\text{ht}} \\ M_y^{\text{ht}} \\ M_{xy}^{\text{ht}} \end{Bmatrix} = \int_{-h_{\text{b}}}^{h_{\text{t}}} z[\overline{Q}] \left(\Delta T \begin{Bmatrix} \widetilde{\alpha}_x \\ \widetilde{\alpha}_y \\ \widetilde{\alpha}_{xy} \end{Bmatrix} + c \begin{Bmatrix} \widetilde{\beta}_x \\ \widetilde{\beta}_y \\ \widetilde{\beta}_{xy} \end{Bmatrix} \right) dz. \tag{4.247}$$

With the definitions of the $[A]$, $[B]$, and $[D]$ matrices (Section 3.2.2), Eqs. (4.244)–(4.247) may be combined to yield

$$\begin{Bmatrix} N_x \\ N_y \\ N_{xy} \\ M_x \\ M_y \\ M_{xy} \end{Bmatrix} = \begin{bmatrix} A_{11} & A_{12} & A_{16} & B_{11} & B_{12} & B_{16} \\ A_{12} & A_{22} & A_{26} & B_{12} & B_{22} & B_{26} \\ A_{16} & A_{26} & A_{66} & B_{16} & B_{26} & B_{66} \\ B_{11} & B_{12} & B_{16} & D_{11} & D_{12} & D_{16} \\ B_{12} & B_{22} & B_{26} & D_{12} & D_{22} & D_{26} \\ B_{16} & B_{26} & B_{66} & D_{16} & D_{26} & D_{66} \end{bmatrix} \begin{Bmatrix} \epsilon_x^{\mathrm{o}} \\ \epsilon_y^{\mathrm{o}} \\ \gamma_{xy}^{\mathrm{o}} \\ \kappa_x \\ \kappa_y \\ \kappa_{xy} \end{Bmatrix} - \begin{Bmatrix} N_x^{\mathrm{ht}} \\ N_y^{\mathrm{ht}} \\ N_{xy}^{\mathrm{ht}} \\ M_x^{\mathrm{ht}} \\ M_y^{\mathrm{ht}} \\ M_{xy}^{\mathrm{ht}} \end{Bmatrix} \tag{4.248}$$

$$\begin{Bmatrix} \epsilon_x^{\mathrm{o}} \\ \epsilon_y^{\mathrm{o}} \\ \gamma_{xy}^{\mathrm{o}} \\ \kappa_x \\ \kappa_y \\ \kappa_{xy} \end{Bmatrix} = \begin{bmatrix} \alpha_{11} & \alpha_{12} & \alpha_{16} & \beta_{11} & \beta_{12} & \beta_{16} \\ \alpha_{12} & \alpha_{22} & \alpha_{26} & \beta_{21} & \beta_{22} & \beta_{26} \\ \alpha_{16} & \alpha_{26} & \alpha_{66} & \beta_{61} & \beta_{62} & \beta_{66} \\ \beta_{11} & \beta_{21} & \beta_{61} & \delta_{11} & \delta_{12} & \delta_{16} \\ \beta_{12} & \beta_{22} & \beta_{62} & \delta_{12} & \delta_{22} & \delta_{26} \\ \beta_{16} & \beta_{26} & \beta_{66} & \delta_{16} & \delta_{26} & \delta_{66} \end{bmatrix} \left(\begin{Bmatrix} N_x \\ N_y \\ N_{xy} \\ M_x \\ M_y \\ M_{xy} \end{Bmatrix} + \begin{Bmatrix} N_x^{\mathrm{ht}} \\ N_y^{\mathrm{ht}} \\ N_{xy}^{\mathrm{ht}} \\ M_x^{\mathrm{ht}} \\ M_y^{\mathrm{ht}} \\ M_{xy}^{\mathrm{ht}} \end{Bmatrix} \right), \tag{4.249}$$

where α_{ij}, β_{ij}, and δ_{ij} are the elements of the compliance matrices (Eq. 3.22). We define the following generalized hygrothermal strains and curvatures:

$$\begin{Bmatrix} \epsilon_x^{\mathrm{o,ht}} \\ \epsilon_y^{\mathrm{o,ht}} \\ \gamma_{xy}^{\mathrm{o,ht}} \\ \kappa_x^{\mathrm{ht}} \\ \kappa_y^{\mathrm{ht}} \\ \kappa_{xy}^{\mathrm{ht}} \end{Bmatrix} = \begin{bmatrix} \alpha_{11} & \alpha_{12} & \alpha_{16} & \beta_{11} & \beta_{12} & \beta_{16} \\ \alpha_{12} & \alpha_{22} & \alpha_{26} & \beta_{21} & \beta_{22} & \beta_{26} \\ \alpha_{16} & \alpha_{26} & \alpha_{66} & \beta_{61} & \beta_{62} & \beta_{66} \\ \beta_{11} & \beta_{21} & \beta_{61} & \delta_{11} & \delta_{12} & \delta_{16} \\ \beta_{12} & \beta_{22} & \beta_{62} & \delta_{12} & \delta_{22} & \delta_{26} \\ \beta_{16} & \beta_{26} & \beta_{66} & \delta_{16} & \delta_{26} & \delta_{66} \end{bmatrix} \begin{Bmatrix} N_x^{\mathrm{ht}} \\ N_y^{\mathrm{ht}} \\ N_{xy}^{\mathrm{ht}} \\ M_x^{\mathrm{ht}} \\ M_y^{\mathrm{ht}} \\ M_{xy}^{\mathrm{ht}} \end{Bmatrix}. \tag{4.250}$$

These generalized hygrothermal strains would occur in the reference plane of an unrestrained plate subjected to changes in temperature and moisture content.

Expressions for calculating N^{ht}, M^{ht} (Eqs. 4.246 and 4.247) are given in Table 4.13 for piecewise linear, linear, and uniform temperature distributions (Fig. 4.49).

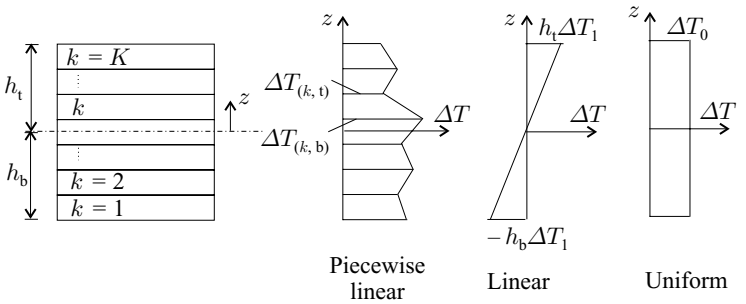

Figure 4.49: Piecewise linear, linear, and uniform temperature distributions across the plate.

Table 4.13. The hygrothermal forces N^{ht},M^{ht} for piecewise linear, linear, and uniform temperature distributions (Fig. 4.49). The $\Delta T_{(k,t)}$ and $\Delta T_{(k,b)}$ refer to the top and bottom of the kth layer. For piecewise linear, linear, and uniform moisture distributions ΔT and $\widetilde{\alpha}$ are replaced by c and $\widetilde{\beta}$.

Piecewise linear temperature distribution

$$\begin{Bmatrix} N_x^{ht} \\ N_y^{ht} \\ N_{xy}^{ht} \end{Bmatrix} = \sum_{k=1}^{K} \left(\frac{z_k - z_{k-1}}{2} [\overline{Q}]_k (\Delta T_{(k,t)} + \Delta T_{(k,b)}) \begin{Bmatrix} \widetilde{\alpha}_x \\ \widetilde{\alpha}_y \\ \widetilde{\alpha}_{xy} \end{Bmatrix}_k \right)$$

$$\begin{Bmatrix} M_x^{ht} \\ M_y^{ht} \\ M_{xy}^{ht} \end{Bmatrix} = \sum_{k=1}^{K} \frac{z_k^3 - z_{k-1}^3}{3(z_k - z_{k-1})} [\overline{Q}]_k (\Delta T_{(k,t)} - \Delta T_{(k,b)}) \begin{Bmatrix} \widetilde{\alpha}_x \\ \widetilde{\alpha}_y \\ \widetilde{\alpha}_{xy} \end{Bmatrix}_k + \sum_{k=1}^{K} \frac{z_k + z_{k-1}}{2} [\overline{Q}]_k (z_k \Delta T_{(k,b)} - z_{k-1} \Delta T_{(k,t)}) \begin{Bmatrix} \widetilde{\alpha}_x \\ \widetilde{\alpha}_y \\ \widetilde{\alpha}_{xy} \end{Bmatrix}_k$$

Linear temperature distribution

$$\begin{Bmatrix} N_x^{ht} \\ N_y^{ht} \\ N_{xy}^{ht} \end{Bmatrix} = \Delta T_1 \sum_{k=1}^{K} \frac{z_k^2 - z_{k-1}^2}{2} [\overline{Q}]_k \begin{Bmatrix} \widetilde{\alpha}_x \\ \widetilde{\alpha}_y \\ \widetilde{\alpha}_{xy} \end{Bmatrix}_k$$

$$\begin{Bmatrix} M_x^{ht} \\ M_y^{ht} \\ M_{xy}^{ht} \end{Bmatrix} = \Delta T_1 \sum_{k=1}^{K} \frac{z_k^3 - z_{k-1}^3}{3} [\overline{Q}]_k \begin{Bmatrix} \widetilde{\alpha}_x \\ \widetilde{\alpha}_y \\ \widetilde{\alpha}_{xy} \end{Bmatrix}_k$$

Constant temperature distribution

$$\begin{Bmatrix} N_x^{ht} \\ N_y^{ht} \\ N_{xy}^{ht} \end{Bmatrix} = \Delta T_0 \sum_{k=1}^{K} \left((z_k - z_{k-1}) [\overline{Q}]_k \begin{Bmatrix} \widetilde{\alpha}_x \\ \widetilde{\alpha}_y \\ \widetilde{\alpha}_{xy} \end{Bmatrix}_k \right)$$

$$\begin{Bmatrix} M_x^{ht} \\ M_y^{ht} \\ M_{xy}^{ht} \end{Bmatrix} = \Delta T_0 \sum_{k=1}^{K} \left(\frac{z_k^2 - z_{k-1}^2}{2} [\overline{Q}]_k \begin{Bmatrix} \widetilde{\alpha}_x \\ \widetilde{\alpha}_y \\ \widetilde{\alpha}_{xy} \end{Bmatrix}_k \right)$$

With the preceding definition of the hygrothermal strains Eqs. (4.248) and (4.249) may be written in the following forms:

$$\begin{Bmatrix} N_x \\ N_y \\ N_{xy} \\ M_x \\ M_y \\ M_{xy} \end{Bmatrix} = \begin{bmatrix} A_{11} & A_{12} & A_{16} & B_{11} & B_{12} & B_{16} \\ A_{12} & A_{22} & A_{26} & B_{12} & B_{22} & B_{26} \\ A_{16} & A_{26} & A_{66} & B_{16} & B_{26} & B_{66} \\ B_{11} & B_{12} & B_{16} & D_{11} & D_{12} & D_{16} \\ B_{12} & B_{22} & B_{26} & D_{12} & D_{22} & D_{26} \\ B_{16} & B_{26} & B_{66} & D_{16} & D_{26} & D_{66} \end{bmatrix} \left(\begin{Bmatrix} \epsilon_x^o \\ \epsilon_y^o \\ \gamma_{xy}^o \\ \kappa_x \\ \kappa_y \\ \kappa_{xy} \end{Bmatrix} - \begin{Bmatrix} \epsilon_x^{o,ht} \\ \epsilon_y^{o,ht} \\ \gamma_{xy}^{o,ht} \\ \kappa_x^{ht} \\ \kappa_y^{ht} \\ \kappa_{xy}^{ht} \end{Bmatrix} \right) \tag{4.251}$$

$$\begin{Bmatrix} \epsilon_x^{\mathrm{o}} \\ \epsilon_y^{\mathrm{o}} \\ \gamma_{xy}^{\mathrm{o}} \\ \kappa_x \\ \kappa_y \\ \kappa_{xy} \end{Bmatrix} = \begin{bmatrix} \alpha_{11} & \alpha_{12} & \alpha_{16} & \beta_{11} & \beta_{12} & \beta_{16} \\ \alpha_{12} & \alpha_{22} & \alpha_{26} & \beta_{21} & \beta_{22} & \beta_{26} \\ \alpha_{16} & \alpha_{26} & \alpha_{66} & \beta_{61} & \beta_{62} & \beta_{66} \\ \beta_{11} & \beta_{21} & \beta_{61} & \delta_{11} & \delta_{12} & \delta_{16} \\ \beta_{12} & \beta_{22} & \beta_{62} & \delta_{12} & \delta_{22} & \delta_{26} \\ \beta_{16} & \beta_{26} & \beta_{66} & \delta_{16} & \delta_{26} & \delta_{66} \end{bmatrix} \begin{Bmatrix} N_x \\ N_y \\ N_{xy} \\ M_x \\ M_y \\ M_{xy} \end{Bmatrix} + \begin{Bmatrix} \epsilon_x^{\mathrm{o,ht}} \\ \epsilon_y^{\mathrm{o,ht}} \\ \gamma_{xy}^{\mathrm{o,ht}} \\ \kappa_x^{\mathrm{ht}} \\ \kappa_y^{\mathrm{ht}} \\ \kappa_{xy}^{\mathrm{ht}} \end{Bmatrix}. \tag{4.252}$$

Rectangular plates with free edges. We consider a rectangular unsupported plate, that is, all four of the edges are free. The plate is subjected to pure bending, in-plane mechanical loads, and to hygrothermal loads. Such a plate can be analyzed by Eq. (4.248). In these equations the temperature and moisture distributions across the plate must be specified as well as 6 of the following 12 quantities (Table 4.14):

$$\begin{array}{llllll} N_x & \text{or} & \epsilon_x^{\mathrm{o}} & M_x & \text{or} & \kappa_x \\ N_y & \text{or} & \epsilon_y^{\mathrm{o}} & M_y & \text{or} & \kappa_y \\ N_{xy} & \text{or} & \epsilon_{xy}^{\mathrm{o}} & M_{xy} & \text{or} & \kappa_{xy}\,. \end{array} \tag{4.253}$$

The deflection of the plate is calculated by Eq. (4.16).

When the unsupported plate is subjected only to a temperature change ΔT and moisture c, the mechanical loads are zero (Table 4.14) as follows:

$$N_x = 0 \qquad N_y = 0 \qquad N_{xy} = 0 \tag{4.254}$$

$$M_x = 0 \qquad M_y = 0 \qquad M_{xy} = 0. \tag{4.255}$$

In this case the strains and curvatures are (see Eqs. 4.249 and 4.250)

$$\begin{Bmatrix} \epsilon_x^{\mathrm{o}} \\ \epsilon_y^{\mathrm{o}} \\ \gamma_{xy}^{\mathrm{o}} \\ \kappa_x \\ \kappa_y \\ \kappa_{xy} \end{Bmatrix} = \begin{Bmatrix} \epsilon_x^{\mathrm{o,ht}} \\ \epsilon_y^{\mathrm{o,ht}} \\ \gamma_{xy}^{\mathrm{o,ht}} \\ \kappa_x^{\mathrm{ht}} \\ \kappa_y^{\mathrm{ht}} \\ \kappa_{xy}^{\mathrm{ht}} \end{Bmatrix}. \tag{4.256}$$

Rectangular plates with built-in edges. When a plate with built-in edges is subjected only to a temperature change ΔT and moisture c, the strains and curvatures are zero (Table 4.14) as follows:

$$\epsilon_x^{\mathrm{o}} = 0 \qquad \epsilon_y^{\mathrm{o}} = 0 \qquad \gamma_{xy}^{\mathrm{o}} = 0 \tag{4.257}$$

$$\kappa_x = 0 \qquad \kappa_y = 0 \qquad \kappa_{xy} = 0. \tag{4.258}$$

The normal forces and moments are calculated by Eqs. (4.246)–(4.248).

Long rectangular plates. When the plate is long and is subjected only to a change in temperature ΔT and moisture content c, some of the strains, curvatures, moments, and in-plane loads are zero, as shown in Table 4.14. The response of the plate is then calculated by setting equal to zero in Eq. (4.248) the quantities indicated in this table. The deflections of the plate are calculated by Eq. (4.16).

Table 4.14. Rectangular plates subjected to hygrothermal and mechanical loads.

Loading	Conditions
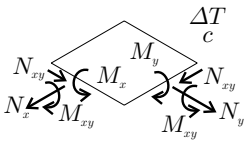	N_x or ϵ_x^o N_y or ϵ_y^o N_{xy} or ϵ_{xy}^o M_x or κ_x M_y or κ_y M_{xy} or κ_{xy}
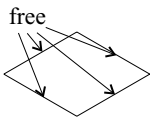	$N_x = 0 \quad N_y = 0 \quad N_{xy} = 0$ $M_x = 0 \quad M_y = 0 \quad M_{xy} = 0$
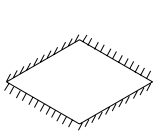	$\epsilon_x^o = 0 \quad \epsilon_y^o = 0 \quad \gamma_{xy}^o = 0$ $\kappa_x = 0 \quad \kappa_y = 0 \quad \kappa_{xy} = 0$
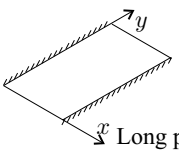	$\epsilon_x^o = 0 \quad \epsilon_y^o = 0 \quad \gamma_{xy}^o = 0$ $\kappa_x = 0 \quad \kappa_y = 0 \quad \kappa_{xy} = 0$
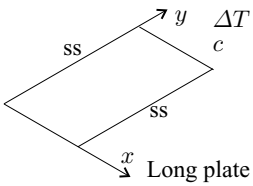	$\epsilon_y^o = 0 \quad \kappa_y = 0 \quad \kappa_{xy} = 0$ $N_x = 0 \quad N_{xy} = 0 \quad M_x = 0$
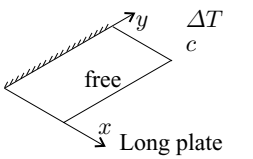	$\epsilon_y^o = 0 \quad \kappa_y = 0 \quad \kappa_{xy} = 0$ $N_x = 0 \quad N_{xy} = 0 \quad M_x = 0$

4.17 Example. *A 1-m-long and 1-m-wide plate is made of graphite epoxy unidirectional plies. The layup is* $[45_6/0_4]_s$. *The edges of the plate are free. The temperature of the bottom surface is raised by* 80 °*C and the top surface by* 120 °*C (Fig. 4.50). Estimate the temperature-induced change in the dimensions of the plate. The ply*

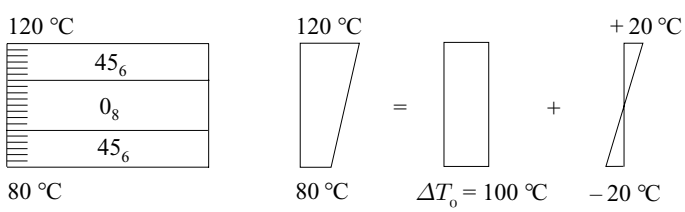

Figure 4.50: Illustration of the plate in Example 4.17.

properties are given in Table 3.6, (page 81) the thermal expansion coefficients are $\widetilde{\alpha}_1 = -0.7 \times 10^{-6} \frac{1}{^\circ C}$ *and* $\widetilde{\alpha}_2 = 25 \times 10^{-6} \frac{1}{^\circ C}$.

Solution. The temperature distribution across the plate is represented by the sum of a constant and a linearly varying temperature distribution, as shown in Figure 4.50. The temperature differences shown in this figure are

$$\Delta T_0 = \frac{80 + 120}{2} = 100\ ^\circ\text{C} \qquad \Delta T_1 = \frac{120 - 80}{h} = 20\,000\ ^\circ\text{C/m}, \tag{4.259}$$

where $h = 0.002$ m is the thickness of the plate. The hygrothermal forces are (Table 4.13, page 154)

$$\left\{ \begin{array}{c} N_x^{\text{ht}} \\ N_y^{\text{ht}} \\ N_{xy}^{\text{ht}} \end{array} \right\}_{\Delta T_0} = \Delta T_0 \sum_{k=1}^{K} \left((z_k - z_{k-1}) \, [\overline{Q}]_k \left\{ \begin{array}{c} \widetilde{\alpha}_x \\ \widetilde{\alpha}_y \\ \widetilde{\alpha}_{xy} \end{array} \right\}_k \right) \tag{4.260}$$

$$\left\{ \begin{array}{c} M_x^{\text{ht}} \\ M_y^{\text{ht}} \\ M_{xy}^{\text{ht}} \end{array} \right\}_{\Delta T_0} = \Delta T_0 \sum_{k=1}^{K} \left(\frac{z_k^2 - z_{k-1}^2}{2} [\overline{Q}]_k \left\{ \begin{array}{c} \widetilde{\alpha}_x \\ \widetilde{\alpha}_y \\ \widetilde{\alpha}_{xy} \end{array} \right\}_k \right) \tag{4.261}$$

$$\left\{ \begin{array}{c} N_x^{\text{ht}} \\ N_y^{\text{ht}} \\ N_{xy}^{\text{ht}} \end{array} \right\}_{\Delta T_1} = \Delta T_1 \sum_{k=1}^{K} \frac{z_k^2 - z_{k-1}^2}{2} [\overline{Q}]_k \left\{ \begin{array}{c} \widetilde{\alpha}_x \\ \widetilde{\alpha}_y \\ \widetilde{\alpha}_{xy} \end{array} \right\}_k \tag{4.262}$$

$$\left\{ \begin{array}{c} M_x^{\text{ht}} \\ M_y^{\text{ht}} \\ M_{xy}^{\text{ht}} \end{array} \right\}_{\Delta T_1} = \Delta T_1 \sum_{k=1}^{K} \frac{z_k^3 - z_{k-1}^3}{3} [\overline{Q}]_k \left\{ \begin{array}{c} \widetilde{\alpha}_x \\ \widetilde{\alpha}_y \\ \widetilde{\alpha}_{xy} \end{array} \right\}_k . \tag{4.263}$$

The stiffness matrices $[\overline{Q}]$ for the zero and 45-degree plies are (Eqs. 3.49 and 3.52)

$$[\overline{Q}]^0 = \begin{bmatrix} 148.87 & 2.91 & 0 \\ 2.91 & 9.71 & 0 \\ 0 & 0 & 4.55 \end{bmatrix} 10^9 \frac{\text{N}}{\text{m}^2} \quad [\overline{Q}]^{45} = \begin{bmatrix} 45.65 & 36.55 & 34.79 \\ 36.55 & 45.65 & 34.79 \\ 34.79 & 34.79 & 38.19 \end{bmatrix} 10^9 \frac{\text{N}}{\text{m}^2}. \tag{4.264}$$

The thermal expansion coefficients of the 0-degree plies are

$$\left\{ \begin{array}{c} \widetilde{\alpha}_x \\ \widetilde{\alpha}_y \\ 0 \end{array} \right\}^0 = \left\{ \begin{array}{c} \widetilde{\alpha}_1 \\ \widetilde{\alpha}_2 \\ 0 \end{array} \right\} = \left\{ \begin{array}{c} -0.7 \\ 25 \\ 0 \end{array} \right\} 10^{-6} \frac{1}{^\circ\text{C}}, \tag{4.265}$$

where $\widetilde{\alpha}_1 = -0.7 \times 10^{-6} \frac{1}{^\circ\text{C}}$ and $\widetilde{\alpha}_2 = 25 \times 10^{-6} \frac{1}{^\circ\text{C}}$ are the thermal expansion coefficients parallel and perpendicular to the fibers. The thermal expansion coefficients

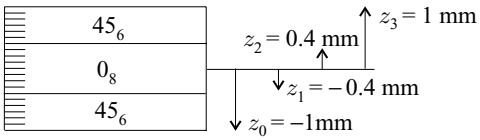

Figure 4.51: The layup of the plate in Example 4.17.

transform as the strains. By replacing ϵ by $\widetilde{\alpha}$ in Eq. (2.188) we obtain

$$\begin{Bmatrix} \widetilde{\alpha}_1 \\ \widetilde{\alpha}_2 \\ 0 \end{Bmatrix} = [T_\epsilon] \begin{Bmatrix} \widetilde{\alpha}_x \\ \widetilde{\alpha}_y \\ \widetilde{\alpha}_{xy} \end{Bmatrix}^{45}, \tag{4.266}$$

where $[T_\epsilon]$ is given by Eq. (3.51). Hence, in the 45-degree direction the thermal expression coefficients are

$$\begin{Bmatrix} \widetilde{\alpha}_x \\ \widetilde{\alpha}_y \\ \widetilde{\alpha}_{xy} \end{Bmatrix}^{45} = \begin{bmatrix} 0.5 & 0.5 & 0.5 \\ 0.5 & 0.5 & -0.5 \\ -1.0 & 1.0 & 0 \end{bmatrix}^{-1} \begin{Bmatrix} \widetilde{\alpha}_1 \\ \widetilde{\alpha}_2 \\ 0 \end{Bmatrix} = \begin{Bmatrix} 12.15 \\ 12.15 \\ -25.70 \end{Bmatrix} 10^{-6} \frac{1}{^{\circ}\text{C}}, \tag{4.267}$$

where z is the distance from the midplane (Fig. 4.51, $z_0 = -0.001$ m, $z_1 = -0.0004$ m, $z_2 = 0.0004$ m, $z_3 = 0.001$ m) and K is the number of ply groups ($K = 3$). With the preceding values of $[\overline{Q}]$ and $\widetilde{\alpha}$ the hygrothermal forces and moments are

$$\begin{Bmatrix} N_x^{\text{ht}} \\ N_y^{\text{ht}} \\ N_{xy}^{\text{ht}} \end{Bmatrix}_{\Delta T_0} = \begin{Bmatrix} 10\,041 \\ 31\,804 \\ -16\,323 \end{Bmatrix} \frac{\text{N}}{\text{m}} \qquad \begin{Bmatrix} M_x^{\text{ht}} \\ M_y^{\text{ht}} \\ M_{xy}^{\text{ht}} \end{Bmatrix}_{\Delta T_0} = \begin{Bmatrix} 0 \\ 0 \\ 0 \end{Bmatrix} \tag{4.268}$$

$$\begin{Bmatrix} N_x^{\text{ht}} \\ N_y^{\text{ht}} \\ N_{xy}^{\text{ht}} \end{Bmatrix}_{\Delta T_1} = \begin{Bmatrix} 0 \\ 0 \\ 0 \end{Bmatrix} \qquad \begin{Bmatrix} M_x^{\text{ht}} \\ M_y^{\text{ht}} \\ M_{xy}^{\text{ht}} \end{Bmatrix}_{\Delta T_1} = \begin{Bmatrix} 16.195 \\ 5.143 \\ -4.697 \end{Bmatrix} 10^6 \text{N}. \tag{4.269}$$

The hygrothermal strains are given by (Eq. 4.250)

$$\begin{Bmatrix} \epsilon_x^{0,\text{ht}} \\ \epsilon_y^{0,\text{ht}} \\ \gamma_{xy}^{0,\text{ht}} \\ \kappa_x^{\text{ht}} \\ \kappa_y^{\text{ht}} \\ \kappa_{xy}^{\text{ht}} \end{Bmatrix} = \begin{bmatrix} \alpha_{11} & \alpha_{12} & \alpha_{16} & \beta_{11} & \beta_{12} & \beta_{16} \\ \alpha_{12} & \alpha_{22} & \alpha_{26} & \beta_{21} & \beta_{22} & \beta_{26} \\ \alpha_{16} & \alpha_{26} & \alpha_{66} & \beta_{61} & \beta_{62} & \beta_{66} \\ \beta_{11} & \beta_{21} & \beta_{61} & \delta_{11} & \delta_{12} & \delta_{16} \\ \beta_{12} & \beta_{22} & \beta_{62} & \delta_{12} & \delta_{22} & \delta_{26} \\ \beta_{16} & \beta_{26} & \beta_{66} & \delta_{16} & \delta_{26} & \delta_{66} \end{bmatrix} \begin{Bmatrix} N_x^{\text{ht}} \\ N_y^{\text{ht}} \\ N_{xy}^{\text{ht}} \\ M_x^{\text{ht}} \\ M_y^{\text{ht}} \\ M_{xy}^{\text{ht}} \end{Bmatrix}. \tag{4.270}$$

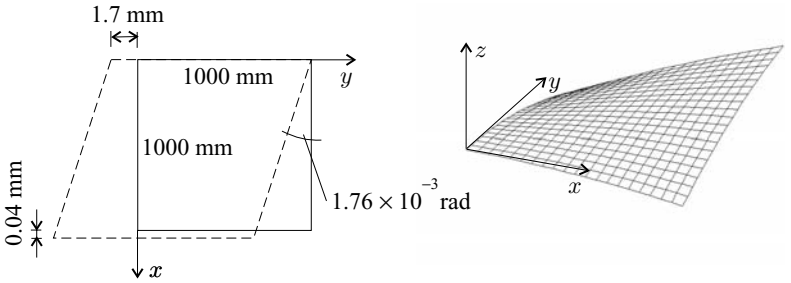

Figure 4.52: The deformed shape of the plate in Example 4.17.

The layup is symmetrical ($[\beta] = 0$), and the compliance matrices are (Table 3.8, page 85)

$$[\alpha] = [a] = \begin{bmatrix} 7.45 & -2.99 & -3.77 \\ -2.99 & 37.81 & -29.39 \\ -3.77 & -29.39 & 48.20 \end{bmatrix} 10^{-9} \frac{\text{m}}{\text{N}} \tag{4.271}$$

$$[\delta] = [d] = \begin{bmatrix} 71.24 & -25.43 & -41.40 \\ -25.43 & 116.82 & -82.58 \\ -41.40 & -82.58 & 153.66 \end{bmatrix} 10^{-3} \frac{1}{\text{N} \cdot \text{m}}. \tag{4.272}$$

Equations (4.270), (4.271), and (4.272) give the hygrothermal strains:

$$\begin{Bmatrix} \epsilon_x^{\text{o,ht}} \\ \epsilon_y^{\text{o,ht}} \\ \gamma_{xy}^{\text{o,ht}} \end{Bmatrix}_{\Delta T_0} = \begin{Bmatrix} 0.041 \\ 1.653 \\ -1.760 \end{Bmatrix} 10^{-3} \qquad \begin{Bmatrix} \kappa_x^{\text{ht}} \\ \kappa_y^{\text{ht}} \\ \kappa_{xy}^{\text{ht}} \end{Bmatrix}_{\Delta T_0} = \begin{Bmatrix} 0 \\ 0 \\ 0 \end{Bmatrix} \tag{4.273}$$

$$\begin{Bmatrix} \epsilon_x^{\text{o,ht}} \\ \epsilon_y^{\text{o,ht}} \\ \gamma_{xy}^{\text{o,ht}} \end{Bmatrix}_{\Delta T_1} = \begin{Bmatrix} 0 \\ 0 \\ 0 \end{Bmatrix} \qquad \begin{Bmatrix} \kappa_x^{\text{ht}} \\ \kappa_y^{\text{ht}} \\ \kappa_{xy}^{\text{ht}} \end{Bmatrix}_{\Delta T_1} = \begin{Bmatrix} 123.0 \\ 284.2 \\ -438.6 \end{Bmatrix} 10^{-3} \frac{1}{\text{m}}. \tag{4.274}$$

The sum $\{\}_{\Delta T_0} + \{\}_{\Delta T_1}$ gives the total hygrothermal strains

$$\begin{Bmatrix} \epsilon_x^{\text{o,ht}} \\ \epsilon_y^{\text{o,ht}} \\ \gamma_{xy}^{\text{o,ht}} \\ \kappa_x^{\text{ht}} \\ \kappa_y^{\text{ht}} \\ \kappa_{xy}^{\text{ht}} \end{Bmatrix} = \begin{Bmatrix} 0.041 \\ 1.653 \\ -1.760 \\ 123.0 \\ 284.2 \\ -438.6 \end{Bmatrix} 10^{-3}.$$

The deformed shape of the plate is illustrated in Figure 4.52.

4.18 Example. *A plate is made of graphite epoxy unidirectional plies. The layup is* $[45_6/0_4]_s$. *The 0-degree plies are parallel to the x axis. The plate is long in the y direction, and one of the long edges is built-in and the other one is free (Fig. 4.53). The temperature of the bottom surface is raised by* 80 °C *and the top surface by* 120 °C *(Fig. 4.50). Estimate the temperature-induced change in the dimensions of the plate. The ply properties are given in Table 3.6 (page 81), the thermal expansion coefficients are* $\widetilde{\alpha}_1 = -0.7 \times 10^{-6} \frac{1}{^\circ C}$ *and* $\widetilde{\alpha}_2 = 25 \times 10^{-6} \frac{1}{^\circ C}$.

Solution. The strains in the laminate are given by Eq. (4.249)

$$\begin{Bmatrix} \epsilon_x^{\mathrm{o}} \\ \epsilon_y^{\mathrm{o}} \\ \gamma_{xy}^{\mathrm{o}} \\ \kappa_x \\ \kappa_y \\ \kappa_{xy} \end{Bmatrix} = \begin{bmatrix} \alpha_{11} & \alpha_{12} & \alpha_{16} & \beta_{11} & \beta_{12} & \beta_{16} \\ \alpha_{12} & \alpha_{22} & \alpha_{26} & \beta_{21} & \beta_{22} & \beta_{26} \\ \alpha_{16} & \alpha_{26} & \alpha_{66} & \beta_{61} & \beta_{62} & \beta_{66} \\ \beta_{11} & \beta_{21} & \beta_{61} & \delta_{11} & \delta_{12} & \delta_{16} \\ \beta_{12} & \beta_{22} & \beta_{62} & \delta_{12} & \delta_{22} & \delta_{26} \\ \beta_{16} & \beta_{26} & \beta_{66} & \delta_{16} & \delta_{26} & \delta_{66} \end{bmatrix} \left(\begin{Bmatrix} N_x \\ N_y \\ N_{xy} \\ M_x \\ M_y \\ M_{xy} \end{Bmatrix} + \begin{Bmatrix} N_x^{\mathrm{ht}} \\ N_y^{\mathrm{ht}} \\ N_{xy}^{\mathrm{ht}} \\ M_x^{\mathrm{ht}} \\ M_y^{\mathrm{ht}} \\ M_{xy}^{\mathrm{ht}} \end{Bmatrix} \right). \tag{4.275}$$

The hygrothermal forces are given in Eqs. (4.268) and (4.269). The compliance matrices are given in Eqs. (4.271) and (4.272). From Table 4.14, sixth row (page 156), we have

$$\epsilon_y^o = 0 \qquad \kappa_y = 0 \qquad \kappa_{xy} = 0 \tag{4.276}$$

$$N_x = 0 \qquad N_{xy} = 0 \qquad M_x = 0 \tag{4.277}$$

Equation (4.275) represents six equations that contain the six unknowns N_y, M_y, M_{xy}, ϵ_x^{o}, γ_{xy}^{o}, κ_x.

The temperature distribution across the plate is represented by the sum of a constant and a linearly varying temperature distribution, as shown in Figure 4.50. The temperature differences shown in this figure are

$$\Delta T_0 = \frac{80 + 120}{2} = 100\ ^{\mathrm{o}}\mathrm{C} \qquad \Delta T_1 = \frac{120 - 80}{h} = 20\,000\ ^{\mathrm{o}}\mathrm{C/m}. \tag{4.278}$$

The corresponding hygrothermal forces are given in Eqs. (4.268) and (4.269), respectively. By substituting the values of the hygrothermal forces given in these equations into Eq. (4.275) we obtain

$$\left(\epsilon_x^{\mathrm{o}}\right)_{\Delta T_0} = 0.172 \times 10^{-3} \qquad \left(\gamma_{xy}^{\mathrm{o}}\right)_{\Delta T_0} = -0.475 \times 10^{-3} \qquad \left(\kappa_x\right)_{\Delta T_0} = 0 \tag{4.279}$$

$$\left(\epsilon_x^{\mathrm{o}}\right)_{\Delta T_1} = 0 \qquad \left(\gamma_{xy}^{\mathrm{o}}\right)_{\Delta T_1} = 0 \qquad \left(\kappa_x\right)_{\Delta T_1} = 36.71 \times 10^{-3} \frac{1}{\mathrm{m}}. \tag{4.280}$$

The sum $()_{\Delta T_0} + ()_{\Delta T_1}$ gives the hygrothermal strains

$$\epsilon_x^{\mathrm{o}} = 0.172 \times 10^{-3} \qquad \gamma_{xy}^{\mathrm{o}} = -0.475 \times 10^{-3} \qquad \kappa_x = 36.71 \times 10^{-3} \frac{1}{\mathrm{m}}. \tag{4.281}$$

The deformed shape of the plate is illustrated in Figure 4.53.

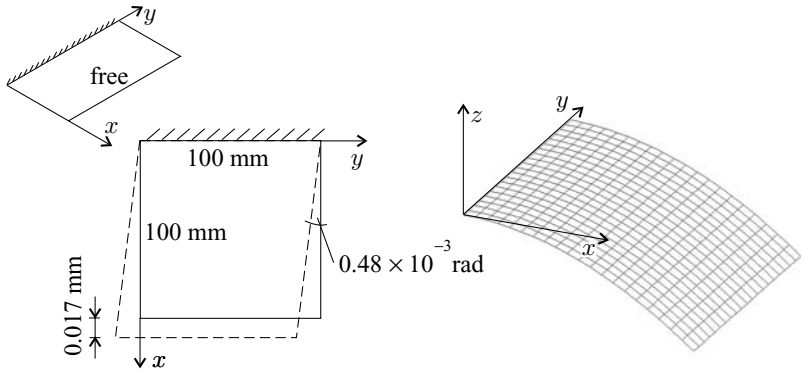

Figure 4.53: Deformed shape of a 100 by 100-mm element of the plate in Example 4.18.

4.5.1 Change in Thickness Due to Hygrothermal Effects

Owing to changes in temperature and moisture content the thickness of the plate changes. The change is (Fig. 4.54)

$$\Delta h = \int_{-h_b}^{h_t} \epsilon_z dz. \tag{4.282}$$

From Eqs. (2.133) and (2.165) the normal strain in a ply is

$$\epsilon_z = \epsilon_3 = [S_{13} \quad S_{23} \quad S_{36}] \begin{Bmatrix} \sigma_1 \\ \sigma_2 \\ \tau_{12} \end{Bmatrix} + \Delta T \widetilde{\alpha}_3 + c\widetilde{\beta}_3. \tag{4.283}$$

In the x_1, x_2 coordinate system the ply stresses are

$$\begin{Bmatrix} \sigma_1 \\ \sigma_2 \\ \tau_{12} \end{Bmatrix} = [T_\sigma] \begin{Bmatrix} \sigma_x \\ \sigma_y \\ \tau_{xy} \end{Bmatrix}, \tag{4.284}$$

where $[T_\sigma]$ is given by Eq. (2.182). In the x, y laminate coordinate system the

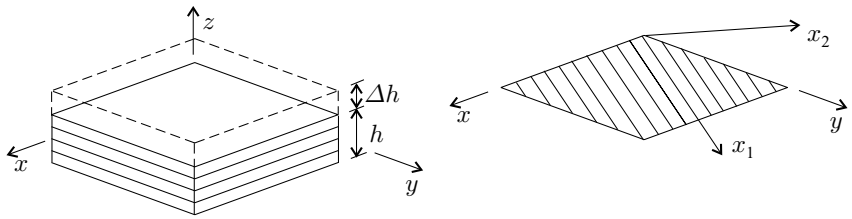

Figure 4.54: Change in thickness of a composite plate and the laminate and ply coordinate systems.

stresses in the ply are (Eqs. 2.126 and 2.165)

$$\begin{Bmatrix} \sigma_x \\ \sigma_y \\ \tau_{xy} \end{Bmatrix} = [\overline{Q}] \left(\begin{Bmatrix} \epsilon_x \\ \epsilon_y \\ \gamma_{xy} \end{Bmatrix} - \Delta T \begin{Bmatrix} \widetilde{\alpha}_x \\ \widetilde{\alpha}_y \\ \widetilde{\alpha}_{xy} \end{Bmatrix} - c \begin{Bmatrix} \widetilde{\beta}_x \\ \widetilde{\beta}_y \\ \widetilde{\beta}_{xy} \end{Bmatrix} \right). \tag{4.285}$$

The strains are (see Eq. 3.7)

$$\begin{Bmatrix} \epsilon_x \\ \epsilon_y \\ \gamma_{xy} \end{Bmatrix} = \begin{Bmatrix} \epsilon_x^{\mathrm{o}} \\ \epsilon_y^{\mathrm{o}} \\ \gamma_{xy}^{\mathrm{o}} \end{Bmatrix} + z \begin{Bmatrix} \kappa_x \\ \kappa_y \\ \kappa_{xy} \end{Bmatrix}. \tag{4.286}$$

Equations (4.282)–(4.286) describe the change in thickness. For a plate subjected to a uniform ΔT_0 change in temperature these equations may be combined to yield

$$\Delta h = \sum_{k=1}^{K} \left\{ [S_{13} \quad S_{23} \quad S_{36}][T_\sigma]_k \left((z_k - z_{k-1}) [\overline{Q}]_k \left(\begin{Bmatrix} \epsilon_x^{\mathrm{o}} \\ \epsilon_y^{\mathrm{o}} \\ \gamma_{xy}^{\mathrm{o}} \end{Bmatrix} - \Delta T_0 \begin{Bmatrix} \widetilde{\alpha}_x \\ \widetilde{\alpha}_y \\ \widetilde{\alpha}_{xy} \end{Bmatrix}_k \right) \right. \right.$$
$$\left. \left. + \frac{z_k^2 - z_{k-1}^2}{2} [\overline{Q}]_k \begin{Bmatrix} \kappa_x \\ \kappa_y \\ \kappa_{xy} \end{Bmatrix} \right) + (z_k - z_{k-1}) \left(\Delta T_0 \left(\widetilde{\alpha}_3 \right)_k \right) \right\}, \tag{4.287}$$

where k is the ply number, K is the total number of plies, and z is the coordinate of the ply (Fig. 3.12). For uniform moisture distribution the change in thickness is calculated by replacing ΔT_0 and $\widetilde{\alpha}$ by c and $\widetilde{\beta}$, respectively.

When the mechanical loads are zero, the strains in, and the curvatures of the reference surface are due only to hygrothermal effects and, from Eq. (4.252), we have

$$\begin{Bmatrix} \epsilon_x^{\mathrm{o}} \\ \epsilon_y^{\mathrm{o}} \\ \gamma_{xy}^{\mathrm{o}} \end{Bmatrix} = \begin{Bmatrix} \epsilon_x^{\mathrm{o,ht}} \\ \epsilon_y^{\mathrm{o,ht}} \\ \gamma_{xy}^{\mathrm{o,ht}} \end{Bmatrix} \qquad \begin{Bmatrix} \kappa_x \\ \kappa_y \\ \kappa_{xy} \end{Bmatrix} = \begin{Bmatrix} \kappa_x^{\mathrm{ht}} \\ \kappa_y^{\mathrm{ht}} \\ \kappa_{xy}^{\mathrm{ht}} \end{Bmatrix}, \tag{4.288}$$

where $\epsilon_x^{\mathrm{o,ht}}$, $\epsilon_y^{\mathrm{o,ht}}$, $\gamma_{xy}^{\mathrm{o,ht}}$, κ_x^{ht}, κ_y^{ht}, $\kappa_{xy}^{\mathrm{ht}}$ are obtained from Eq. (4.250).

4.19 Example. *A rectangular plate is made of graphite epoxy unidirectional plies. The layup is* $[45_6/0_4]_{\mathrm{s}}$. *The edges of the plate are free. The temperature of the plate is raised by* 80 °C. *Estimate the temperature-induced change in the thickness of the plate. The ply properties are given in Table 3.6 (page 81), the thermal expansion coefficients are* $\widetilde{\alpha}_1 = -0.7 \times 10^{-6} \frac{1}{^\circ C}$ *and* $\widetilde{\alpha}_2 = 25 \times 10^{-6} \frac{1}{^\circ C}$.

Solution. The temperature distribution across the plate is uniform and is

$$\Delta T_0 = 80\ ^{\mathrm{o}}\mathrm{C}. \tag{4.289}$$

The change in thickness is (see Eq. 4.287)

$$\Delta h = \sum_{k=1}^{K} \left\{ [S_{13} \quad S_{23} \quad S_{36}][T_\sigma]_k \left((z_k - z_{k-1})[\overline{Q}]_k \left(\begin{Bmatrix} \epsilon_x^o \\ \epsilon_y^o \\ \gamma_{xy}^o \end{Bmatrix} - \Delta T_0 \begin{Bmatrix} \widetilde{\alpha}_x \\ \widetilde{\alpha}_y \\ \widetilde{\alpha}_{xy} \end{Bmatrix}_k \right) \right) + (z_k - z_{k-1}) \left(\Delta T_0 \left(\widetilde{\alpha}_3 \right)_k \right) \right\}. \tag{4.290}$$

The stiffness matrices are (Eq. 4.264)

$$[\overline{Q}]^0 = \begin{bmatrix} 148.87 & 2.91 & 0 \\ 2.91 & 9.71 & 0 \\ 0 & 0 & 4.55 \end{bmatrix} 10^9 \frac{\mathrm{N}}{\mathrm{m}^2} \quad [\overline{Q}]^{45} = \begin{bmatrix} 45.65 & 36.55 & 34.79 \\ 36.55 & 45.65 & 34.79 \\ 34.79 & 34.79 & 38.19 \end{bmatrix} 10^9 \frac{\mathrm{N}}{\mathrm{m}^2}. \tag{4.291}$$

The thermal expansion coefficients are (Eqs. 4.265 and 4.267)

$$\begin{Bmatrix} \widetilde{\alpha}_x \\ \widetilde{\alpha}_y \\ \widetilde{\alpha}_{xy} \end{Bmatrix}^0 = \begin{Bmatrix} -0.7 \\ 25 \\ 0 \end{Bmatrix} 10^{-6} \frac{1}{^{\mathrm{o}}\mathrm{C}} \qquad \begin{Bmatrix} \widetilde{\alpha}_x \\ \widetilde{\alpha}_y \\ \widetilde{\alpha}_{xy} \end{Bmatrix}^{45} = \begin{Bmatrix} 12.15 \\ 12.15 \\ -25.70 \end{Bmatrix} 10^{-6} \frac{1}{^{\mathrm{o}}\mathrm{C}}, \tag{4.292}$$

where z is the distance from the midplane: $z_0 = -0.001$ m, $z_1 = -0.0004$ m, $z_2 = 0.0004$ m, $z_3 = 0.001$ m (Fig. 4.51) and K is the number of ply groups ($K = 3$). The stress transformation matrix $[T_\sigma]$ in the 45-degree direction is obtained from Eq. (3.51)

$$[T_\sigma] = \begin{bmatrix} 0.5 & 0.5 & 1.0 \\ 0.5 & 0.5 & -1.0 \\ -0.5 & 0.5 & 0 \end{bmatrix}. \tag{4.293}$$

The strains and curvatures of the midplane are given by Eq. (4.273) as follows:

$$\begin{array}{lll} \epsilon_x^o = 0.041 \times 10^{-3} & \epsilon_y^o = 1.653 \times 10^{-3} & \gamma_{xy}^o = -1.760 \times 10^{-3} \\ \kappa_x = 0 & \kappa_y = 0 & \kappa_{xy} = 0. \end{array} \tag{4.294}$$

With these values Eq. (4.290) gives

$$\Delta h = 5.899 \times 10^{-6} \text{ m}. \tag{4.295}$$

4.6 Plates with a Circular or an Elliptical Hole

We consider a plate with symmetrical layup containing either a circular or an elliptical hole (Fig. 4.55). The dimensions of the hole are small compared with the dimensions of the plate. We assume that at some distance from the hole there is a region where the in-plane forces and strains are nearly uniform. These "farfield" forces and strains are taken to be those that would exist in the plate in the absence of the hole. We wish to determine the strains near the hole in terms of the farfield forces and strains.

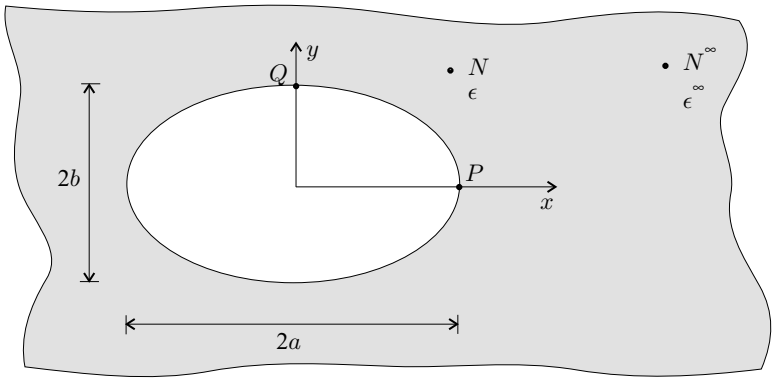

Figure 4.55: Elliptical hole in a plate.

Far from the hole the "farfield" in-plane forces are denoted by N_x^∞, N_y^∞, N_{xy}^∞ and the "farfield" in-plane strains are denoted by $\epsilon_x^{o,\infty}$, $\epsilon_y^{o,\infty}$, $\gamma_{xy}^{o,\infty}$. These forces and strains are related by (Eq. 3.26)

$$\begin{Bmatrix} N_x^\infty \\ N_y^\infty \\ N_{xy}^\infty \end{Bmatrix} = [A] \begin{Bmatrix} \epsilon_x^{o,\infty} \\ \epsilon_y^{o,\infty} \\ \gamma_{xy}^{o,\infty} \end{Bmatrix}. \tag{4.296}$$

At a point near the hole, the in-plane forces are

$$\begin{Bmatrix} N_x \\ N_y \\ N_{xy} \end{Bmatrix} = \begin{Bmatrix} N_x^\infty \\ N_y^\infty \\ N_{xy}^\infty \end{Bmatrix} + \begin{Bmatrix} N_x^* \\ N_y^* \\ N_{xy}^* \end{Bmatrix}, \tag{4.297}$$

where N_x^*, N_y^*, N_{xy}^* are modification terms that depend on x and y. Expressions

Table 4.15. The modification terms in Eq. (4.297)

$N_x^* = 2\,\mathrm{Re}\left\{\mu_1^2\Phi_1'(Z_1) + \mu_2^2\Phi_2'(Z_2)\right\}$
$N_y^* = 2\,\mathrm{Re}\left\{\Phi_1'(Z_1) + \Phi_2'(Z_2)\right\}$
$N_{xy}^* = -2\,\mathrm{Re}\left\{\mu_1\Phi_1'(Z_1) + \mu_2\Phi_2'(Z_2)\right\}$
$\Phi_k(Z_k) = A_k\zeta_k^{-1} \quad (k = 1, 2)$
$\zeta_k = \frac{Z_k + \sqrt{Z_k^2 - a^2 - \mu_k^2 b^2}}{a - i\mu_k b}$ (at the interface $\zeta_k = e^{i\vartheta}$)
$Z_k = x + y\mu_k \quad (k = 1, 2)$
μ_k's are the roots of the characteristic polynomial ($\mu_1 = \overline{\mu}_3$, $\mu_2 = \overline{\mu}_4$)
$a_{11}\mu^4 - 2a_{16}\mu^3 + (2a_{12} + a_{66})\mu^2 - 2a_{26}\mu + a_{22} = 0,$

where Re refers to the real part, i the imaginary unit;
$\overline{\mu}$ is the complex conjugate of μ;
$()'$ refers to the derivative with respect to Z_k;
a and b are shown in Figure 4.55;
$[a_{ij}] = [A_{ij}]^{-1}$ are the in-plane compliances of the plate.

for these parameters are given by Lekhnitskii[40] and are presented in Table 4.15. The modification terms depend on $\Phi_k(Z_k) = A_k \zeta_k^{-1}$, where A_k represents two unknown complex numbers whose real and imaginary parts constitute four unknown constants. These constants are determined from the condition that the surface traction is zero along the surface of the hole. It suffices to enforce this condition only at two points on the boundary

$$\begin{aligned} N_x \left(= N_x^{\infty} + N_x^*\right) &= 0 \qquad \text{at point } P \\ N_{xy} \left(= N_{xy}^{\infty} + N_{xy}^*\right) &= 0 \qquad \text{at point } P \\ N_y \left(= N_y^{\infty} + N_y^*\right) &= 0 \qquad \text{at point } Q \\ N_{xy} \left(= N_{xy}^{\infty} + N_{xy}^*\right) &= 0 \qquad \text{at point } Q. \end{aligned} \tag{4.298}$$

The four unknown constants in A_k are calculated by the following steps:

1. The constants A_k are assumed in the form

$$A_1 = C_1 + C_2 i \qquad A_2 = C_3 + C_4 i, \tag{4.299}$$

where $i = \sqrt{-1}$.

2. The roots μ_1 and μ_2 of the characteristic polynomial given in Table 4.15 are calculated.
3. Modification terms N_x^*, N_{xy}^* at point P and N_y^*, N_{xy}^* at point Q are calculated for four different sets of C_1, C_2, C_3, C_4.

Set 1 $C_1 = 1, C_2 = C_3 = C_4 = 0$, resulting in
$(N_x^*)_1^P$, $(N_{xy}^*)_1^P$ and $(N_y^*)_1^Q$, $(N_{xy}^*)_1^Q$

Set 2 $C_2 = 1, C_1 = C_3 = C_4 = 0$, resulting in
$(N_x^*)_2^P$, $(N_{xy}^*)_2^P$ and $(N_y^*)_2^Q$, $(N_{xy}^*)_2^Q$

Set 3 $C_3 = 1, C_1 = C_2 = C_4 = 0$, resulting in
$(N_x^*)_3^P$, $(N_{xy}^*)_3^P$ and $(N_y^*)_3^Q$, $(N_{xy}^*)_3^Q$

Set 4 $C_4 = 1, C_1 = C_2 = C_3 = 0$, resulting in
$(N_x^*)_4^P$, $(N_{xy}^*)_4^P$ and $(N_y^*)_4^Q$, $(N_{xy}^*)_4^Q$.

For arbitrary values of C_1–C_4 we have

$$\begin{Bmatrix} N_x^{*P} \\ N_{xy}^{*P} \\ N_y^{*Q} \\ N_{xy}^{*Q} \end{Bmatrix} = \begin{bmatrix} (N_x^*)_1^P & (N_x^*)_2^P & (N_x^*)_3^P & (N_x^*)_4^P \\ (N_{xy}^*)_1^P & (N_{xy}^*)_2^P & (N_{xy}^*)_3^P & (N_{xy}^*)_4^P \\ (N_y^*)_1^Q & (N_y^*)_2^Q & (N_y^*)_3^Q & (N_y^*)_4^Q \\ (N_{xy}^*)_1^Q & (N_{xy}^*)_2^Q & (N_{xy}^*)_3^Q & (N_{xy}^*)_4^Q \end{bmatrix} \begin{Bmatrix} C_1 \\ C_2 \\ C_3 \\ C_4 \end{Bmatrix}. \tag{4.300}$$

4. Equations (4.298) and (4.300) give

$$\begin{Bmatrix} N_x^{\infty} \\ N_{xy}^{\infty} \\ N_y^{\infty} \\ N_{xy}^{\infty} \end{Bmatrix} + \begin{bmatrix} (N_x^*)_1^P & (N_x^*)_2^P & (N_x^*)_3^P & (N_x^*)_4^P \\ (N_{xy}^*)_1^P & (N_{xy}^*)_2^P & (N_{xy}^*)_3^P & (N_{xy}^*)_4^P \\ (N_y^*)_1^Q & (N_y^*)_2^Q & (N_y^*)_3^Q & (N_y^*)_4^Q \\ (N_{xy}^*)_1^Q & (N_{xy}^*)_2^Q & (N_{xy}^*)_3^Q & (N_{xy}^*)_4^Q \end{bmatrix} \begin{Bmatrix} C_1 \\ C_2 \\ C_3 \\ C_4 \end{Bmatrix} = 0. \tag{4.301}$$

5. Equations (4.301) are solved for the C_1, C_2, C_3, C_4 constants.

[40] S. G. Lekhnitskii, *Anisotropic Plates*. Gordon and Breach Science Publishers, New York, 1968, p. 31.

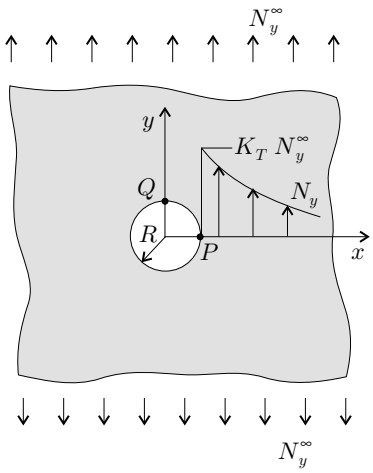

Figure 4.56: Orthotropic plate with a circular hole.

Next we apply the preceding equations to orthotropic plates containing a circular hole with radius R and subjected to a uniform tensile load N_y^∞ (Fig. 4.56). The maximum forces (per unit length) at the surface of the hole are[41]

$$N_y\,(R, 0) = K_T N_y^\infty \qquad \text{force at point } P \tag{4.302}$$

$$N_x\,(0,\, R) = -\sqrt{\frac{A_{11}}{A_{22}}}\,N_y^\infty \qquad \text{force at point } Q, \tag{4.303}$$

where K_T is the stress intensity factor

$$K_T = 1 + \sqrt{\frac{2}{A_{11}}\left(\sqrt{A_{11}A_{22}} - A_{12} + \frac{A_{11}A_{22} - A_{12}^2}{2A_{66}}\right)}, \tag{4.304}$$

x and y are in the directions of orthotropy, and the elements of the stiffness matrix are to be calculated in this coordinate system. The force distribution N_y along the x-axis may be approximated by[42] (Fig 4.56)

$$N_y\,(x, 0) = \frac{N_y^\infty}{2}\left\{2 + \left(\frac{R}{x}\right)^2 + 3\left(\frac{R}{x}\right)^4 - (K_T - 3)\left[5\left(\frac{R}{x}\right)^6 - 7\left(\frac{R}{x}\right)^8\right]\right\}. \tag{4.305}$$

4.7 Interlaminar Stresses

Laminate plate theory is formulated on the basis of the assumption that the laminate as well as all the layers are in a state of plane stress. Correspondingly, all

[41] Ibid., p. 175.

[42] H. J. Konish and J. M. Whitney, Approximate Stresses in an Orthotropic Plate Containing a Circular Hole. *Journal of Composite Materials*, Vol. 9, 157–166, 1975.

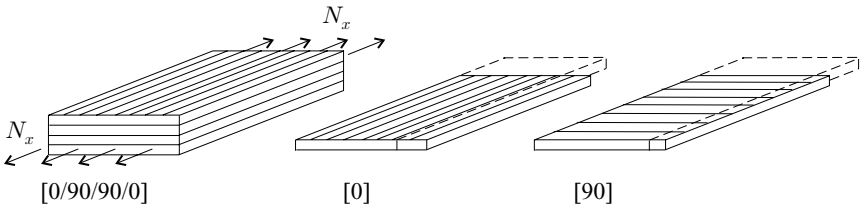

Figure 4.57: $[0/90]_s$ laminate loaded in tension and the deformations of unbonded 0- and 90-degree layers.

out-of-plane stress components are zero ($\sigma_z = 0$, $\tau_{yz} = 0$, $\tau_{xz} = 0$). This assumption is reasonable in regions away from free edges. Near free edges, both shear and normal stresses may arise between the layers. These interlaminar stresses may significantly alter the stress field existing away from the free edge and, importantly, may cause separation (delamination) of adjacent layers.

We illustrate the stresses near a free edge through the example of a $[0/90]_s$ cross-ply laminate (Fig. 4.57). The laminate is subjected to a unidirectional force (per unit length) N_x with x being in the direction of the 0-degree fibers. The axial load is shared by the plies, and the axial deformation of each ply is the same ($\epsilon_x^0 = \epsilon_x^{90}$). We now consider one of the 0-degree plies and the adjacent 90-degree ply. Their transverse Poisson ratios are different ($\nu_{xy}^0 \neq \nu_{xy}^{90}$). Hence, if the two plies were allowed to move freely, they would deform by different amounts in the transverse y direction (Fig. 4.57). In reality, the two plies are bonded together, and their transverse deformations (and transverse strains) are equal. Obviously, one of the plies (in this example the 0-degree ply) must be in tension, and the other one (90-degree ply) must be in compression.

The stresses on a 0-degree ply element are shown in Figure 4.58. Away from the free edge, on a small element the σ_y stresses equilibrate each other, and there is no interlaminar shear stress ($\tau_{yz} = 0$). At the free edge σ_y is unbalanced and is

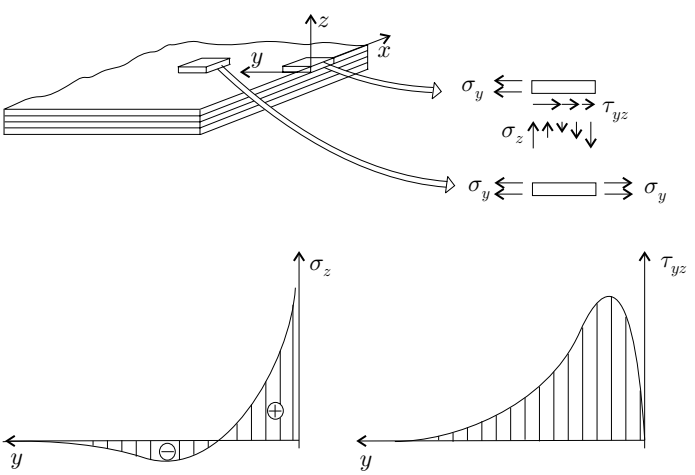

Figure 4.58: Free-body diagrams and the stress distributions near a free edge.

equilibrated by the interlaminar stresses ($\tau_{yz} \neq 0$). Furthermore, σ_y and τ_{yz} create a moment, which must be equilibrated by the interlaminar normal stress σ_z shown in Figure 4.58. The normal stress, as well as τ_{yz}, diminishes in regions away from the edge.

Care must be taken in calculating the interlaminar stresses. Under the assumption that the material is linearly elastic, the calculations result in infinite stresses at free edges.